Environmental Impact Assessment Report
Volume 3, Appendix 6.1: Physical Processes Modelling

MarramWind Offshore Wind Farm

December 2025

MarramWind

Document code:	MAR-GEN-ENV-REP-WSP-000077
Contractor document number:	852346-WEIS-IA-O1-RP-M6-107495
Version:	Final for Submission
Date:	08/12/2025
Prepared by:	ABPmer Limited
Checked by:	WSP UK Limited
Approved by:	MarramWind Limited

Contents

1. Introduction

1.1.1.1 This Appendix outlines the technical studies undertaken, including numerical modelling and empirical analysis, to inform **Volume 1, Chapter 6: Marine Geology, Oceanography and Physical Processes** of the MarramWind Offshore Wind Farm (hereafter, referred to as 'the Project') Environmental Impact Assessment (EIA) Report.

1.1 Overview

1.1.1.2 A range of technical assessments have been developed to infer the potential changes relative to the baseline (existing) coastal and marine environment caused by the construction, operation and maintenance (O&M) and decommissioning of the Project, specifically changes to:

- waves: characterise the impact of floating and fixed foundations on the wave regime (wave height, period and direction) during the O&M stage;
- stratification and frontal systems: characterise the impact of wind turbine generator (WTG) floating units on the strength and timing of seasonal stratification during the O&M stage; and
- scour: characterise the patterns of local and global scour associated with near-bed infrastructure during the O&M stage.

1.1.1.3 The information from this Appendix informs the technical analysis and the assessment of the likely significant environmental effects of the Project on physical processes across the physical processes study area. This Appendix accompanies **Volume 1, Chapter 6: Marine Geology, Oceanography and Physical Processes** to support the consent application for the Project.

1.2 Physical processes study area

1.1.1.4 The study area for the marine geology, oceanography, and physical processes assessment has previously been presented within the Project Scoping Report (MarramWind Limited, 2023) and is also shown in **Figure 1**. It includes the Option Agreement Area (OAA), the offshore export cable corridor, and the wider surrounding marine area across which potentially significant effects could occur.

1.1.1.5 The study area has been informed by expert judgement, based on understanding of region-scale marine geology, oceanography, and physical processes, in particular that of the prevailing wave direction, tidal excursion distances and sediment transport pathways.

1.1.1.6 The study area is located off the northeast coast of Aberdeenshire (**Figure 1**). It has been defined on the basis of:

- The distance away from the Project which suspended sediment plumes may be advected (and interact with potentially sensitive receptors). This has been defined by a spring tidal excursion ellipse buffer around the OAA and offshore export cable corridor.
- The distance up / down drift from the landfall, that littoral processes could theoretically be impacted by offshore infrastructure associated with the Project. This has been defined through consideration of coastal sub-cell information set out in Ramsay and Brampton (2000a; 2000b).

- The distance from the OAA that wave blockage impacts could theoretically be detected. This has been informed by expert judgement, drawing upon (amongst other things), the evidence base from other projects and consideration of the prevailing wave directions.

1.1.1.7 Direct changes to the seabed will be confined to the OAA and offshore export cable corridor, with indirect changes (for example, due to disruption of waves, tides or sediment pathways) experienced both inside and outside of the site boundary. These indirect changes are expected to diminish with distance from the OAA and offshore export cable corridor.

1.1.1.8 The study area overlaps with several nationally and internationally designated nature conservation sites, some of which are designated on the basis of the geological and geomorphological features contained within them. These include the Southern Trench Nature Conservation Marine Protected Area (NCMPA) and Rosehearty to Fraserburgh Coast Site of Special Scientific Interest, both designated in part for the geodiversity features they contain.

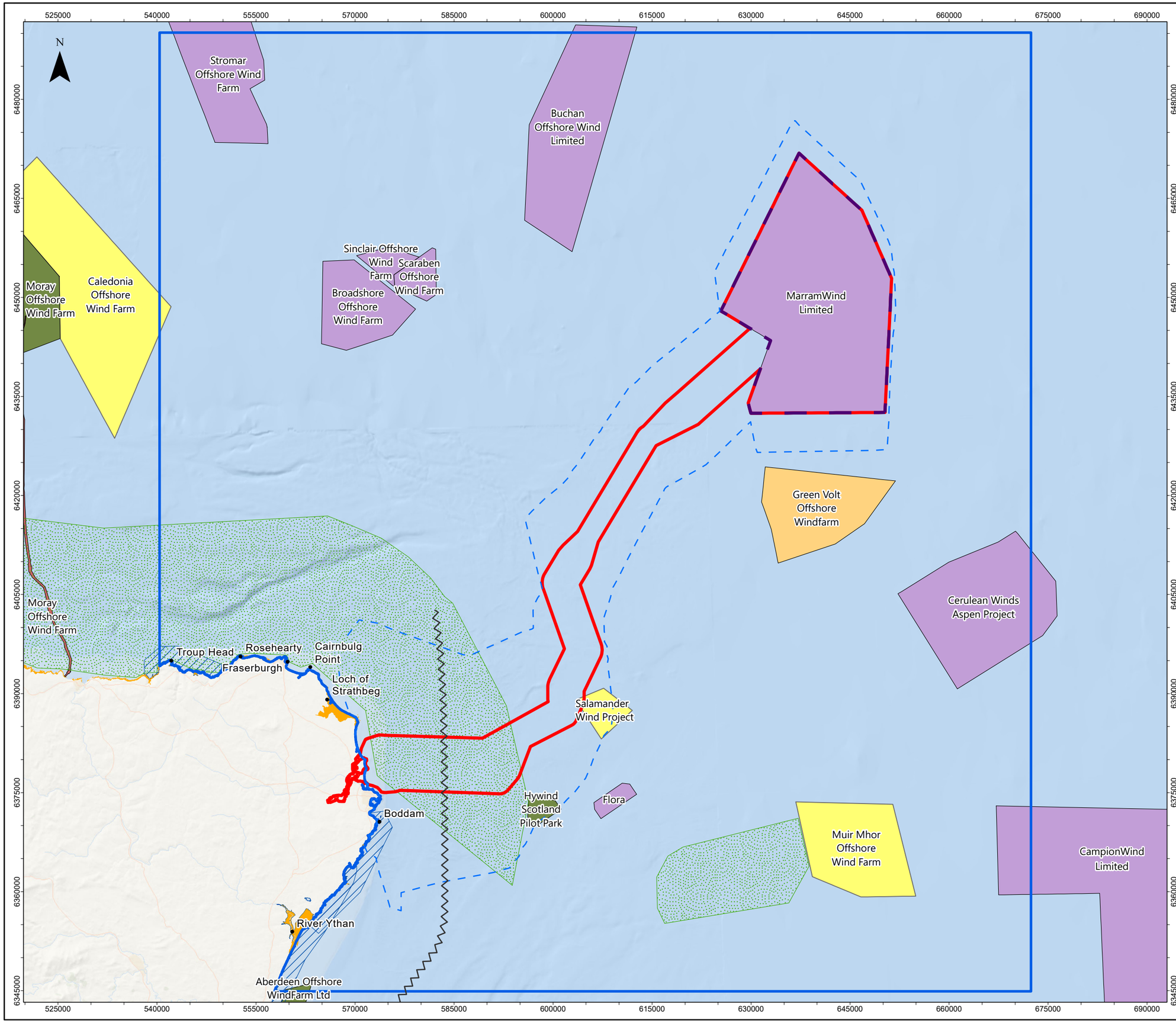

- Red Line Boundary
- Option Agreement Area
- Marine geology, oceanography, and physical processes study area
- Approximate position of Buchan front
- Spring tidal excursion ellipse buffer
- Site of Special Scientific Interest
- Marine Protected Area
- Special Protection Area

Offshore Wind - Project Phase

- Consented
- In Planning
- Operational
- Pre Planning
- Under Construction

0 10 20 Kilometres

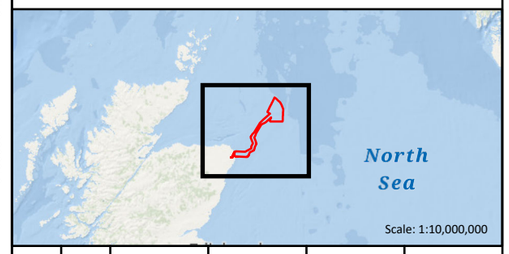

REV	REV DATE	GIS CREATOR	GIS REVIEWER	TECHNICAL CHECKER	TECHNICAL APPROVER
		--	--	--	--
	--	--	--	--	--
2	18/09/2025	AW	ND	AB	AB

WSP DRAWING NUMBER	808368-WEIS-IA-E5-FG-M7-18716
MarramWind DRAWING NUMBER	MAR-GEN-ENV-MAP-WSP-000359
DATUM	ETRS 89
PROJECTION	UTM Zone 30N
SCALE	1:550,000
PAGE SIZE	A3

PROJECT TITLE
MarramWind Offshore Wind Farm

DRAWING TITLE
Figure 1 Marine geology, oceanography, and physical processes study area

Environmental Impact Assessment Report
Appendix 6.1

NOT TO BE USED FOR NAVIGATION

wsp MarramWind

2. Waves

2.1.1.1 This Section describes the design, validation and results of a suite of numerical spectral wave (SW) models covering the study area. The SW models are used to simulate baseline conditions (patterns of wave height, period and direction), and the impact of the Project on baseline conditions during the O&M stage.

2.2 Introduction

2.2.1.1 The interaction between waves and the foundations of the offshore infrastructure WTGs, offshore substations and reactive compensation platforms (RCPs) may result in a reduction in wave energy locally around foundations, and across the wider physical processes study area. Where the wave climate is important to local processes and is persistently modified, these changes may potentially alter the frequency or pattern of sediment transport and therefore seabed morphology in affected offshore areas, and / or the rate and direction of longshore sediment transport and therefore coastal morphology on affected coastlines.

2.2.1.2 To quantitatively assess the likely magnitude and extent of interaction between the O&M stage of the Project and the wave regime, a numerical wave model has been developed.

2.3 Methods

2.3.1 Wave model design

2.3.1.1 The wave model is built using the MIKE21FM SW module (DHI, 2025), which simulates the growth, decay and transformation of wind-generated waves and swell in offshore and coastal areas.

2.3.1.2 The wave model creates discrete simulations of wave height, period and direction throughout the domain, for a representative range of selected ‘every day’ and extreme wave conditions (return periods and directions).

2.3.2 Wave model mesh

2.3.2.1 The extent and resolution of the wave model mesh is shown in **Plate 2.1**. A flexible mesh design (interlocking triangular ‘elements’ of varying shape and orientation) is used, providing tailored spatially variable resolution within a single model mesh. The horizontal model resolution is highest, approximately 100 metres (m), within the Project OAA, and OAAs of other offshore wind farms included in the cumulative assessment. Resolution within the central area of the model domain and covering the coastline is approximately 250m, gradually reducing to approximately 1 kilometre (km) at the open boundaries.

Plate 2.1 SW model mesh

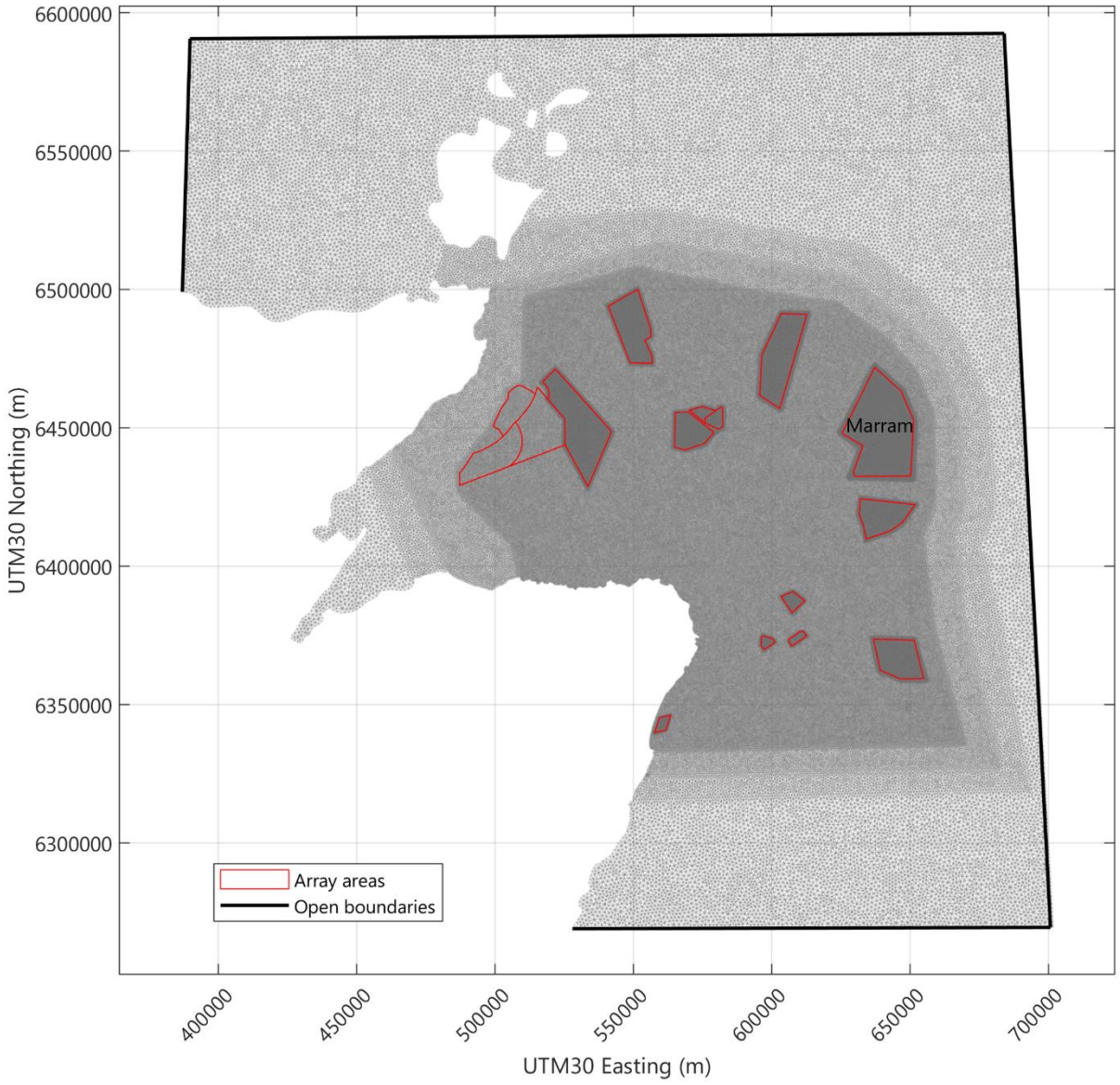

2.3.3 Wave model bathymetry

2.3.3.1 The SW model bathymetry (**Plate 2.2**) is sourced from EMODnet (EMODnet, 2025), which is a freely available and reliable data source that incorporates survey data from national hydrographic survey programmes in the UK and throughout Europe. Depth values from EMODnet across the OAA and offshore export cable corridor were compared with those obtained from the 2022 / 2023 geophysical surveys (Fugro, 2023a; 2024). The comparison shows good correlation and consistency between the two data sets.

2.3.3.2 Spatially varying adjustments are made to convert the bathymetry data from the standard Lowest Astronomical Tide (LAT) datum at source, to Mean Sea Level (MSL), as is required for use in the model. Adjustments are made using a combination of (Vertical Offshore Reference Frames) (University College London and United Kingdom Hydrographic Office, 2005).

2.3.3.3 The SW models are run with a constant 'MSL' condition (fixed at MSL with no tidal water level variation). This provides a central description of the range of total water depths that might be experienced within the physical processes study area. The timing of larger extreme wave events is independent of the timing of tidal processes (high water / low water / spring / neap). A relatively higher water level might allow larger waves to extend further onto or beyond otherwise shallower areas of the domain, or vice versa. However, the main effect of the foundations on waves is within the relatively deep offshore OAA (approximately 106mMSL), where there is only a small relative difference in total water depth between a mean tidal water level and a mean spring high or low water (±1.8m). Sensitivity testing of the model indicates minimal difference as a result.

Plate 2.2 SW model bathymetry

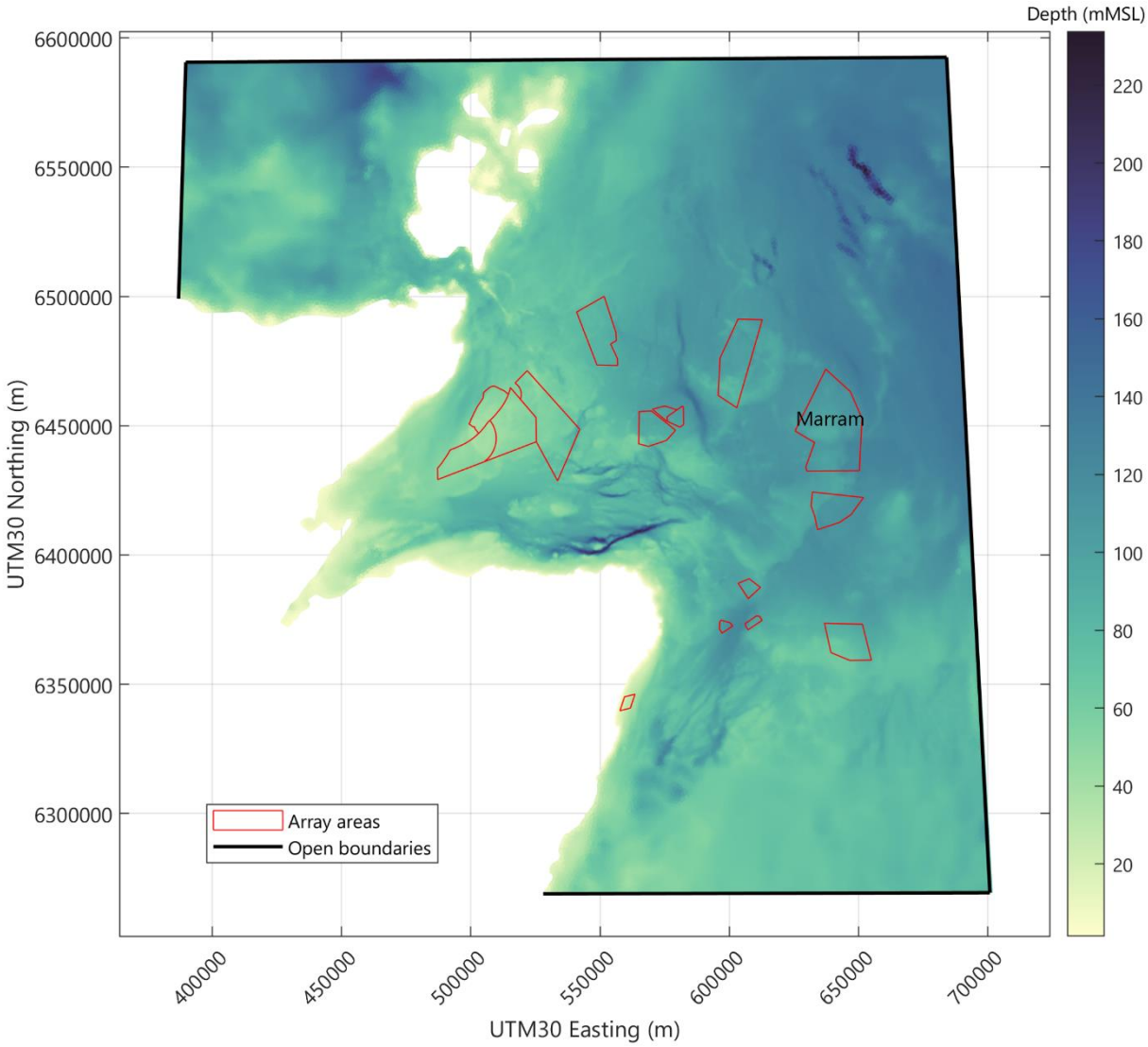

2.3.4 Wave model spectral and time formulations

2.3.4.1 A fully spectral formulation is used. The fully spectral formulation is based on a wave action conservation relationship where the directional-frequency wave action spectrum is the dependent variable (DHI, 2025). Of the available choices, this formulation is considered to be the most appropriate and accurate for the nature of the processes being simulated with respect to both general wave propagation and the effect of the WTG foundations.

2.3.4.2 A quasi-stationary time formulation is used. Time is removed as an independent variable and a steady state solution is calculated for each seastate being simulated. This choice is appropriate for the limited size of the model domain, within which waves are likely to achieve an equilibrium state dependant on the input wave and wind boundary conditions.

2.3.4.3 A logarithmic distribution of 36 spectral frequencies are resolved, equivalent to wave periods in the approximate range from 1 second (s) to 30s, with smaller intervals at smaller wave periods. This exceeds the default number and range (25 spectral frequencies, from 1.8s to 18s) in order to better resolve a wider range of wave periods.

2.3.4.4 Directional calculations are made using 32 directional sectors (each sector covering a range of 11.25 degrees (°)). This exceeds the default number (16 directional sectors, 22.5°) in order to reduce the occurrence of small magnitude 'radial artefacts' in the scheme effect results when obstacles representing the offshore infrastructure are included in the model. The baseline wave maps are largely unaffected by the difference.

2.3.5 Wave model boundary conditions

2.3.5.1 The wave model is forced by wave conditions (height, period, direction and directional spreading) at the four offshore wave boundaries (along the northern, eastern, southern and western extents of the model domain), and by a constant wind speed and direction applied over the whole domain. The wave model is run with a constant MSL (no tidal water level variation) and no currents.

2.3.5.2 The wave condition scenarios considered by the model for the assessment are:

- wave coming directions (east (E), east northeast (ENE), northeast (NE), north northeast (NNE) and north (N)); and
- return periods (50% non-exceedance, 0.1 year; 1 year; 10 year; 50 year; 100 year).

2.3.5.3 An understanding of the potential impacts of offshore infrastructure within this range of conditions will inform the assessments regarding potential impacts on sedimentary / coastal processes and flood risk. These conditions were initially determined using Extreme Value Analysis (EVA) for a location at the central point of the OAA, using hindcast timeseries data from the separately validated ABPmer SEASTATES NW European Shelf Wave Hindcast Model (ABPmer, 2013).

2.3.5.4 The wave boundary condition is applied uniformly along the four offshore wave boundaries. The condition is defined by the significant wave height (Hs), peak wave period (Tp), mean wave direction (DirM) and directional standard deviation (DirStd). The directional return period wave boundary conditions tested are listed in **Table 2.1**. The shortest return period is the wave condition not exceeded 50% of the time, representing a relatively frequent, every day wave condition; more severe but infrequent conditions are described by the associated 'return period' (RP) or likelihood of occurrence expressed in years.

2.3.5.5 The wind forcing is applied uniformly across the whole model domain area, representing the wind speed at 10m above sea level normally associated with the target seastate. The associated wind direction is the same as the wave direction at the boundary. The wind boundary condition is required for natural patterns of wave propagation and development

through the model domain from the offshore boundaries. Wind is also a realistic mechanism contributing to wave recovery in the lee of offshore infrastructure. The associated directional return period values of wind speed and direction used are also shown in **Table 2.1**.

Table 2.1 Wave and wind boundary conditions for seastates modelled

Directional sector	Case	Hs (m)	Tp (s)	DirM (°N, from)	Wind speed at 10m (m/s)	Wind direction at 10m (°N, from)
E	50% no exc.	1.9	9.5	90	8.3	90
	0.1 year RP.	5.2	10.2	90	17.2	90
	1 year RP.	8.2	12.8	90	21.5	90
	10 year RP.	10.9	14.8	90	24.4	90
	50 year RP.	12.6	16.0	90	26.9	90
	100 year RP.	13.4	16.4	90	27.8	90
ENE	50% no exc.	1.6	8.7	67.5	7.7	67.5
	0.1 year RP.	3.5	8.5	67.5	13.2	67.5
	1 year RP.	5.5	10.6	67.5	17.5	67.5
	10 year RP.	7.3	12.3	67.5	19.0	67.5
	50 year RP.	8.5	13.2	67.5	20.0	67.5
	100 year RP.	9.0	13.6	67.5	22.0	67.5
NE	50% no exc.	1.3	7.9	45	6.5	45
	0.1 year RP.	3.1	7.7	45	13.0	45
	1 year RP.	4.9	9.7	45	17.6	45
	10 year RP.	6.6	11.2	45	20.7	45
	50 year RP.	7.7	12.0	45	21.9	45
	100 year RP.	8.1	12.4	45	22.4	45
NNE	50% no exc.	1.4	7.8	22.5	6.2	22.5
	0.1 year RP.	3.9	9.4	22.5	13.6	22.5
	1 year RP.	6.2	11.8	22.5	18.9	22.5
	10 year RP.	8.2	13.6	22.5	20.2	22.5
	50 year RP.	9.6	14.6	22.5	21.7	22.5

Directional sector	Case	Hs (m)	Tp (s)	DirM (°N, from)	Wind speed at 10m (m/s)	Wind direction at 10m (°N, from)
	100 year RP.	10.1	15.1	22.5	23.5	22.5
N	50% no exc.	1.9	9.5	0	8.3	0
	0.1 year RP.	5.0	10.3	0	15.5	0
	1 year RP.	7.9	13.0	0	20.0	0
	10 year RP.	10.6	15.0	0	24.4	0
	50 year RP.	12.3	16.1	0	26.1	0
	100 year RP.	13.0	16.6	0	27.2	0

2.3.6 Wave model parameters

2.3.6.1 The settings and values below are either default settings or within the range of normally recommended values and are consistent with numerous similar recent offshore wind farm modelling studies undertaken by ABPmer (Awel y Môr Offshore Wind Farm Ltd (ABPmer, 2022) and Five Estuaries Offshore Wind Farm Ltd (ABPmer, 2024)).

2.3.6.2 Depth-induced wave breaking is the process by which waves dissipate energy when the waves are too high to be supported by the water depth, (for instance, reach a limiting wave height / depth-ratio). Wave breaking is described in MIKE21SW (DHI, 2025) by standard equations that are scaled by a coefficient ‘Gamma’. A constant Gamma value of 0.8 was used.

2.3.6.3 Bottom friction is relevant where, as waves propagate into shallow water, the orbital wave velocities penetrate throughout the full water depth and the source function due to wave-bottom interaction becomes important. A large part of the model domain (towards the adjacent coastlines) is shallow enough, relative to the waves being simulated, to be affected by choices relating to the implementation of bottom friction. The dissipation source function used in the SW module is based on the quadratic friction law and linear wave kinematic theory. The dissipation coefficient depends on the hydrodynamic and sediment conditions. Sediment roughness is characterised in the MIKE21SW wave model by a Nikuradse Roughness length value of 0.04m.

2.3.6.4 The MIKE21SW wave model (DHI, 2025) also takes account of the following wave transformation processes (using default settings):

- white capping (Dissipation coefficients, constant Cdis = 4.5, constant DELTAdis = 0.5); and
- quadruplet-wave interaction.

2.3.7 Wave model structures

2.3.7.1 To simulate a maximum design scenario blockage scenario for waves, the largest cross-sectional area within the water column for the WTG, offshore substations and RCP foundation types described in **Volume 1, Chapter 4: Project Description**, has been calculated. These sub-grid scale foundations are represented in the model as a single triangular element centred on their locations, each containing a point structure assigned with the appropriate maximum design scenario blockage width and a height exceeding the water column depth.

2.3.7.2 To assess cumulative impacts with neighbouring operational and proposed offshore wind farms including Green Volt, Buchan, Stromar, Caledonia, Scaraben, Sinclair, Broadshore, Salamander, Muir Mhòr, Flora, Hywind Scotland Pilot Park, Aberdeen, Beatrice, Moray West and Moray East - a version of the model was run that includes structures representing WTGs and offshore substations within each array.

2.3.7.3 For operational offshore wind farms, turbine locations and maximum design scenario blockage were derived from the existing infrastructure. For proposed offshore wind farms, these parameters were estimated using information from site-specific EIAs and / or Scoping Reports.

2.3.7.4 Where detailed WTG and offshore substation locations were unavailable - specifically for Stromar, Buchan, Caledonia, Scaraben, Sinclair, Broadshore, Salamander, and Flora - a uniform grid layout was applied to represent turbine positions within each array. Additionally, foundation size data for WTGs and offshore substations was not available for Stromar and Flora. For Stromar, which is expected to be a large floating wind project, foundation dimensions were conservatively assumed based on those of the Project. For Flora, foundation sizes were assumed based on typical dimensions used in smaller floating wind installations.

The Project foundation type and number

2.3.7.5 A range of WTG, offshore substations and RCP foundation types are considered in the project design envelope. The maximum design scenario is identified as the combination of option presenting the greatest total potential blockage to waves passing through the OAA (for instance, the greatest number of foundation and the greatest near-surface dimension). The maximum design scenario for the Project is provided in **Table 2.2**.

Table 2.2 Maximum design scenario for the Project in relation to wave modelling

Parameter	Maximum design scenario
Maximum turbine power output	14 megawatts (MW)
Maximum number of WTGs	225
Maximum dimension of floating unit	120m
Number offshore substations	4

Parameter	Maximum design scenario
Offshore substation foundation type	Jacket foundations secured by driven piles or suction caisson.
Offshore substation maximum dimension	80m
Number of RCPs	2
RCP foundation type	Jacket foundations secured by driven piles or suction caisson.
RCP maximum dimension	35m

Any other combination of foundation type and number would result in a smaller total blockage.

Other offshore windfarm foundation type and number

2.3.7.6 To assess cumulative impacts with neighbouring operational / proposed offshore wind farms (Green Volt, Buchan, Stromar, Caledonia, Scaraben, Sinclair, Broadshore, Salamander, Muir Mhòr, Flora, Hywind Scotland Pilot Park, Aberdeen, Beatrice, Moray West and Moray East), the maximum design scenario for wave blockage based on the site-specific WTG and offshore substation foundations number and dimensions is determined for each other offshore wind farm in **Table 2.3**.

Table 2.3 Maximum design scenario for other offshore wind farms in relation to wave modelling

Offshore wind farm	Maximum design scenario
Green Volt	30 WTGs with maximum dimension of 100m. 1 offshore substation with maximum dimension of 26m.
Buchan	70 WTGs with maximum dimension of 80m. 3 offshore substations with maximum dimension of 18m.
Stromar	71 WTGs with maximum dimension of 130m. 3 offshore substations with maximum dimension of 140m.
Caledonia	101 WTGs with maximum dimension of 28m. 39 WTGs with maximum dimension of 102m. 4 offshore substations with maximum dimension of 28m.
Scaraben	6 WTGs with maximum dimension of 140m.
Sinclair	6 WTGs with maximum dimension of 140m.

Offshore wind farm	Maximum design scenario
Broadshore	60 WTGs with maximum dimension of 140m.
Salamander	70 WTGs with maximum dimension of 140m.
Muir Mhòr	67 WTGs with maximum dimension of 150m. 1 offshore substation with maximum dimension of 18m.
Flora	3 WTGs with maximum dimension of 140m. 1 offshore substation with maximum dimension of 18m.
Hywind Scotland Pilot Park	5 WTGs with maximum dimension of 15.
Aberdeen	11 WTGs with maximum dimensions of 10.5m.
Beatrice	84 WTGs with maximum dimension of 12m. 2 offshore substations with maximum dimension of 12m.
Moray West	60 WTGs with maximum dimension of 10m. 2 offshore substations with maximum dimension of 9.5m.
Moray East	100 WTGs with maximum dimension of 9m. 3 offshore substations with maximum dimension of 9m.

Foundation locations

2.3.7.7 For the Project, the foundation layout provided in **Volume 1, Chapter 4: Project Description** that gives the maximum design scenario for wave blockage is for the greatest number of WTGs (225), offshore substations (4), and RCPs (2) as shown in **Plate 2.3**. This layout is realistically representative of any that might be eventually considered.

2.3.7.8 For Green Volt, Muir Mhòr, Hywind Scotland Pilot Park, Aberdeen, Beatrice, Moray West and Moray East offshore wind farms the foundation locations are determined from site-specific EIA and / or Scoping Reports. For Stromar, Buchan, Caledonia, Scaraben, Sinclair, Broadshore, Salamander, and Flora, information detailing the specific location of foundations could not be found, therefore a uniform grid layout was assumed to estimate the WTG and offshore substation positions within the respective OAAs.

2.3.7.9 All structure locations included in the SW model runs are shown in **Plate 2.3**.

Plate 2.3 SW model structure locations

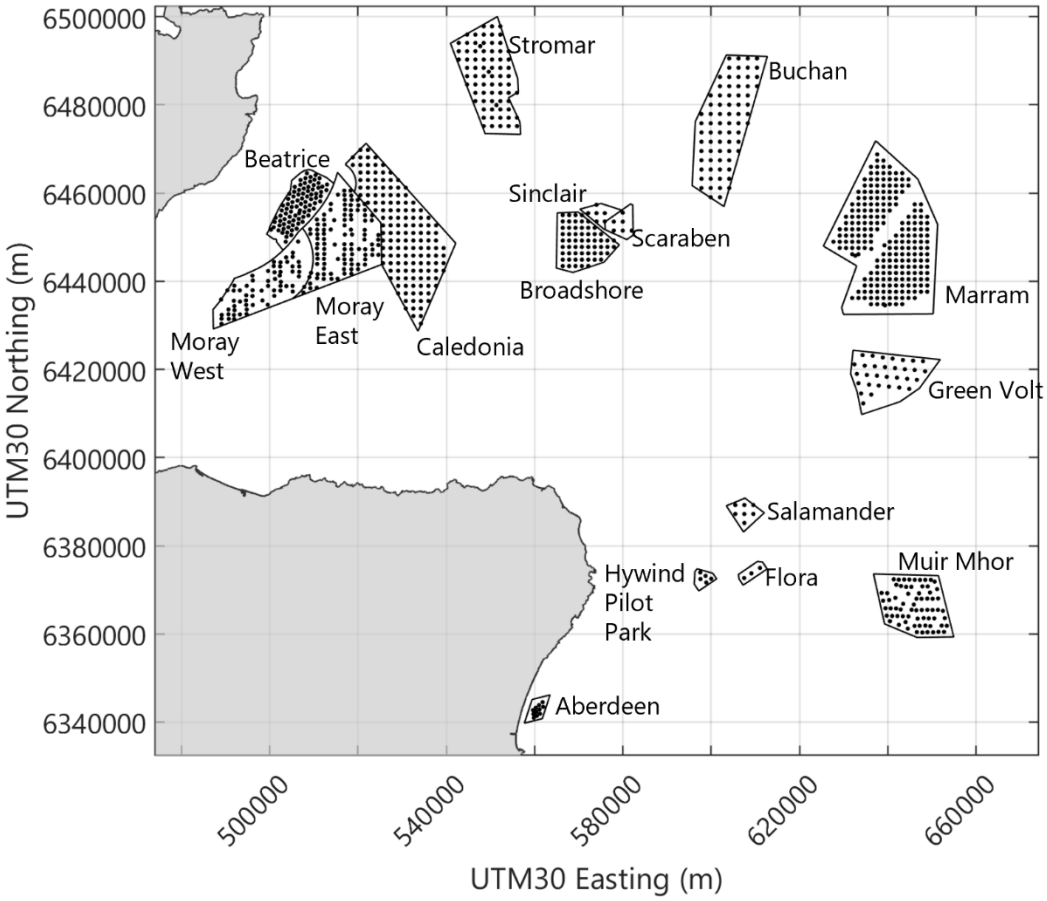

2.3.8 Wave model validation

2.3.8.1 The wave model is not required to provide historical (hindcast) predictions of wave conditions in a timeseries mode, therefore, no direct validation of the project-specific wave model against measured timeseries data is required.

2.3.8.2 Hindcast data from the ABPmer SEASTATES NW European Shelf Wave Hindcast Model are used to inform the boundary conditions. The SEASTATES wave hindcast model is described fully and has already been regionally validated against numerous wave buoys in ABPmer (2013).

2.3.8.3 The SEASTATES wave hindcast model (ABPmer, 2013) is also further locally validated against measured data from a project-specific metocean deployment within the OAA (640916mE, 6458665mN, UTM30). Measured wave data from September 2022 to September 2023 was found to capture a wide range of wave heights (<1m to >6m) and wave directions. Comparison against this period ensures the model performs well over a wide range of conditions.

2.3.8.4 The accuracy of the SEASTATES NW European Shelf Wave Hindcast Model (ABPmer, 2013) in predicting Hs, Tp and mean direction was assessed by comparing measured wave data with coincident timeseries output at the location of the measured data extracted from the SEASTATES Wave Hindcast Model.

2.3.8.5 **Plate 2.4** show timeseries comparison plots of modelled Hs, Tp and mean direction against measured values (Fugro, 2023b). The visual comparison shows the general magnitude and

timing of wave events are reproduced well. The above information validates the SEASTATES hindcast model data (ABPmer, 2013) to provide a realistic representation of wave conditions and climate within the physical processes study area.

2.3.8.6 The local wave model performance is not validated explicitly. However, the important components of the model design and inputs (extent, resolution, bathymetry, coastlines and boundary conditions) have been individually validated to be realistic, accurate and detailed. The resulting model is therefore expected to perform to a similar level.

Plate 2.4 Comparison of measured and modelled wave parameters within the OAA

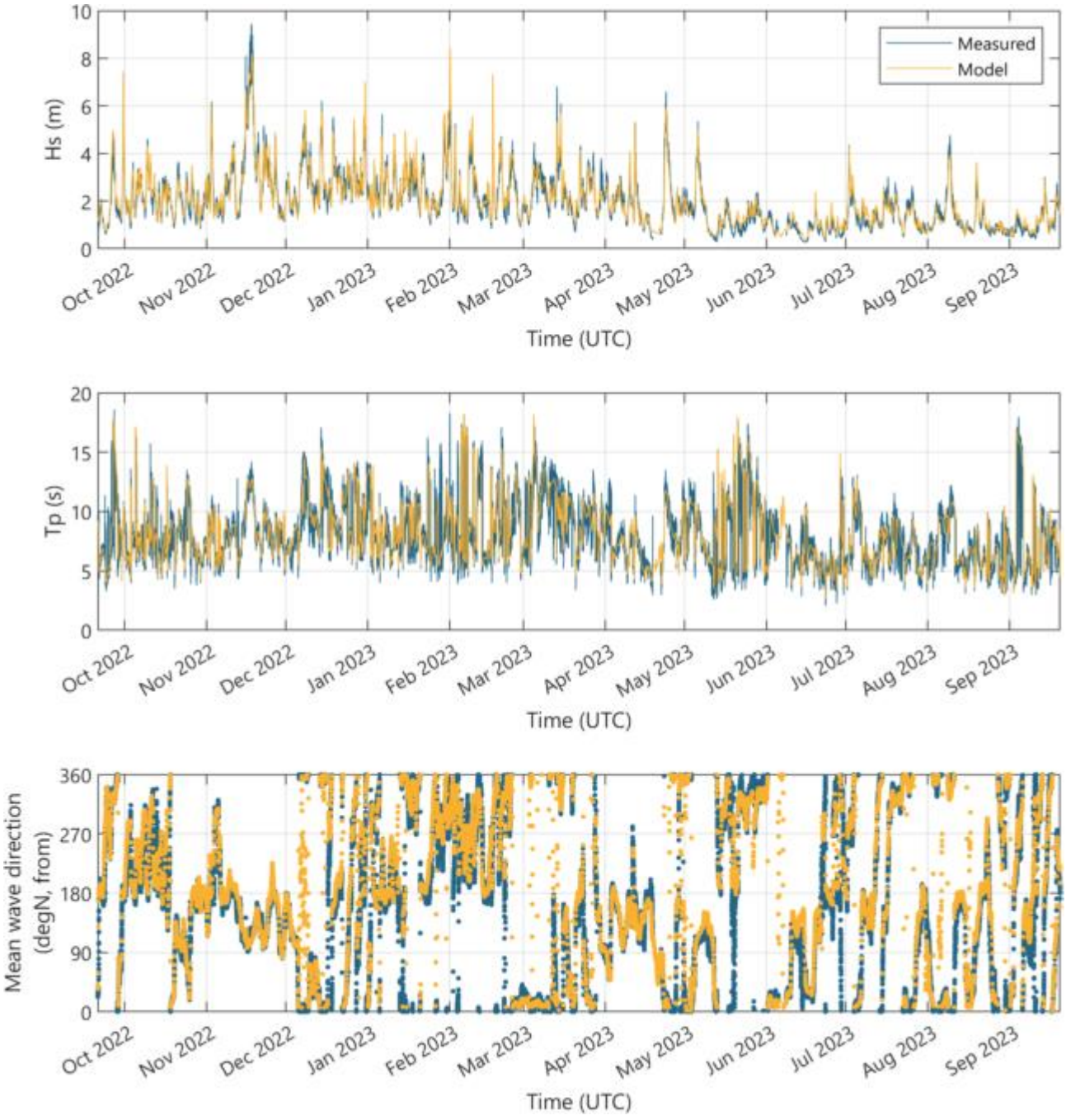

2.3.8.7 The SW numerical models are robust tools but are subject to a number of assumptions. These include the input parameters (for example, using representative wave events), scenario assumptions (for example, the location of foundations) as well as uncertainty in the underpinning datasets (for example, wave data and bathymetry data). Such uncertainty is managed in the design of the modelling study, validation (where appropriate and possible) of models and the interpretation of the model results in the context of the baseline and using expert judgement. The model settings and assumptions applied are within the range of normally recommended values and are consistent with numerous similar recent offshore wind farm modelling studies undertaken by ABPmer (for example, Awel y Môr Offshore Wind Farm Ltd, (ABPmer, 2022) and Five Estuaries Offshore Wind Farm Ltd (ABPmer, 2024)).

2.4 Results

2.4.1.1 This Section sets out the assessment of changes to the wave regime within the physical processes study area, based on SW modelling of the maximum design scenario for the Project, considered both alone and cumulatively with neighbouring operational / proposed offshore wind farms.

2.4.1.2 The wave model simulates the development, propagation and dispersion of wave energy throughout the domain, creating discrete spatial maps of Hs, Tp and DirM, for a representative range of selected every day and extreme wave conditions (return periods and directions). The wave condition scenarios considered by the model for the assessment are:

- wave coming directions (E, ENE, NE, NNE and N); and
- return periods (50% non-exceedance, 0.1 year; 1 year; 10 year; 50 year; 100 year).

2.4.1.3 More detailed information about the design and validation of the wave models is given in **Section 2.3**.

2.4.2 Baseline conditions

2.4.2.1 Plots showing the spatial distribution of wave height and direction for each of the baseline wave conditions without any wind farm infrastructure present are shown in **Plate 2.5** to **Plate 2.9**.

Plate 2.5 Baseline significant wave height, waves from the E, all return periods

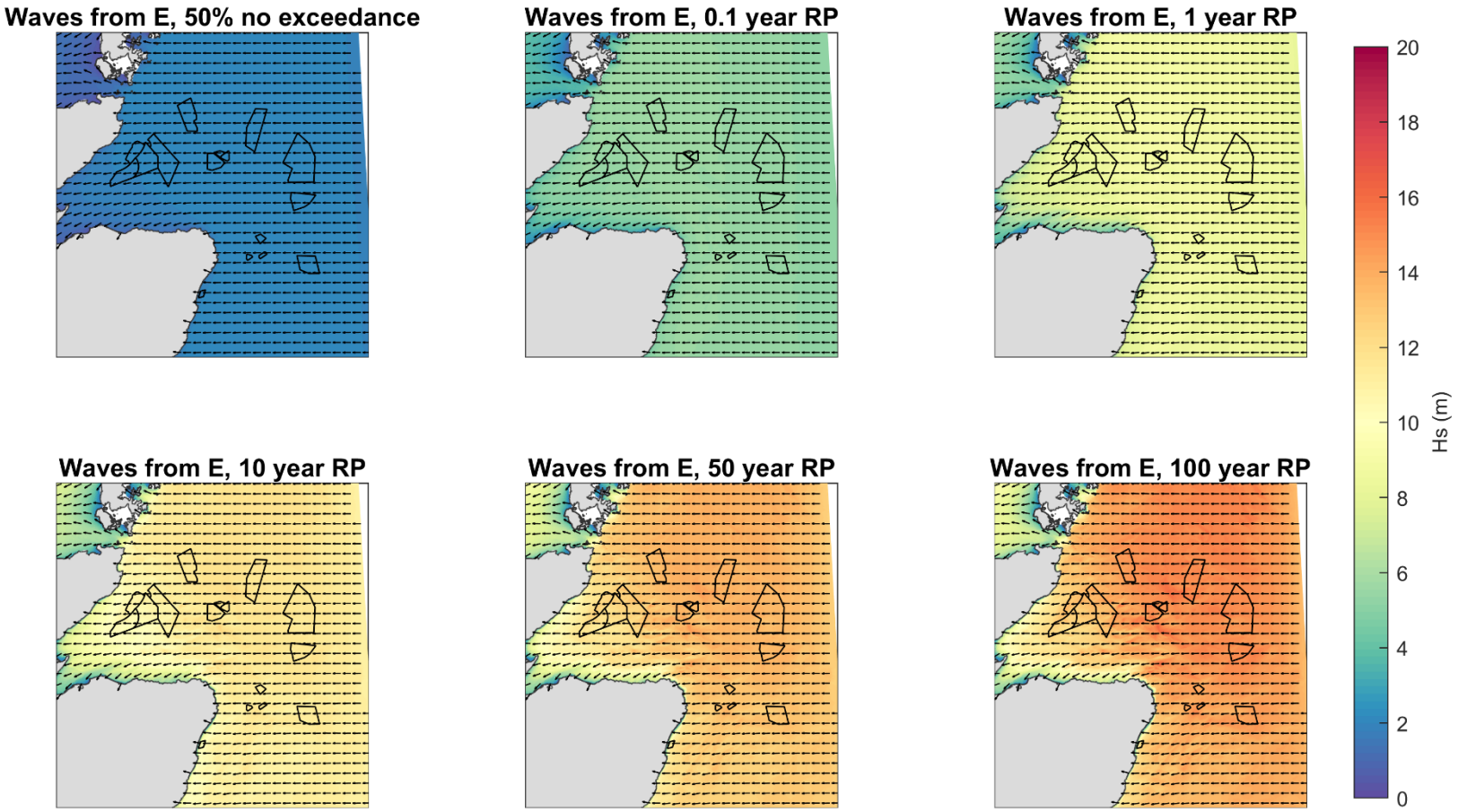

Plate 2.6 Baseline significant wave height, waves from the ENE, all return periods

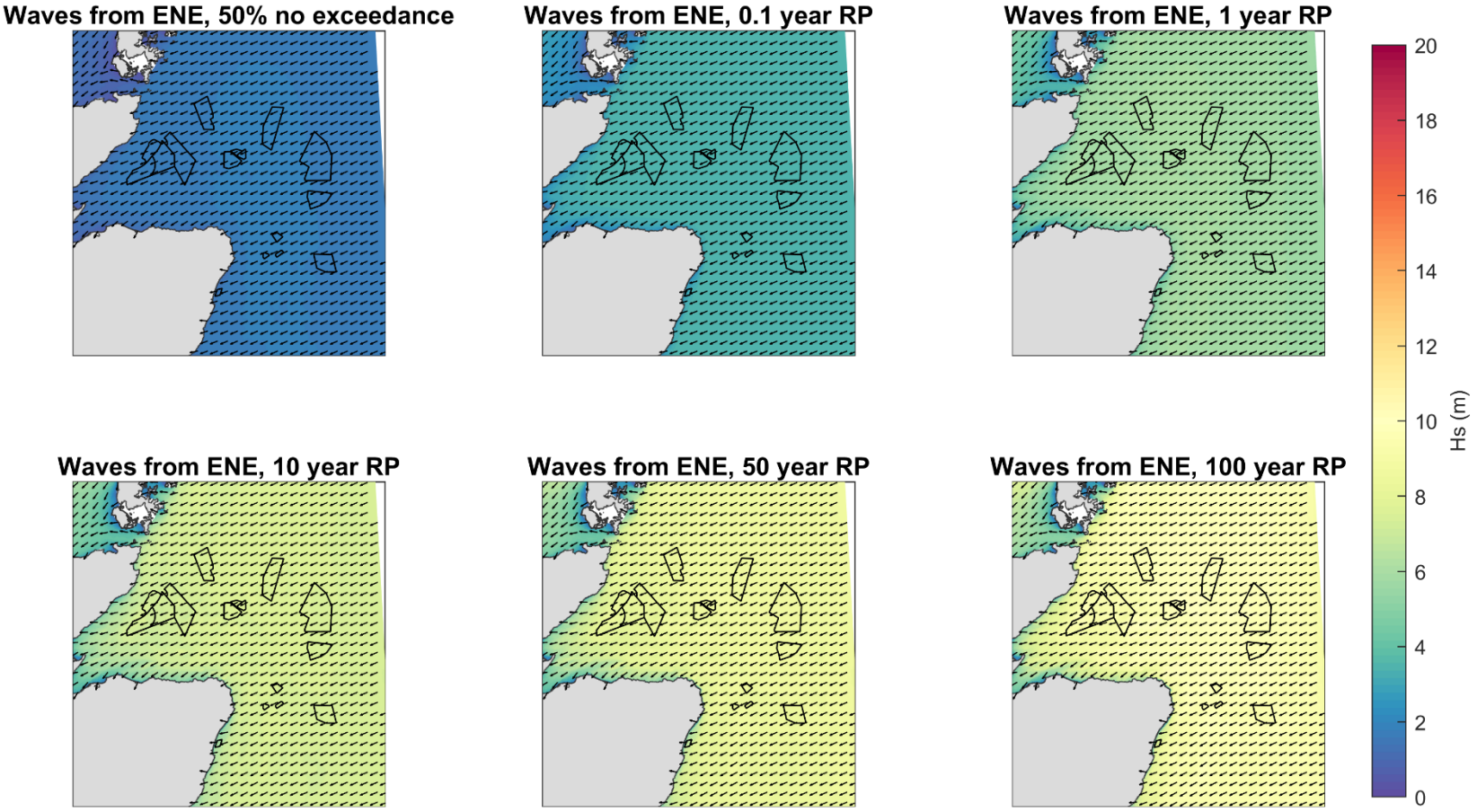

Plate 2.7 Baseline significant wave height, waves from the NE, all return periods

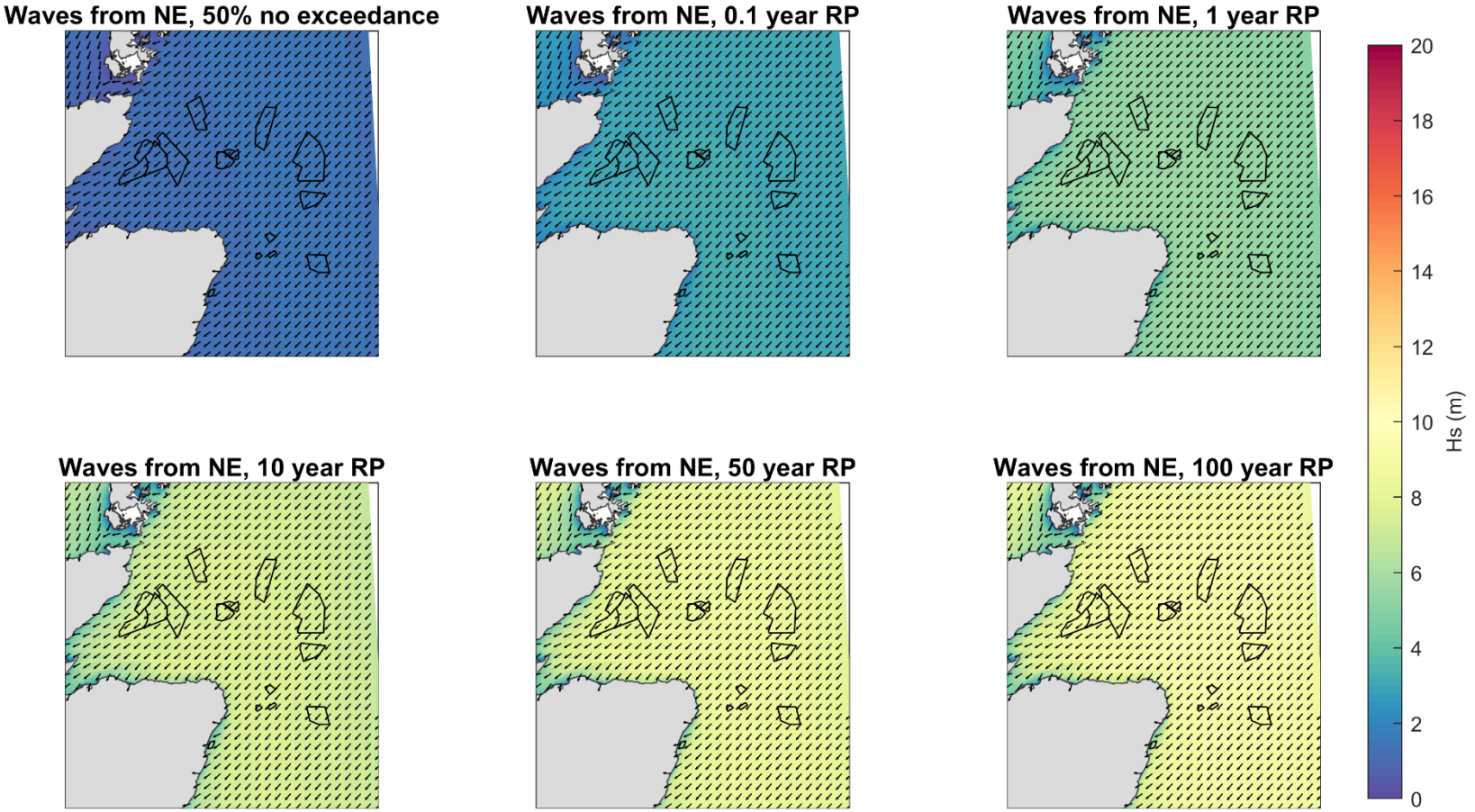

Plate 2.8 Baseline significant wave height, waves from the NNE, all return periods

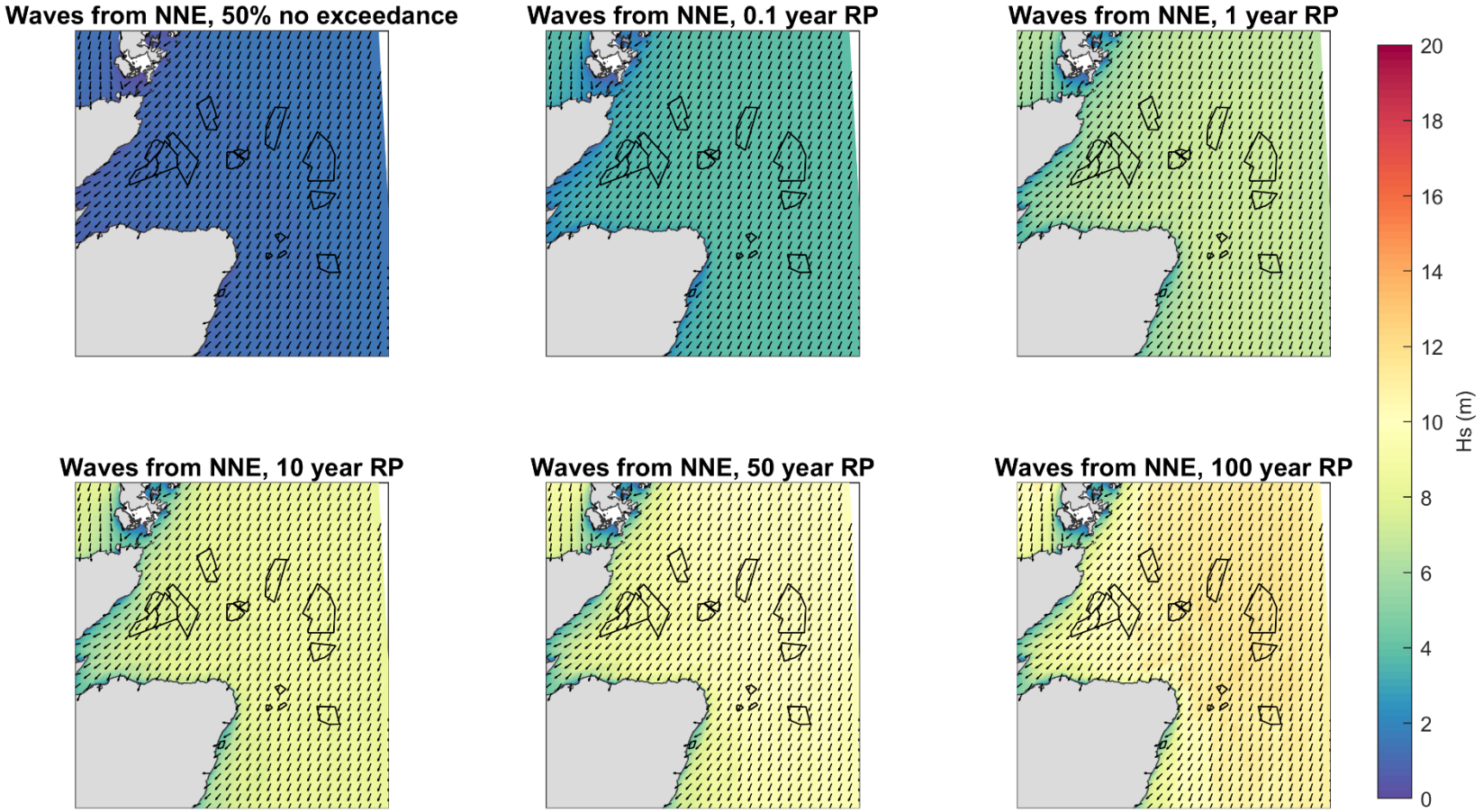

Plate 2.9 Baseline significant wave height, waves from the N, all return periods

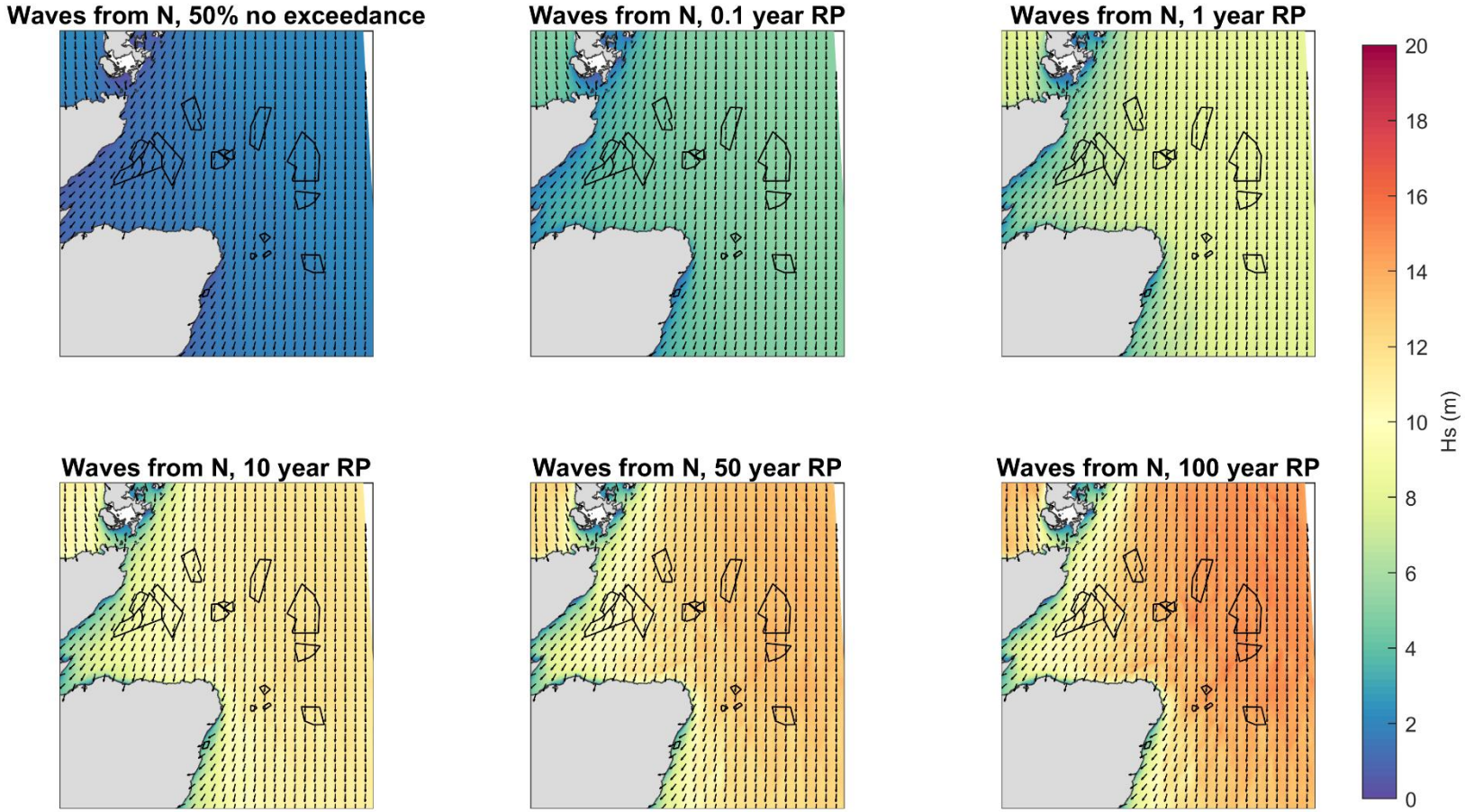

2.4.3 Impact assessment

The Project only

2.4.3.1 Plots showing the spatial distribution of changes to wave height for each of the baseline wave conditions as a result of maximum design scenario for wave blockage for the Project alone are shown in **Plate 2.10** to **Plate 2.14**.

2.4.3.2 Changes less than 5% of the baseline wave height would be indistinguishable from natural variability both within the seastate (difference between individual waves) and compared to normal rates of change (over timescales of one hour or less); such small differences would not be measurable in practice. Changes less than 2.5% are also less than the reasonably expected accuracy of the model and so are excluded from the colour scale.

2.4.3.3 The images show that, due to interaction with consecutive foundations, wave height progressively decreases with distance through the OAA measured in the direction that the waves are traveling. As a result, the maximum reduction in wave height is found downwind of individual wind turbines in the central downwind part of the OAA (15% to 17.5%). Regions of larger relative change (>15%) are restricted to confined areas within or immediately neighbouring the OAA, with the magnitude of change decreasing with distance from the OAA. The majority of the footprint of influence outside the OAA is defined by a reduction of less than 10%.

2.4.3.4 The scale of the change is dependent on the nature of the wave height / period condition, and the main direction of the wave energy with respect to the shape / thickness of the OAA and the alignment of the foundations. The maximum corresponding changes to wave period and wave direction (not shown) are less than 0.1s and 3° respectively, at all locations, in all cases.

2.4.3.5 Wave height begins to recover immediately downwind of the OAA. Recovery occurs mainly due to lateral wave energy spreading from areas to the side of the OAA where waves are less or completely unaffected by interaction with the wind farm. For smaller seastates, recovery of the dominant wave condition can also occur more rapidly as a result of ongoing wind energy input.

2.4.3.6 In the area where changes to wave height are greatest (typically within and immediately to the west through to south of the OAA), water depths are also relatively large (~100mMSL). In such water depths, a minimum wave period (approximately 12s and larger in 100m depth) is required to penetrate deeply enough to cause any water movement at the seabed. Even longer waves in conjunction with a sufficient wave height are needed to cause sufficient motion at the seabed to contribute to sediment transport. As the wave period will not be affected (by more than 0.1s), the ability of individual waves to reach the seabed will be unaffected. The difference is therefore unlikely to result in a measurably different motion of water.

2.4.3.7 Further west and south-west, the water depth progressively decreases towards the coastline and so more / smaller waves may interact with the seabed more strongly and more frequently; however, wave height also recovers rapidly with distance downwind of the OAA and the relative difference in wave height in these shallower areas is even more limited. Differences in wave height are less than 5% in nearshore areas (up to 5km from the coast) and at the adjacent coastlines.

2.4.3.8 For waves coming from the N, where wave pass through the OAA before reaching Turbot Bank NCMPA, no observable difference in wave height is predicted (<5%).

2.4.3.9 For waves coming from the NE, where wave pass through the OAA before reaching the Rosehearty to Fraserburgh Coast Site of Special Scientific Interest (SSSI) and Southern Trench NCMPA, no observable difference in wave height is predicted (<5%).

2.4.3.10 Sediment transport by waves alone in deep water results in a to-and-fro motion with minimal net transport. In conjunction with tidal currents, waves increase the overall rate of sediment transport, but the combined net transport rate and direction is largely controlled by the speed and direction of the coincident tidal current.

2.4.3.11 The differences in wave height, period and direction described above are small in absolute and relative terms and (as a small additional contribution to the tidally dominated transport) could only cause an even smaller change to overall instantaneous sediment transport rates or directions. The differences would not be measurable in practice and are easily within the range of natural variability in wave height from wave to wave, from hour to hour during the passage of a storm, and in the context of seasonal and interannual variation of wave climate.

Plate 2.10 Percentage difference in significant wave height (scheme minus baseline as a proportion of baseline values), waves from the E, all return periods. O&M stage maximum design scenario for the Project

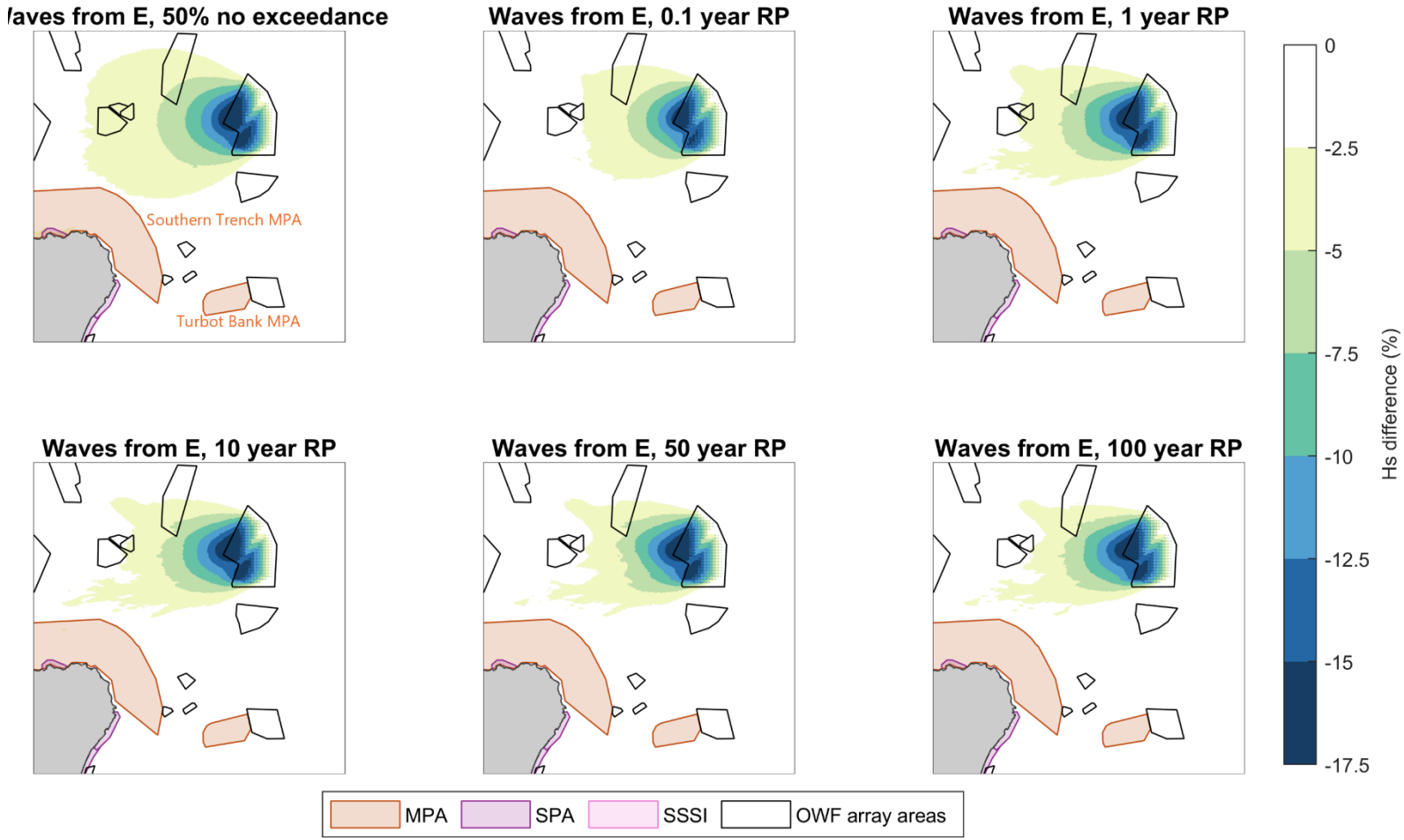

Plate 2.11 Percentage difference in significant wave height (scheme minus baseline as a proportion of baseline values), waves from the ENE, all return periods. O&M stage maximum design scenario for the Project

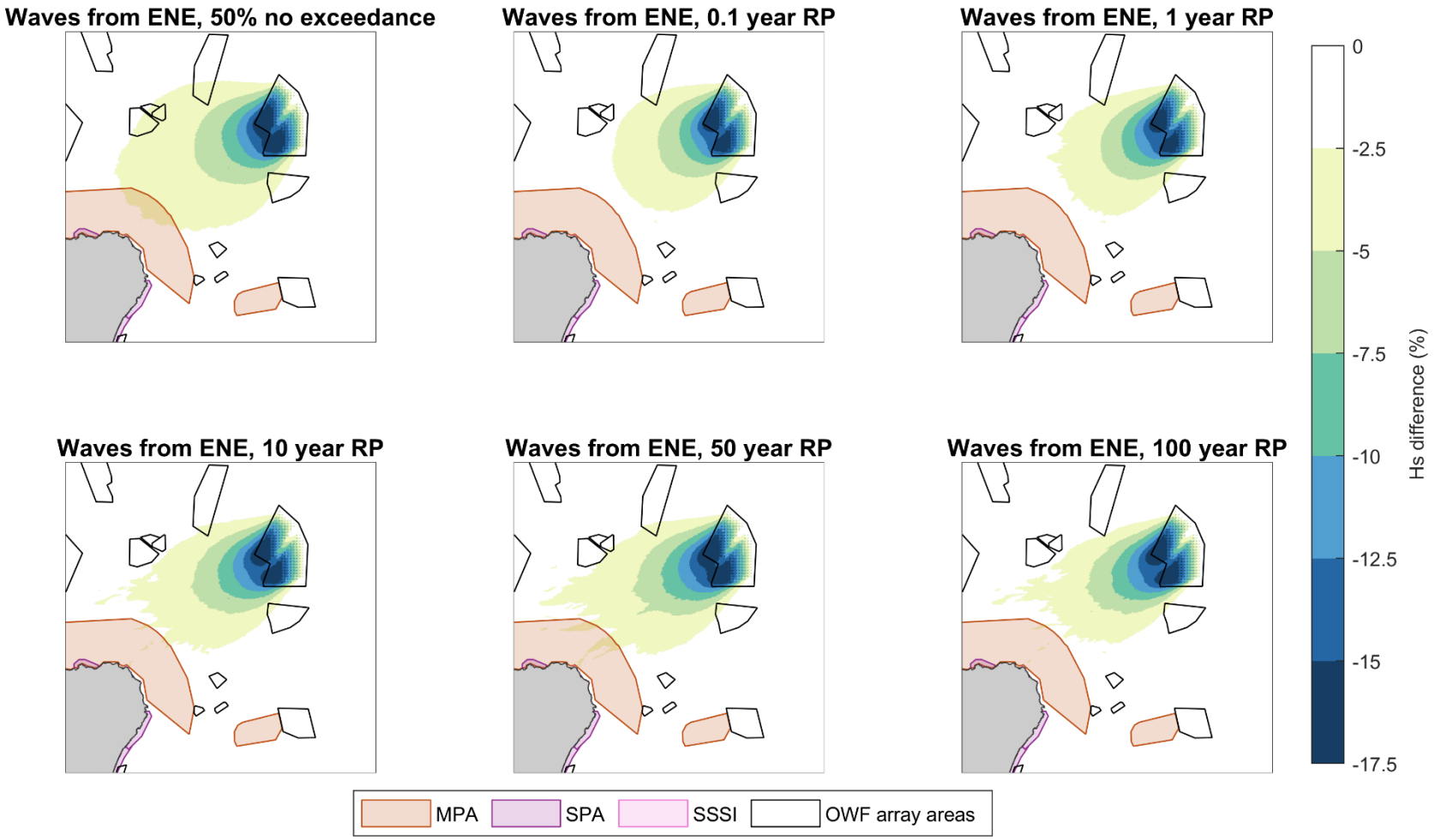

Plate 2.12 Percentage difference in significant wave height (scheme minus baseline as a proportion of baseline values), waves from the NE, all return periods. O&M stage maximum design scenario for the Project

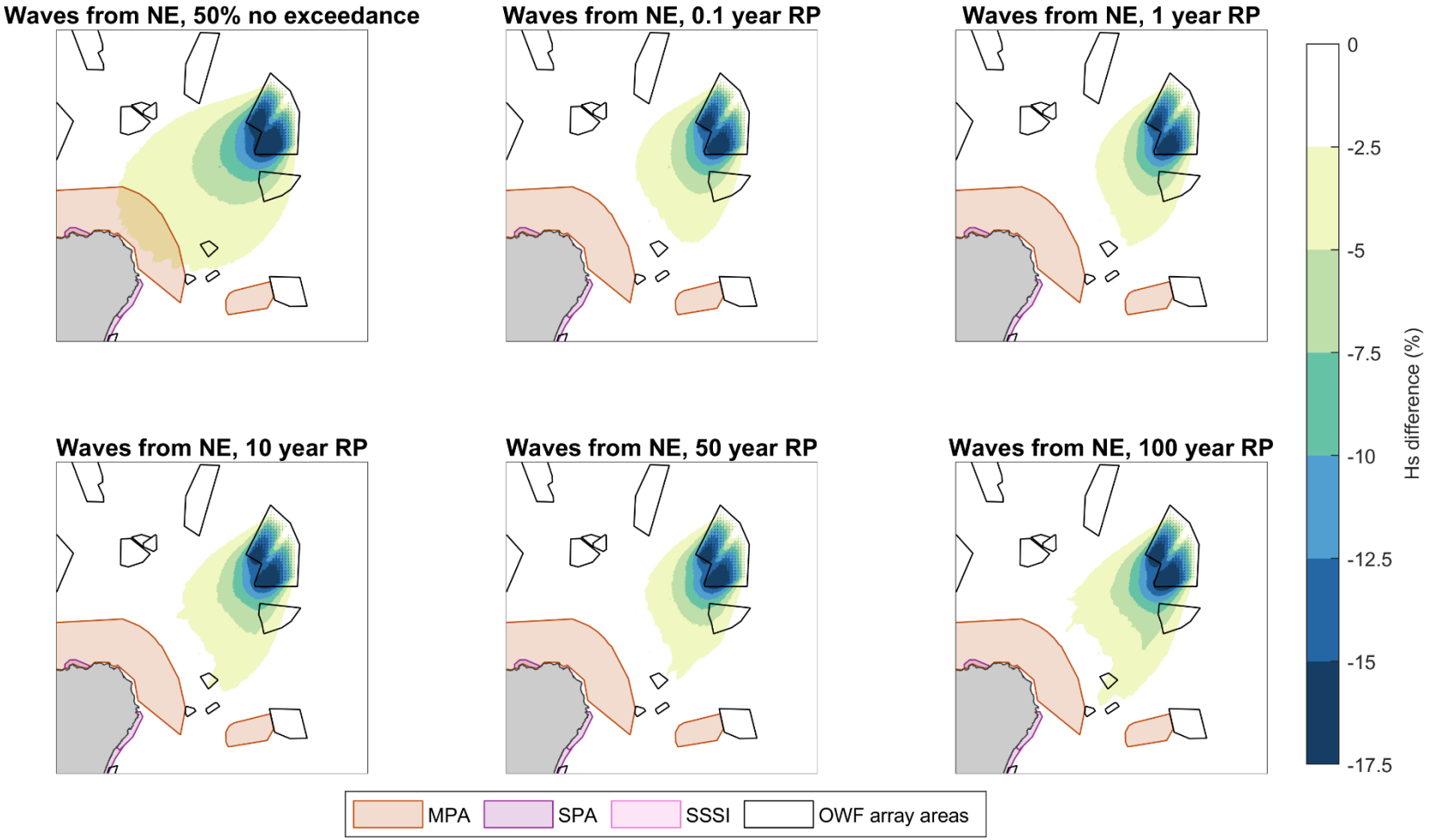

Plate 2.13 Percentage difference in significant wave height (scheme minus baseline as a proportion of baseline values), waves from the NNE, all return periods. O&M stage maximum design scenario for the Project

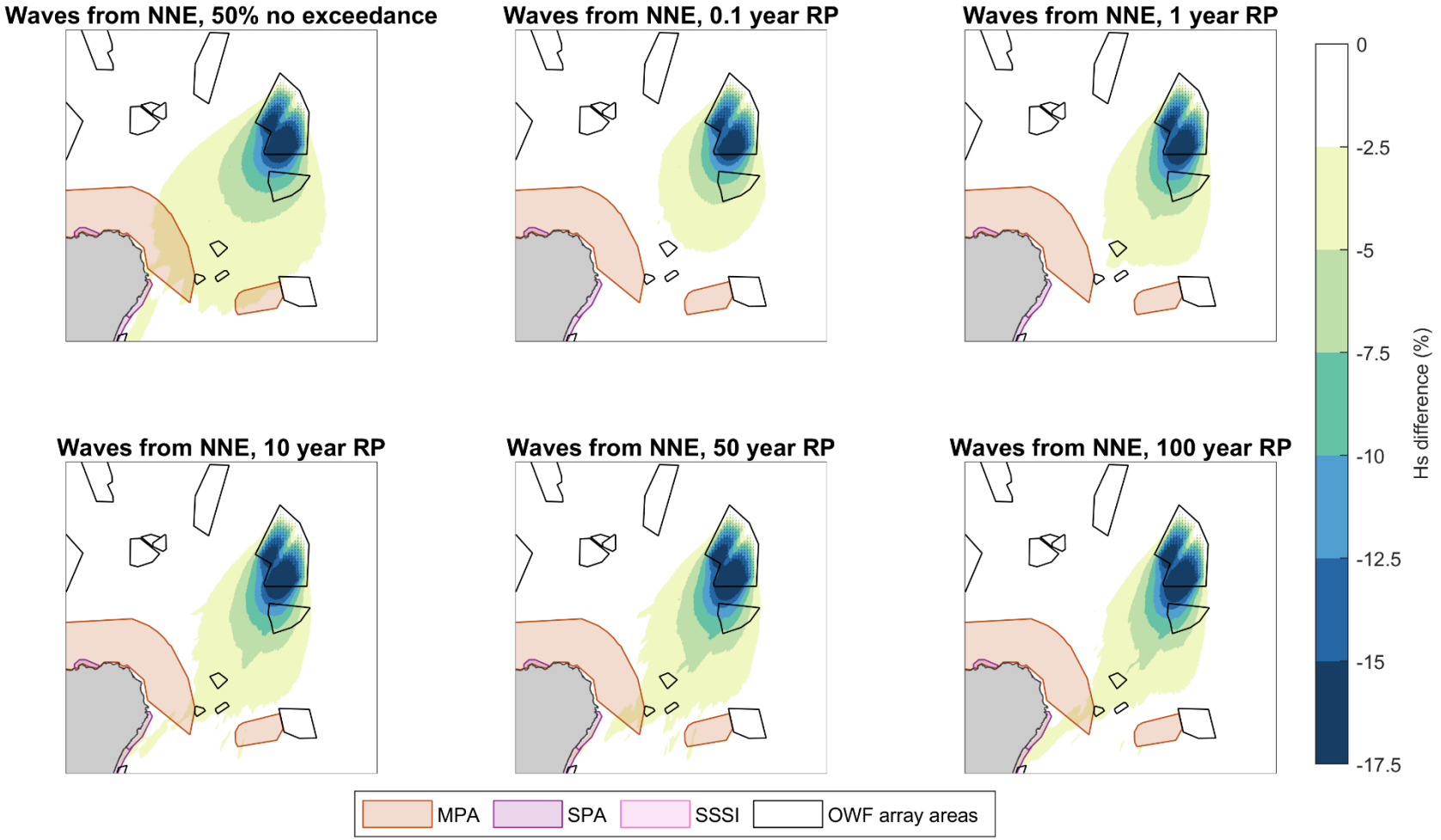

Plate 2.14 Percentage difference in significant wave height (scheme minus baseline as a proportion of baseline values), waves from the N, all return periods. O&M stage maximum design scenario for the Project

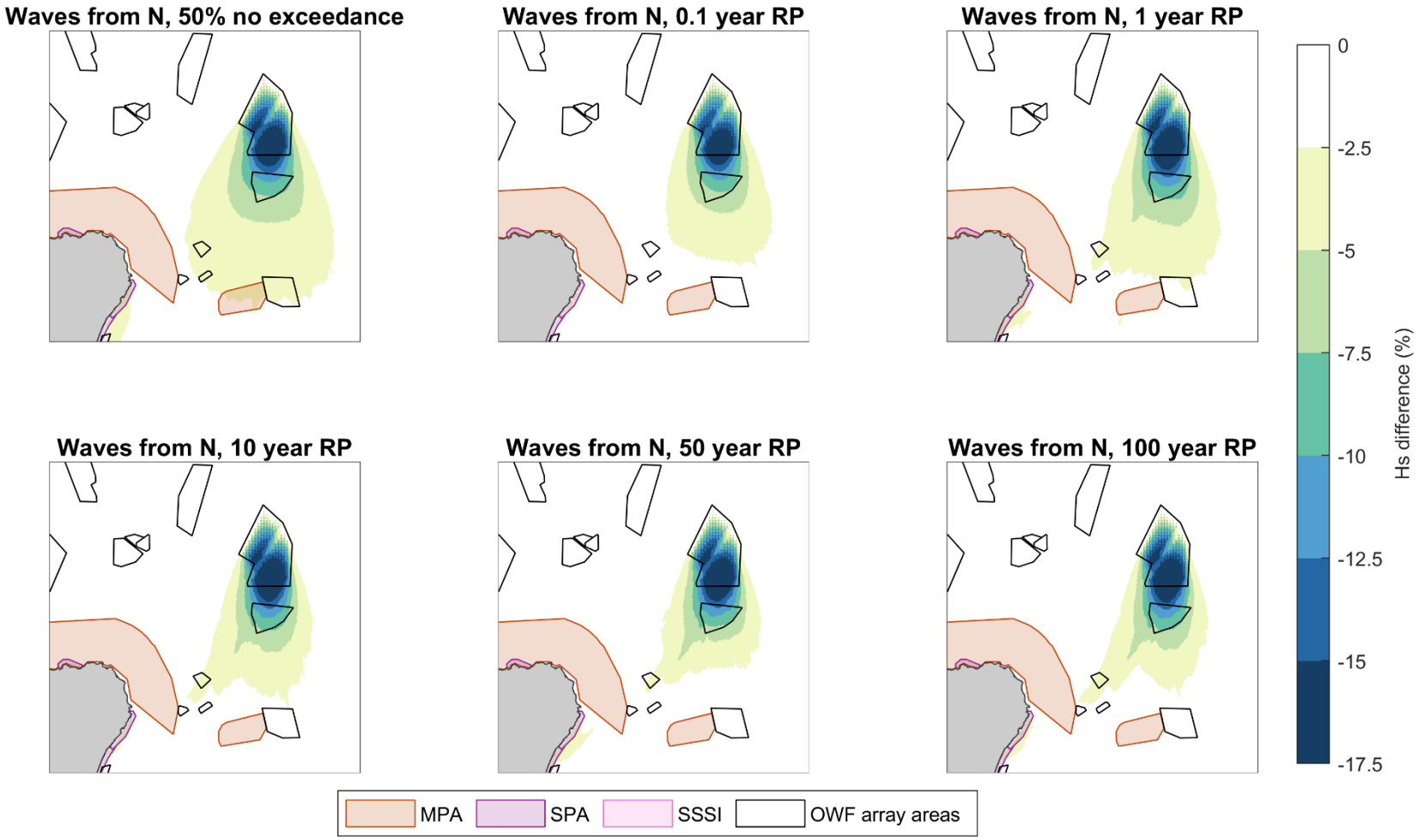

The Project and other offshore windfarms

2.4.3.12 Plots showing the spatial distribution of changes to wave height for each of the baseline wave conditions as a result of maximum design scenario foundation type, number and layout for the Project, alongside operational and planned neighbouring offshore wind farms are shown in **Plate 2.15** to **Plate 2.19**.

2.4.3.13 Changes less than 5% of the baseline wave height would be indistinguishable from natural variability both within the seastate (difference between individual waves) and compared to normal rates of change (over timescales of one hour or less); such small differences would not be measurable in practice. Changes less than 2.5% are also less than the reasonably expected accuracy of the model and so are excluded from the colour scale.

2.4.3.14 The images show that, due to interaction with consecutive foundations, wave height progressively decreases with distance through the individual OAAs measured in the direction that the waves are travelling.

2.4.3.15 Cumulative differences in wave height are less than 5% in most nearshore areas and coastlines. With some regions of up to 7.5% reductions where the coastline aligns with the wave direction passing through multiple offshore wind farms.

2.4.3.16 The maximum corresponding changes to wave period and wave direction (not shown) are less than 0.1s and 3° respectively, at all locations, in all cases.

2.4.3.17 For waves originating from the N, which travel through multiple OAAs (the Project, Green Volt, Hywind Scotland Pilot Park, Flora, Buchan, Salamander, and Muir Mhòr) before reaching the Turbot Bank NCMPA, the modelling predicts a maximum wave height reduction of up to 7.5% within the designated area. This occurs only under the 50% non-exceedance sea state. For all other sea states, wave heights recover quickly with distance from the arrays, resulting in no observable cumulative change in wave height within the NCMPA (reductions remain below 5%).

2.4.3.18 For waves coming from the NE, passing through multiple OAAs (Buchan, Broadshore, Sinclair, Scaraben, and Caledonia), before reaching the Rosehearty to Fraserburgh Coast SSSI and Southern Trench NCMPA, the modelling predicts a maximum wave height reduction of up to 7.5% within the designated areas. This occurs only under the 50% non-exceedance sea state. For all other sea states, wave heights recover quickly with distance from the arrays, resulting in no observable cumulative change in wave height within the NCMPA (reductions remain below 5%).

Plate 2.15 Percentage cumulative difference in significant wave height (scheme minus baseline as a proportion of baseline values), waves from the E, all return periods. O&M stage maximum design scenario for the Project and neighbouring offshore wind farms

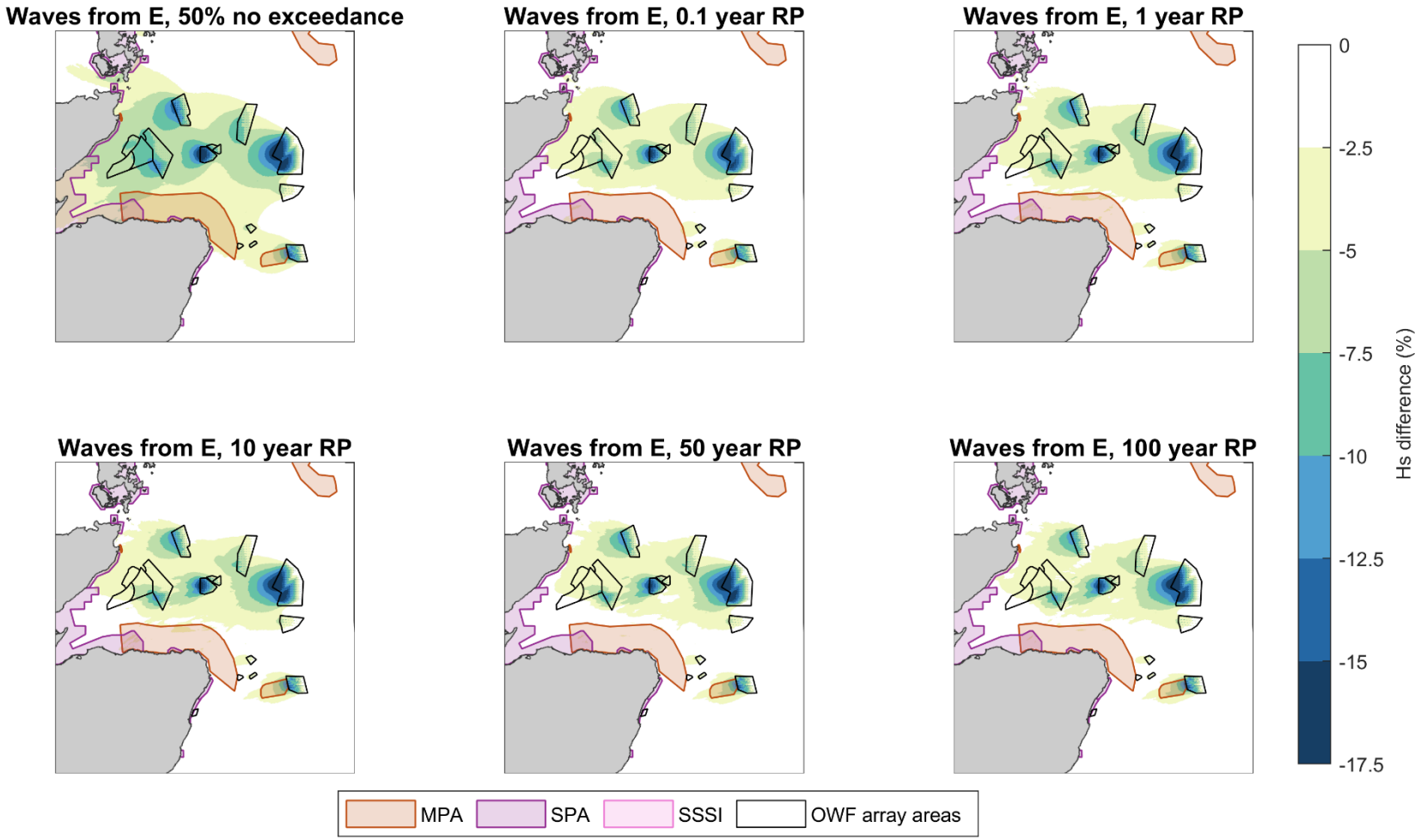

Plate 2.16 Percentage cumulative difference in significant wave height (scheme minus baseline as a proportion of baseline values), waves from the ENE, all return periods. O&M stage maximum design scenario for the Project and neighbouring offshore wind farms

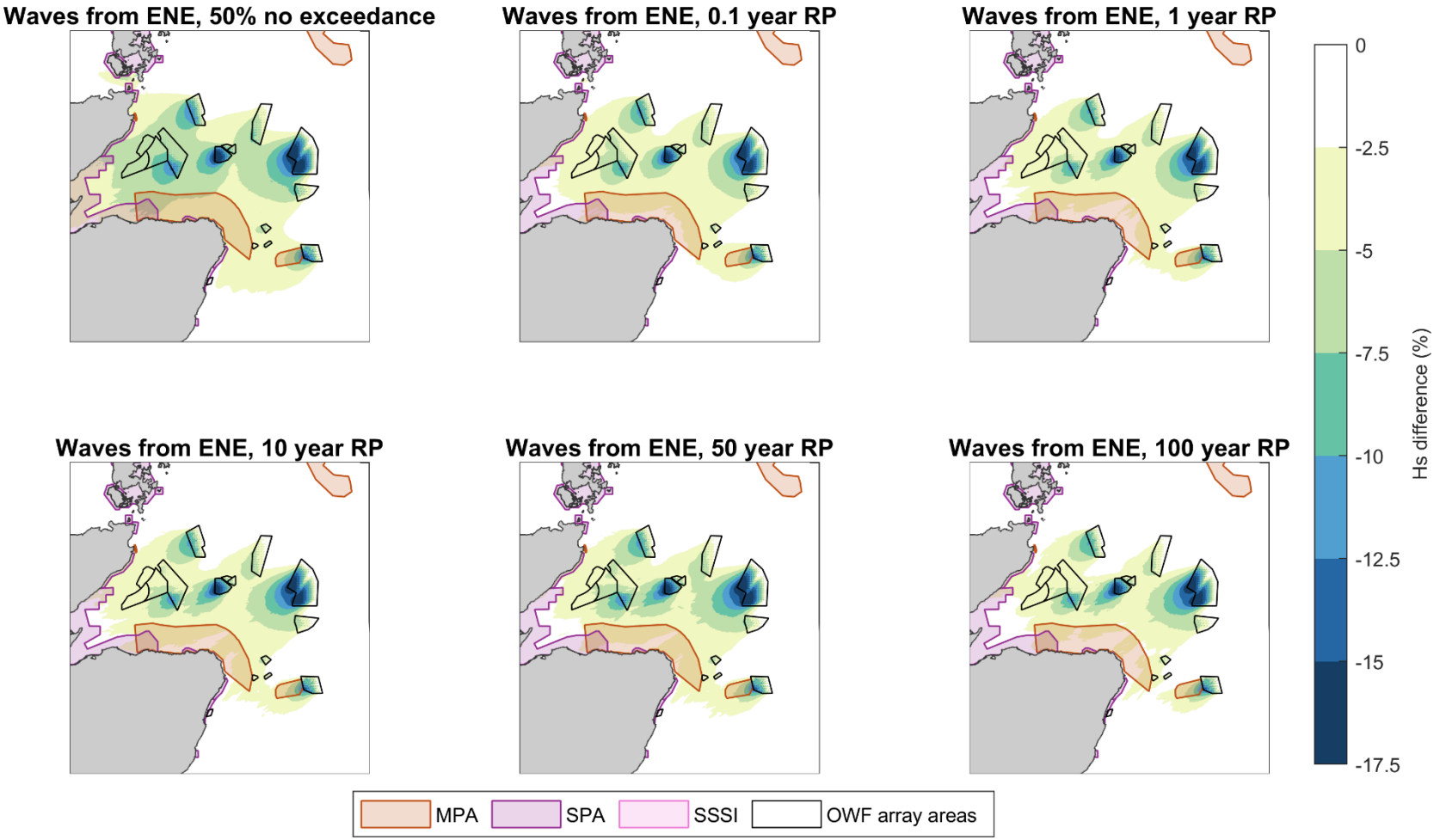

Plate 2.17 Percentage cumulative difference in significant wave height (scheme minus baseline as a proportion of baseline values), waves from the NE, all return periods. O&M stage maximum design scenario for the Project and neighbouring offshore wind farms

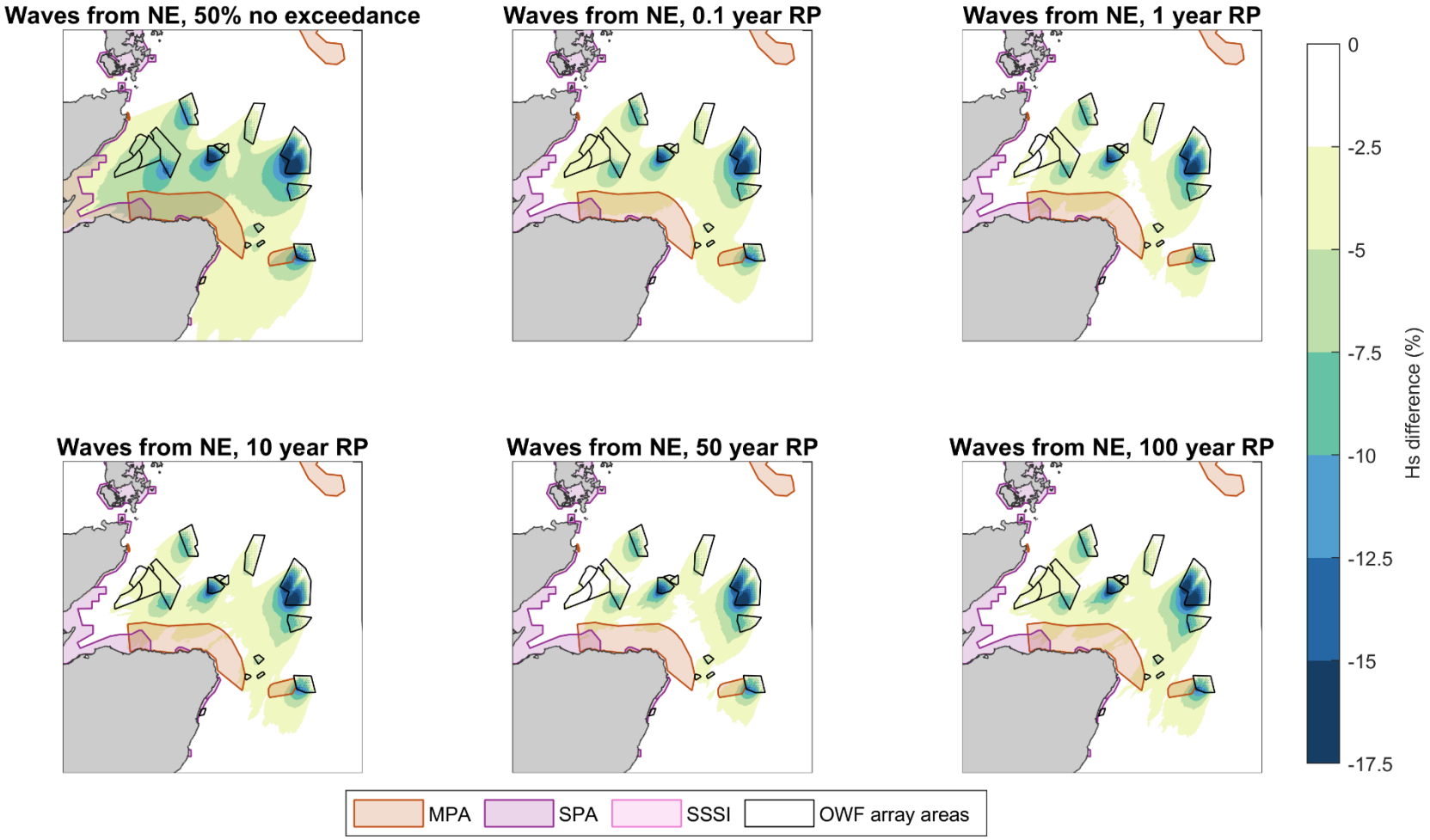

Plate 2.18 Percentage cumulative difference in significant wave height (scheme minus baseline as a proportion of baseline values), waves from the NNE, all return periods. O&M stage maximum design scenario for MarramWind and neighbouring offshore wind farms

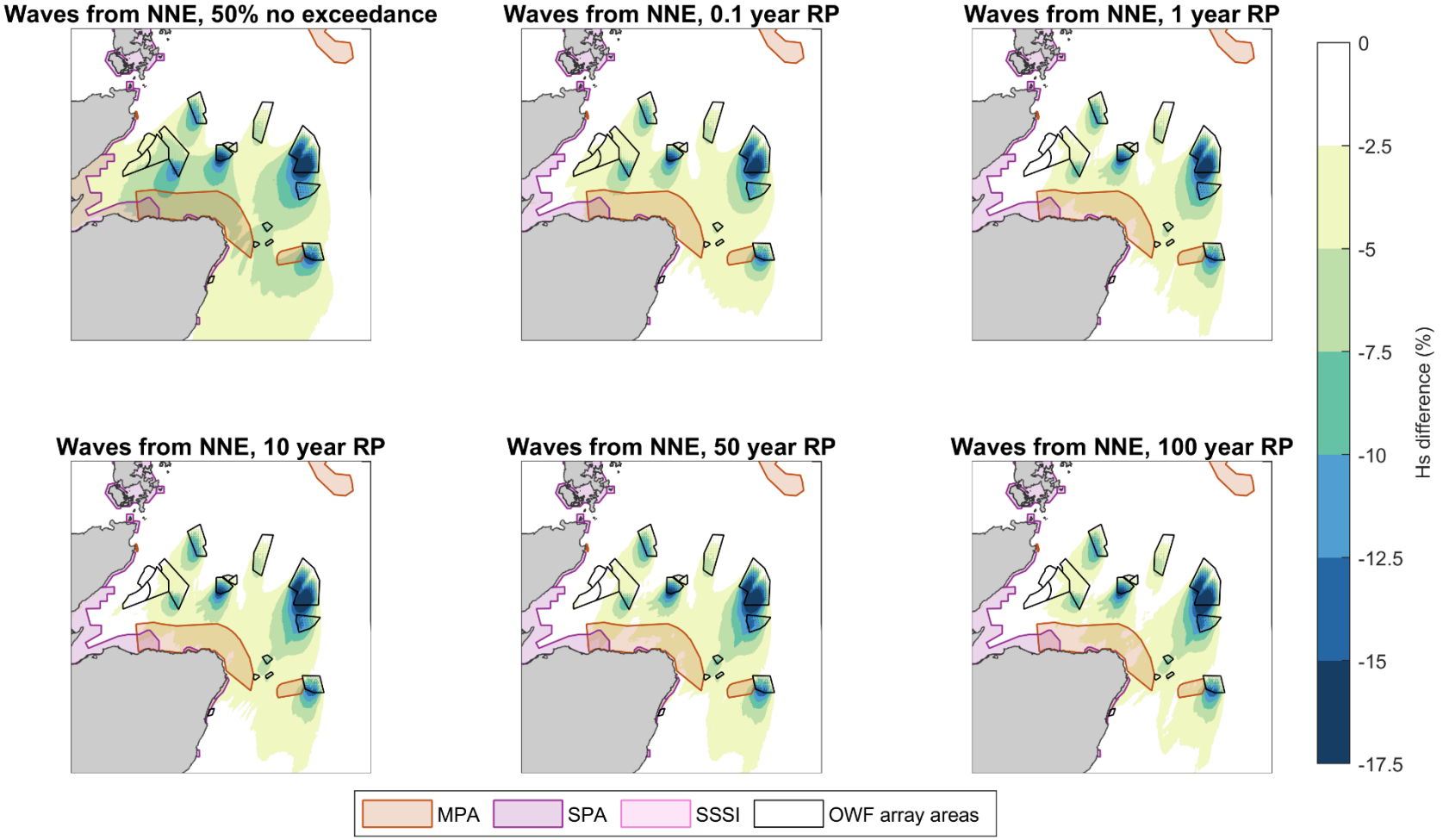

Plate 2.19 Percentage cumulative difference in significant wave height (scheme minus baseline as a proportion of baseline values), waves from the N, all return periods. O&M stage maximum design scenario for the Project and neighbouring offshore wind farms

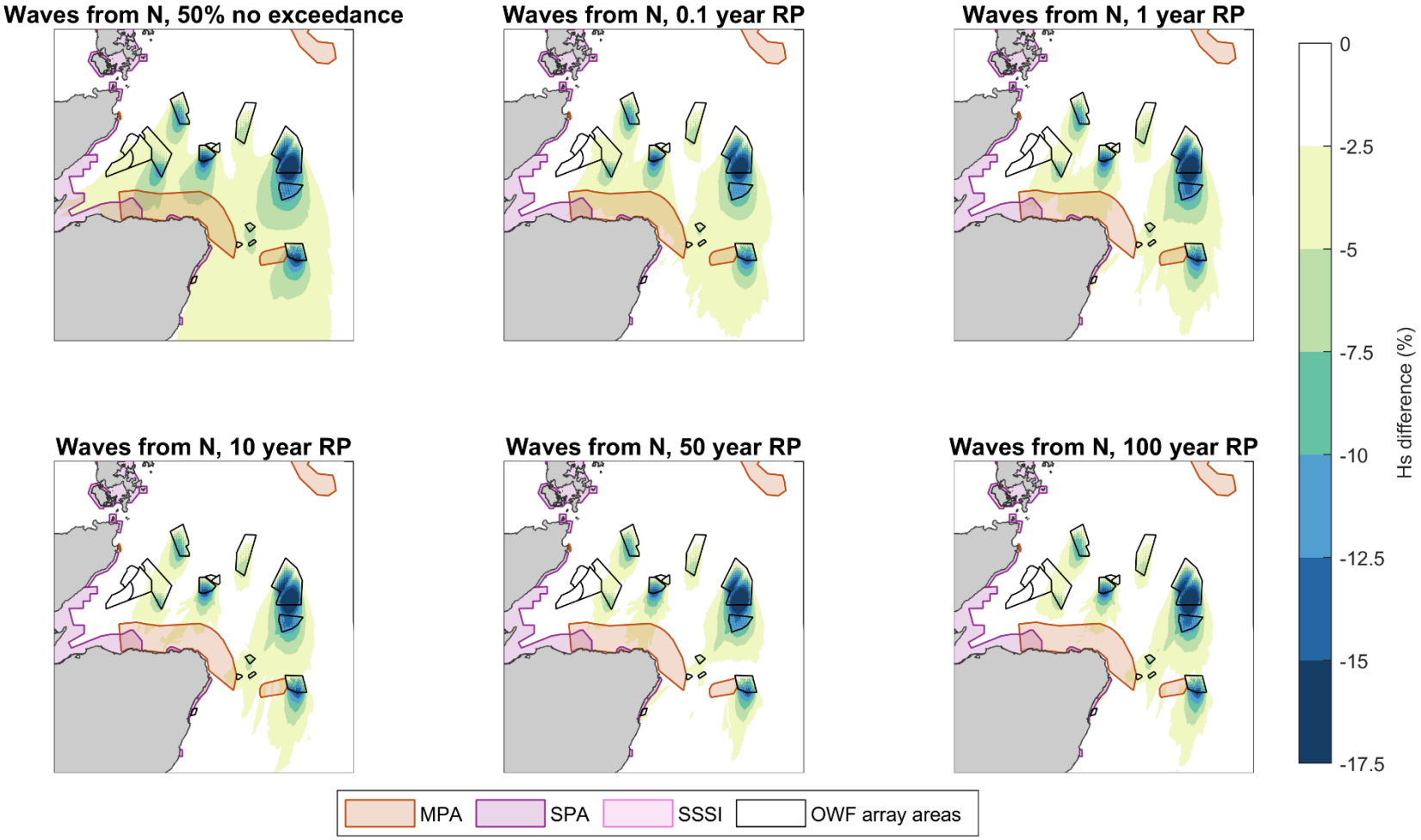

2.5 Summary

2.5.1.1 Wave modelling has been undertaken to characterise the impact of the Project on the wave regime (wave height, period and direction). Cumulative impacts with neighbouring operational / proposed offshore wind farms have also been separately assessed. The wave model was built using DHI's (2025) MIKE21FM SW module, simulating specific wind / wave events for a representative range of selected 'every day' and extreme wave conditions (return periods and directions). To simulate a realistic worst-case blockage scenario for waves, a maximum design scenario blockage width was applied to sub-grid scale model structures representative of the maximum number of WTGs, offshore substations and RCPs.

2.5.1.2 Model results show that wave height (a measure of wave energy) progressively decreases with distance of travel through the OAA, due to the cumulative local blockage effect of the individual foundations. As a result, the maximum reduction in wave height is found downwind of individual foundations in the central downwind part of the OAA (15% to 17.5%). The maximum corresponding changes to wave period and wave direction of the seastates tested are less than 0.1s and 3° respectively. Wave height begins to naturally recover (through lateral spreading of wave energy, and ongoing wind energy input) immediately downwind of the OAA, meaning the magnitude of change progressively decreases (recovers towards baseline conditions) with distance downwind of the OAA. No observable difference in wave height is predicted (<5%) from the Project alone in the designated area within the vicinity of the Project (for example, Turbot Bank NCMPA, Rosehearty to Fraserburgh Coast SSSI and Southern Trench NCMPA).

3. Stratification and Frontal Systems

3.1.1.1 This Section outlines the methods and findings of the assessment of the Project's impact during the O&M stage on stratification and frontal systems in the northern North Sea - a region typically characterised by seasonal water column stratification.

3.2 Introduction

3.2.1.1 There has been increasing interest in the scientific literature on the impact of wind farm developments on stratification, (for example, Carpenter *et al*., (2016); Cazenave *et al*., (2016); Dorrell *et al.,* (2022)). This interest has been driven at least in part by the proliferation of proposed floating offshore wind farms: these projects are generally located further offshore and in deeper water than fixed bottom projects and it is these settings which are characterised by seasonal water column stratification (**Plate 3.1**), and which could therefore potentially be impacted by the installation of wind farm infrastructure (**Plate 3.2**).

Plate 3.1 Northwest Europe Summer Potential Energy Anomaly (PEA), φ, a measure of the amount of stratification, calculated from Copernicus model output. Black circle denotes location of the OAA

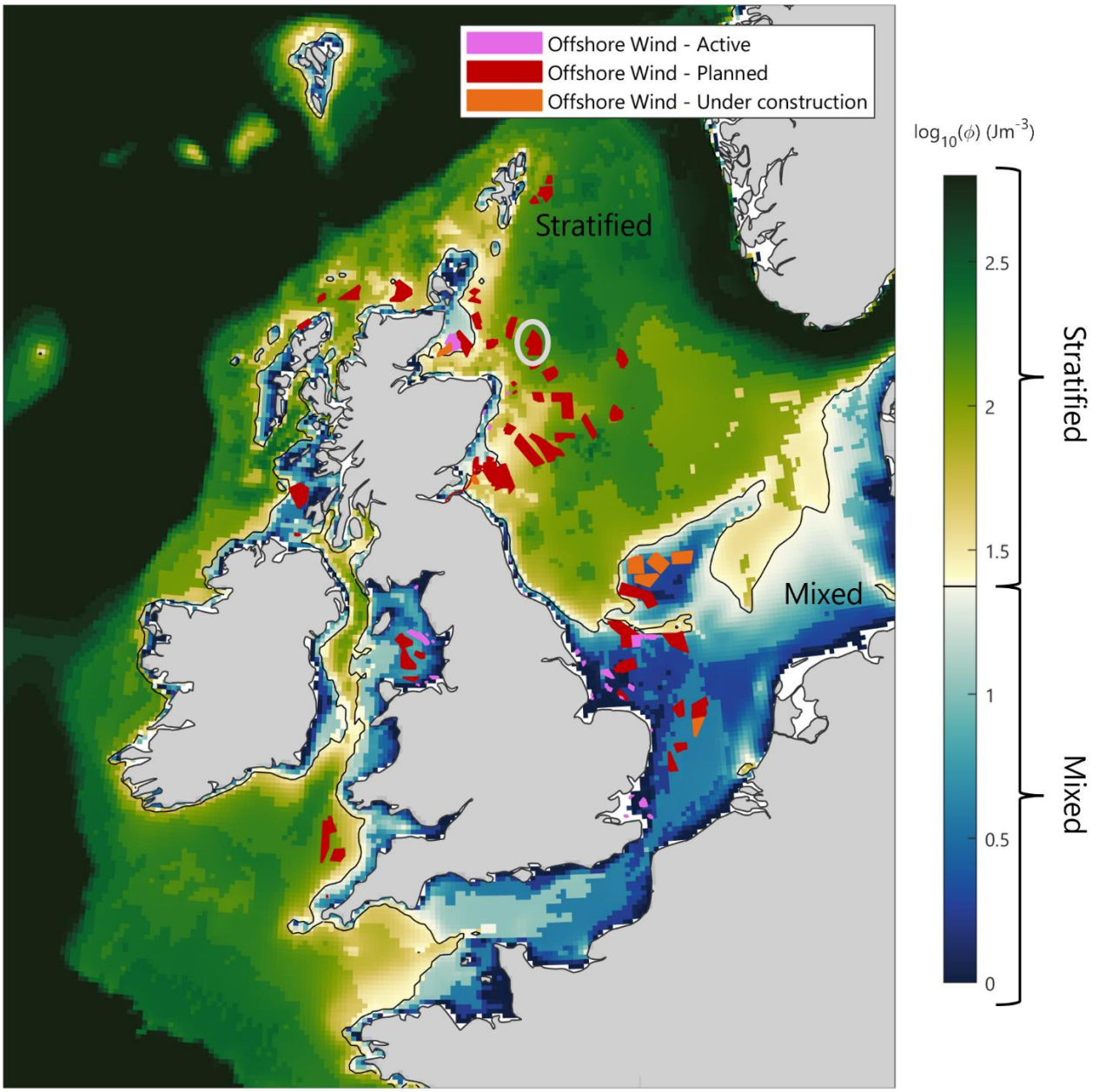

3.2.1.2 Turbulence is generated naturally as a result of near-bed and near-surface shear. The installation of offshore infrastructure creates an additional source of turbulence through flow-structure induced shear, as illustrated in the schematic in **Plate 3.2**. Infrastructure wake turbulence mixes cold nutrient rich bottom water with warm nutrient poor surface water, reducing the strength of stratification and potentially enhancing plankton growth in the subsurface chlorophyll layer. Changes in the subsurface chlorophyll layer would have further impacts on nutrient pathways, ecosystem functioning and oceanic carbon sequestration.

Plate 3.2 Processes contributing to natural stratification, and the effect of additional turbulence generated by offshore infrastructure (from Dorrell *et al.,* 2022)

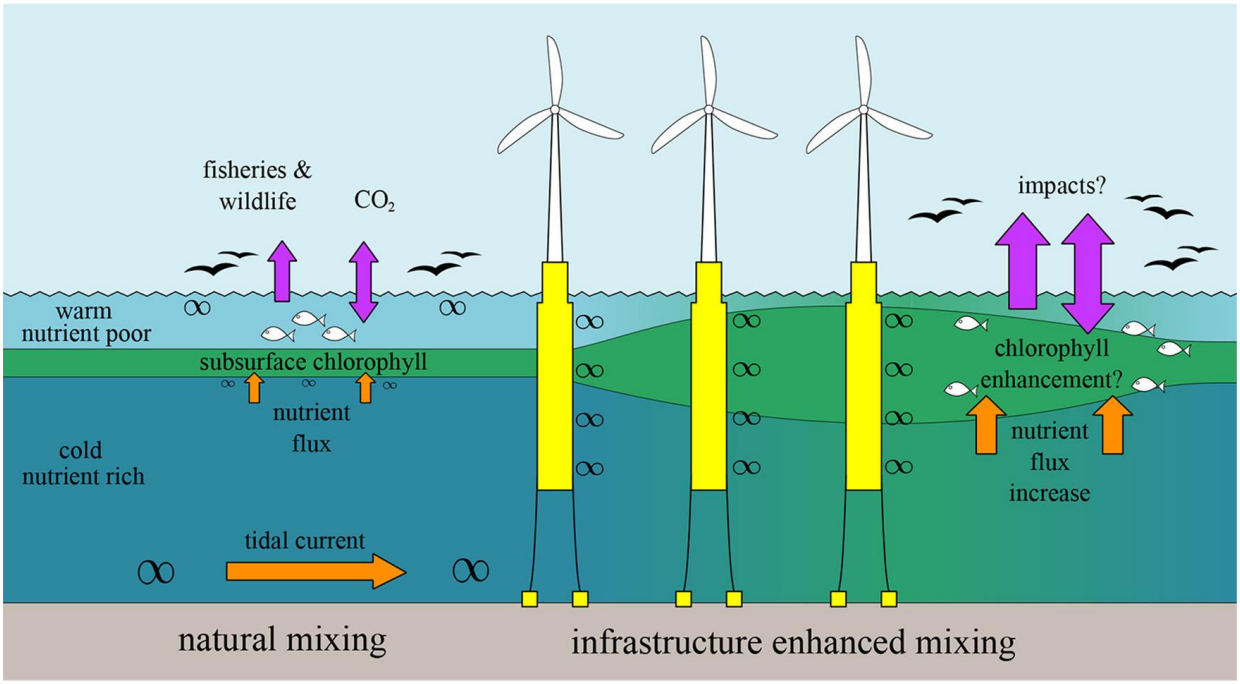

3.2.1.3 The WTG floating unit type for the Project will differ from the spar buoy type shown in the schematic. Instead, semi-submersible or tension-leg platform foundations, which sit higher in the water column, will be used. Nonetheless, turbulence will still be generated as water flows past these structures, following processes similar to those illustrated.

3.3 Methods

3.3.1 Baseline conditions

3.3.1.1 The baseline understanding of the existing temporal / spatial pattern of stratification and positioning of tidal mixing fronts has been developed using readily available three-dimensional numerical model outputs from Copernicus Marine Service (Copernicus, 2024a; 2024b).

3.3.1.2 Temperature, salinity and chlorophyll-a reanalysis datasets across the Northwest European Shelf were generated by integrating past observations from satellites and in situ measurements with coupled physical-biogeochemistry model systems. This dataset provides timeseries from 2010 to 2024, at a 7km horizontal resolution and over 24 standard Intergovernmental Oceanographic Commission geopotential levels, concentrated in the upper 200m of the water column. A detailed description of the model production, calibration and validation is available in Tonani *et al*. (2022) and Ciavatta *et al*. (2018) for the physical and biogeochemical models, respectively.

3.3.1.3 The use of Copernicus reanalysis data allowed for a detailed examination of spatial and temporal variability over a range of scales, from broader seasonal and inter-annual changes to shorter term fluctuations occurring over a tidal cycle. Vertical temperature and salinity profiles facilitated the calculation of density profiles, which were used to assess stratification strength through the PEA. Chlorophyll-a profiles served as a proxy for primary productivity

(PP), with elevated concentrations often indicating increased productivity linked to the onset of stratification or the positioning of tidal mixing fronts.

3.3.2 Impact assessment

3.3.2.1 To assess the impact of offshore infrastructure on water column mixing and stratification, the method outlined by Carpenter *et al*. (2016) was used. This approach uses empirical equations to estimate two key timescales: the mixing timescale, which predicts the time required for complete mixing of stratified layers due to increased Turbulent Kinetic Energy (TKE) generated by flow past the foundation structures, and the advective timescale, which quantifies how long a water parcel remains within the OAA, experiencing enhanced TKE. These estimates provide insight into the influence of offshore infrastructure on local stratification.

3.3.2.2 One-dimensional depth-profile models, such as the General Ocean Turbulence Model (GOTM), could offer a more detailed analysis of mixing processes within a limited distance of individual foundations within the OAA. However, the absence of sufficient measured data for model validation poses a significant challenge, limiting the usefulness of the results. A one-dimensional modelling approach would not provide a suitably realistic description of the two or three-dimensional result of localised turbulent interaction between the flow and individual foundations in an array of widely spaced foundations, and where water passing through the OAA may or may not be repeatedly affected. Whilst a bespoke model might be theoretically possible, the extensive effort required to develop, calibrate / validate, and implement such a model would be disproportionate to the findings.

3.4 Results

3.4.1 Baseline conditions

Overview

3.4.1.1 Stratification is a naturally occurring seasonal hydrodynamic process related to the vertical and horizontal distribution of seawater temperature and salinity. Where present, stratification plays a key role in nutrient availability and the distribution of marine flora and fauna (Simpson and Sharples, 2012).

3.4.1.2 During summer, solar heating and higher air temperatures warm the surface waters, creating a marked temperature difference between the warmer, buoyant upper layer and the colder, denser bottom waters. In the North Sea, this temperature difference can reach up to 10 degrees Celsius (C), forming a sharp vertical density gradient, or pycnocline, which acts as a physical barrier to vertical mixing. This separation limits the upward transport of nutrients from deeper waters, which can limit PP in surface waters as nutrients become depleted over time.

3.4.1.3 The development of stratification is counterbalanced by turbulent mixing, which is generated at the seabed by tidal currents and at the surface by wind and wave action. Consequently, stratification is more likely to form in deeper waters but can also occur in shallower areas with low current speeds and limited wind exposure. The interplay between these forces determines whether stratification will persist or break down, affecting the overall productivity of the ecosystem.

3.4.1.4 Tidal mixing fronts form at the boundaries between well-mixed and stratified waters, creating regions of enhanced biological activity. These fronts, common in shelf seas like the North Sea (Hill and Cota, 2005; *Hill et al.,* 2008), facilitate nutrient exchange between

surface and deeper layers, promoting PP through the stimulation of phytoplankton growth. Fronts act as biological hotspots, concentrating nutrients and attracting higher trophic levels, making them important features for fisheries and marine biodiversity. The strength and position of these fronts are influenced by factors such as tidal current speeds, freshwater inputs, and wind patterns, which can vary on timescales ranging from hours to years.

3.4.1.5 The North Sea is characterised by significant spatial and temporal variation in the vertical distribution of temperature and salinity. An assessment of intra-annual patterns of stratification in the North Sea has been undertaken by van Leeuwen *et al*. (2015), using a long term (51 year) regional scale hydro-biogeochemical model simulation. The OAA is located in an area described by van Leeuwen *et al*. (2015) as being "*seasonally stratified*", defined as >120 days in the year where the water column is stratified and <90 days in the year where the water column is fully mixed.

Stratification

3.4.1.6 The PEA provides a measure of the amount of energy per unit volume (J/m^3) required to completely mix a stratified water column, making density vertically homogenous. The significance of PEA lies in its ability to provide a single, scalar value that captures the complexity of stratification in terms of both temperature and salinity gradients. It is widely used in oceanography to assess the strength of stratification in a water body, for example Simpson (1981); Gowen *et al*. (1995); Yamaguchi *et al*. (2019) and Dorell *et al*. (2022).

3.4.1.7 PEA (ϕ) is calculated as:

$$\phi = \frac{g}{h} \int_{-h}^{0} (\rho - \bar{\rho})\, z \cdot dz$$

3.4.1.8 Where h is the water depth, g is acceleration due to gravity (9.81 metres per second squared (m/s^2)), ρ is the water density and $\bar{\rho}$ is the density calculated using the depth-mean water temperature and salinity. To calculate water density, the Gibbs SeaWater Matlab toolbox is used alongside three-dimensional temperature and salinity data available from the Copernicus reanalysis dataset.

3.4.1.9 The threshold values of PEA can vary depending on the specific water body. Based on the density profiles and calculated PEA values for the physical processes study area and its surrounding regions, along with thresholds used in the literature (Gowen *et al*., 1995; Dorrell *et al*., 2022), the following PEA classifications are applied in this study:

- mixed water column: ϕ < 25 joules per cubic metre (J/m³);
- weakly stratified water column: 25J/m³ ≤ ϕ < 50J/m³;
- moderately stratified water column: 50J/m³ ≤ ϕ < 100J/m³; and
- strongly stratified water column: ϕ > 100J/m³.

3.4.1.10 PEA values were calculated for the physical processes study area and its surrounding region at monthly intervals, from January 2010 to December 2023. This approach enabled the assessment of both seasonal and inter-annual variability in stratification strength.

3.4.1.11 There is variability in the strength of summer stratification from year to year, with mid-summer PEA values ranging from approximately 130J/m³ in 2015 to approximately 170J/m³ in 2014 (**Plate 3.3**).

Plate 3.3 Monthly PEA (ϕ) values, based on the Copernicus Reanalysis monthly temperature and salinity data, in the OAA from 2010 to 2023

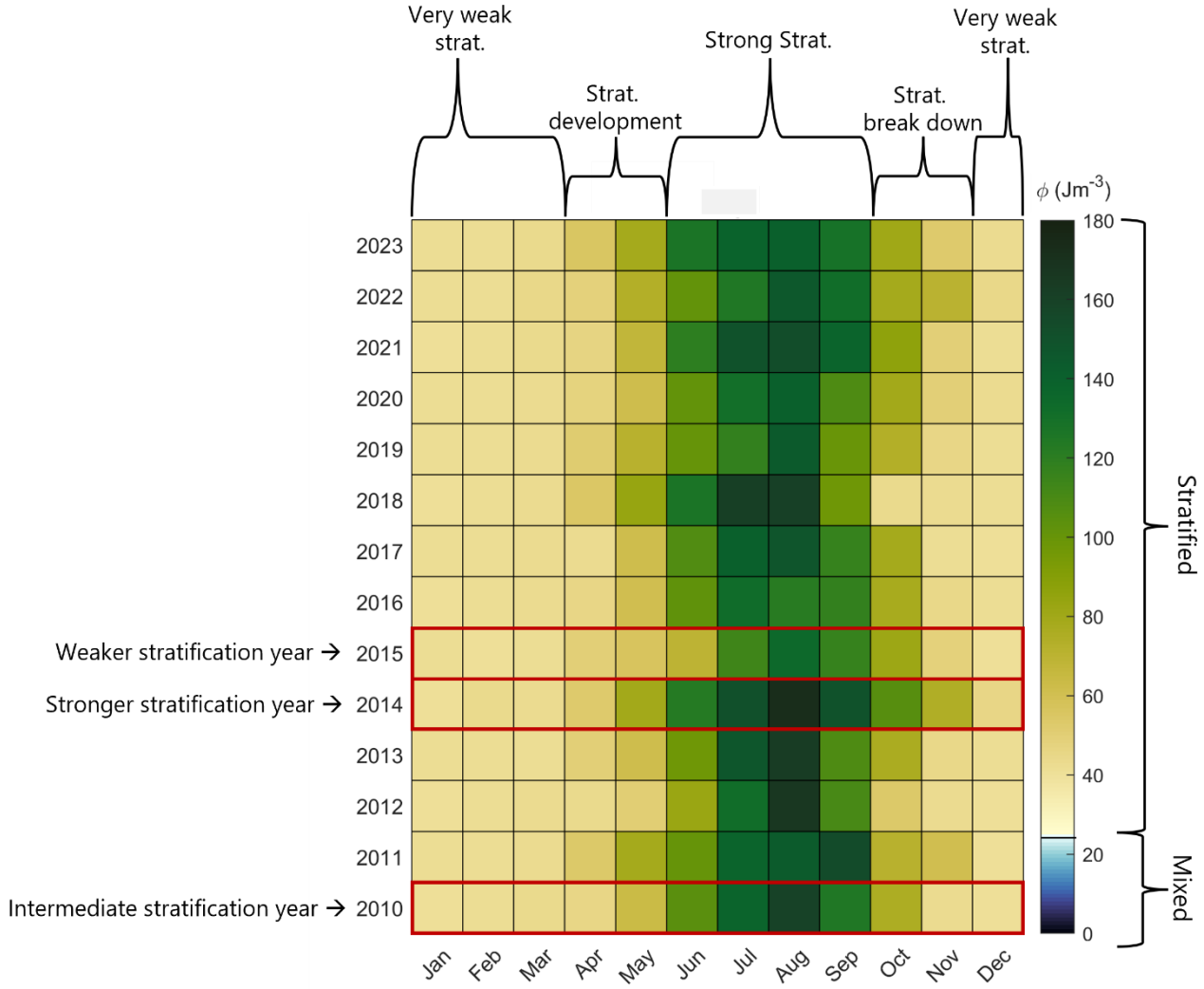

3.4.1.12 **Plate 3.4, Plate 3.5** and **Plate 3.6** illustrate the results for three specific years, 2014, 2010 and 2015, representing years with stronger stratification, intermediate stratification and weaker stratification, respectively. In the figures, seas are partitioned into those defined as mixed (ϕ<25J/m^3) and stratified (ϕ≥25J/m^3).

3.4.1.13 During the winter months (November to April), reduced solar heating and increased turbulent mixing from wind and waves result in very weakly stratified to mixed waters in the OAA, characterised by homogeneous temperature and density profiles, with PEA values around 30J/m³. With the onset of spring and summer, calmer weather and longer, warmer days enhance stratification, overcoming the mixing effects of tide and winds. From May to October, this leads to a vertical temperature gradient and an increase in PEA values. Over the 14 year analysis period (2010 to 2023), PEA typically reaches around 140J/m³ in mid-summer, indicating a strongly stratified water column, consistent with the findings of van Leeuwen *et al*. (2015).

3.4.1.14 To the east of the OAA, increasing depths and weaker tidal currents lead to stronger stratification with greater distance from the OAA. Conversely, closer to the coastline, shallower depths and stronger tidal currents result in reduced stratification. Approximately

60km southwest of the OAA towards the northeast Aberdeenshire coastline, the water column remains well-mixed throughout the year.

Plate 3.4 Calculated PEA (ϕ), based on the Copernicus Reanalysis monthly temperature and salinity data for 2014, a stronger stratification year

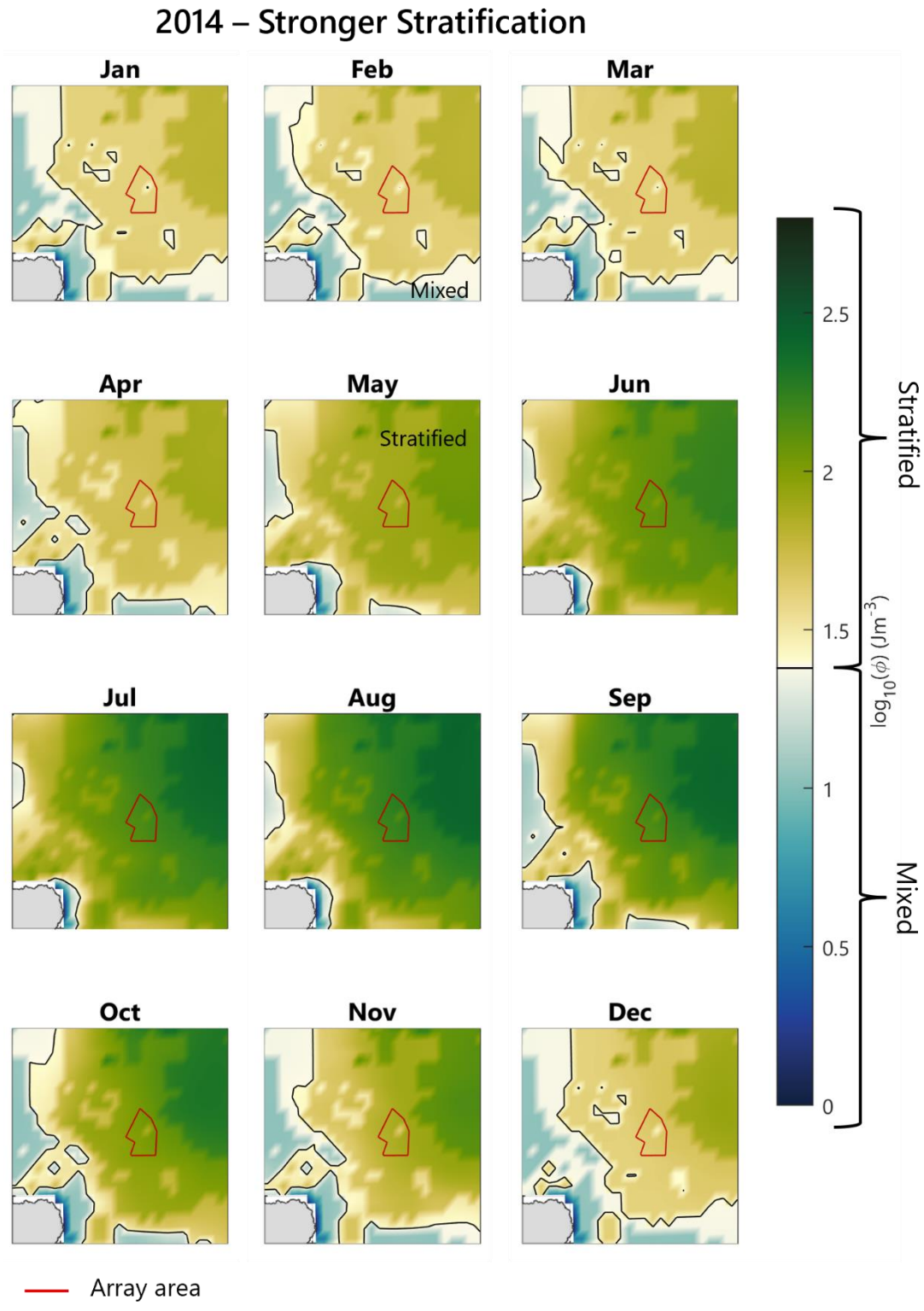

Plate 3.5 Calculated PEA (ϕ), based on the Copernicus Reanalysis monthly temperature and salinity data for 2010, an intermediate stratification year

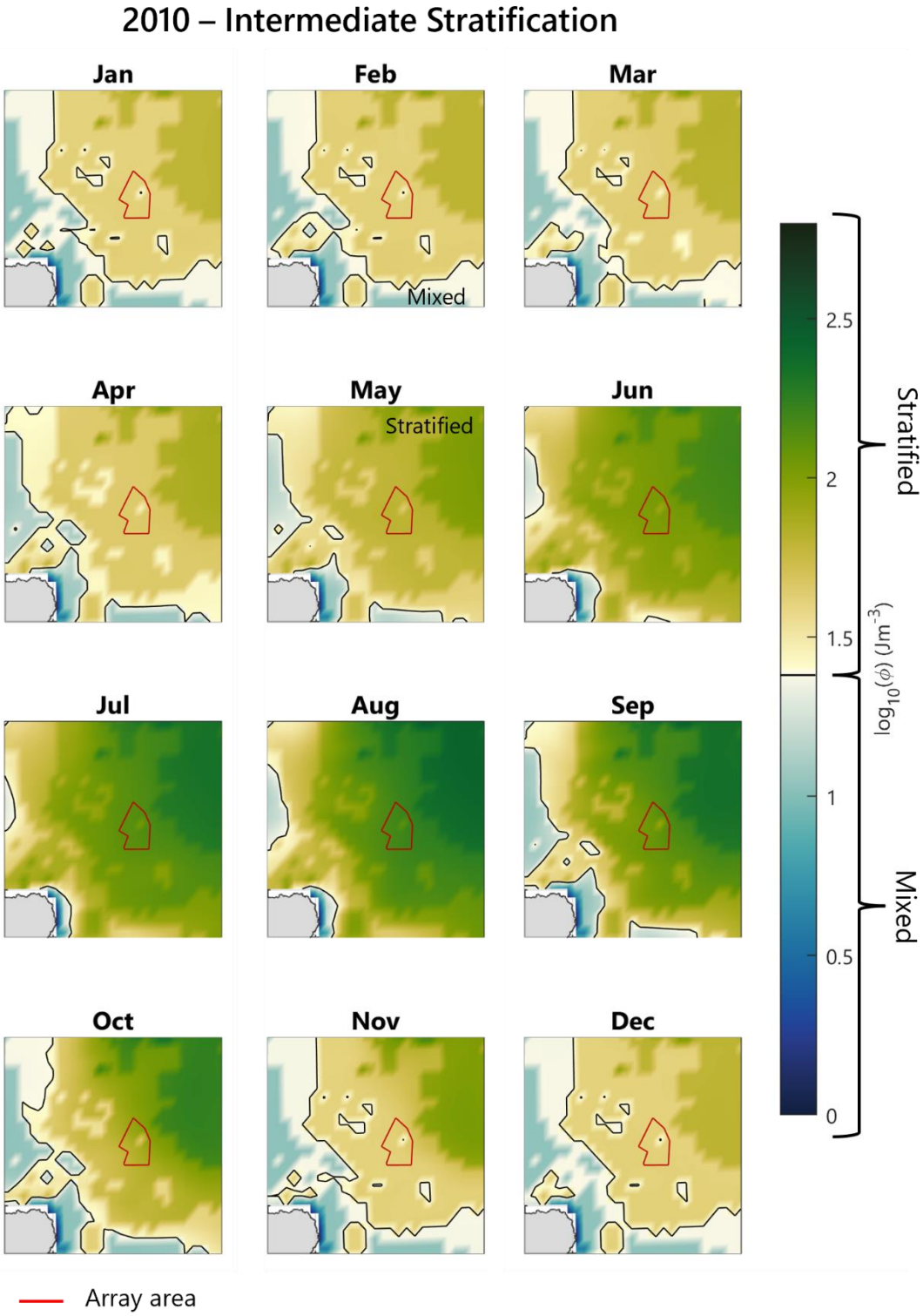

Plate 3.6 Calculated PEA (ϕ), based on the Copernicus Reanalysis monthly temperature and salinity data for 2015, a weaker stratification year

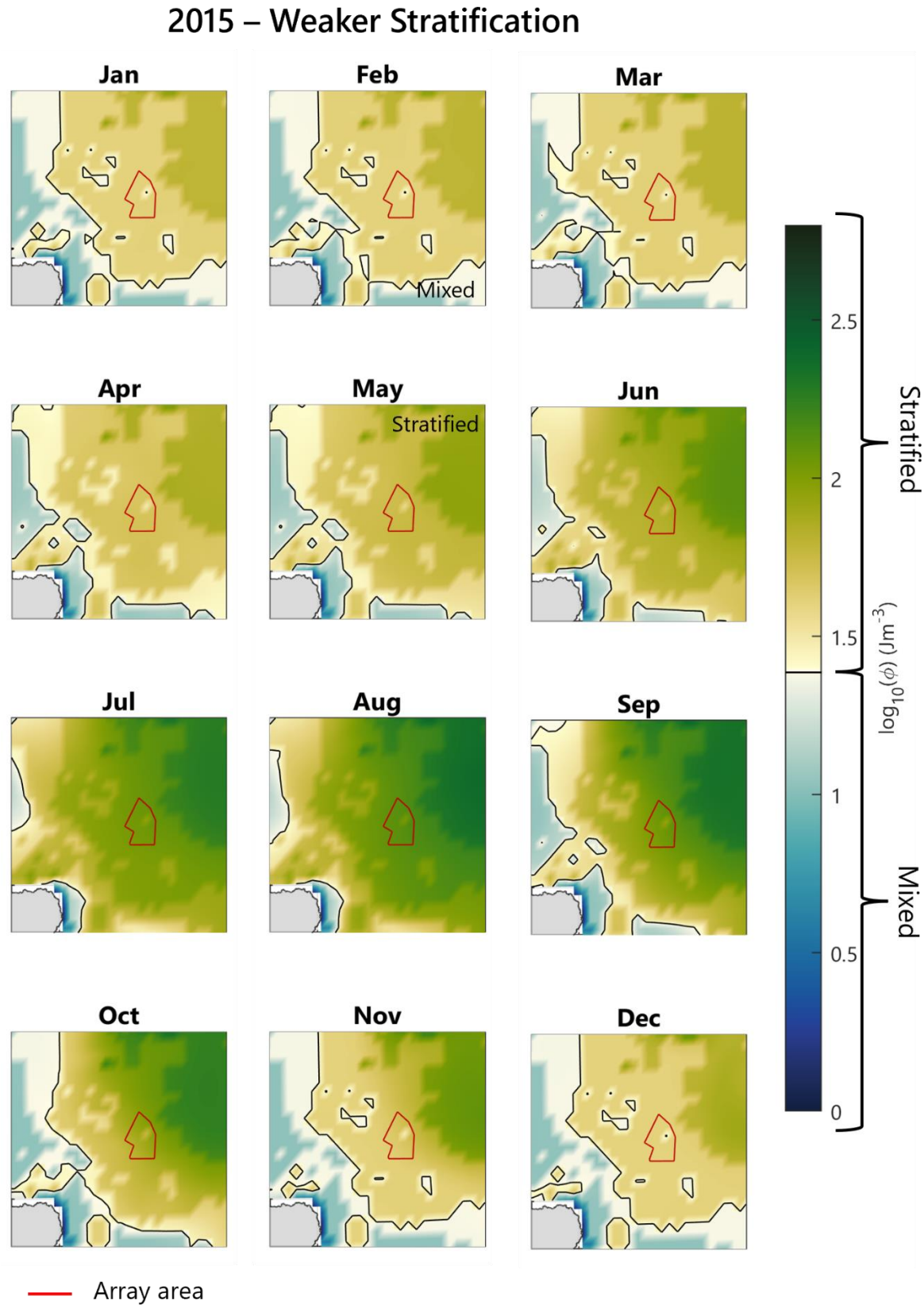

Tidal mixing fronts

3.4.1.15 The relative abundance of chlorophyll-a is proportional to phytoplankton biomass, and local patterns or gradients in concentration can serve as an effective proxy indicator for locating tidal mixing fronts (Garcia-Nieto *et al*., 2024). Phytoplankton rely on sunlight and nutrients for photosynthesis and thrive in areas where both are readily available. In stratified waters, nutrients tend to be trapped below the thermocline, making them inaccessible to phytoplankton in the sunlit surface layer. The physical mixing at fronts locally supplies a relatively higher concentration of nutrients into the sunlit surface layer, therefore creating more favourable conditions for phytoplankton growth by preventing nutrient depletion in the surface layers. As a result, these areas often support higher levels of PP (and chlorophyll-a) compared to both the mixed and stratified waters on either side of the front.

3.4.1.16 **Plate 3.7, Plate 3.8** and **Plate 3.9** illustrate the maximum chlorophyll-a concentrations throughout the water column for the years 2014 (stronger stratification year), 2010 (intermediate stratification year) and 2015 (weaker stratification year), capturing both deep chlorophyll maxima and surface peaks.

3.4.1.17 During summer, elevated chlorophyll-a concentrations - likely associated with a tidal mixing front - are commonly observed west of the OAA. However, their exact positioning varies significantly between years. In years with weaker stratification (for example, 2015), the tidal mixing front forms further offshore, resulting in elevated chlorophyll-a levels within the OAA. Conversely, during years of stronger stratification (for example, 2014), the front / elevated chlorophyll-a concentrations shift closer to the coast.

3.4.1.18 Through analysis of eight day maps of ocean colour, this frontal zone off Rattray Head was also identified in Miller *et al.* (2014) and associated with phytoplankton blooms in the summer months.

Plate 3.7 Copernicus Reanalysis monthly maximum chlorophyll-a concentration throughout the water column for 2014 a stronger stratification year

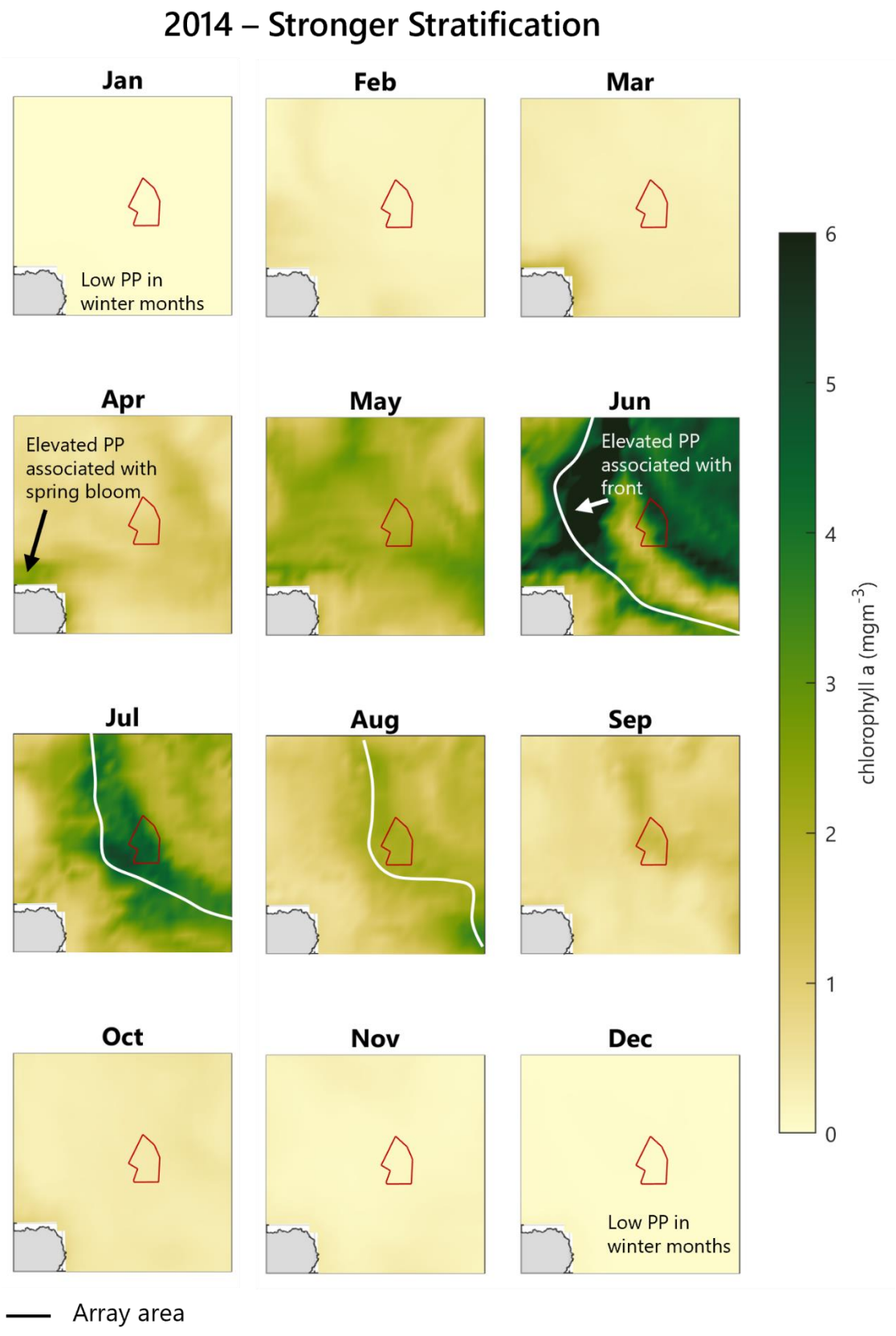

Plate 3.8 Copernicus Reanalysis monthly maximum chlorophyll-a concentration throughout the water column for 2010 an intermediate stratification year

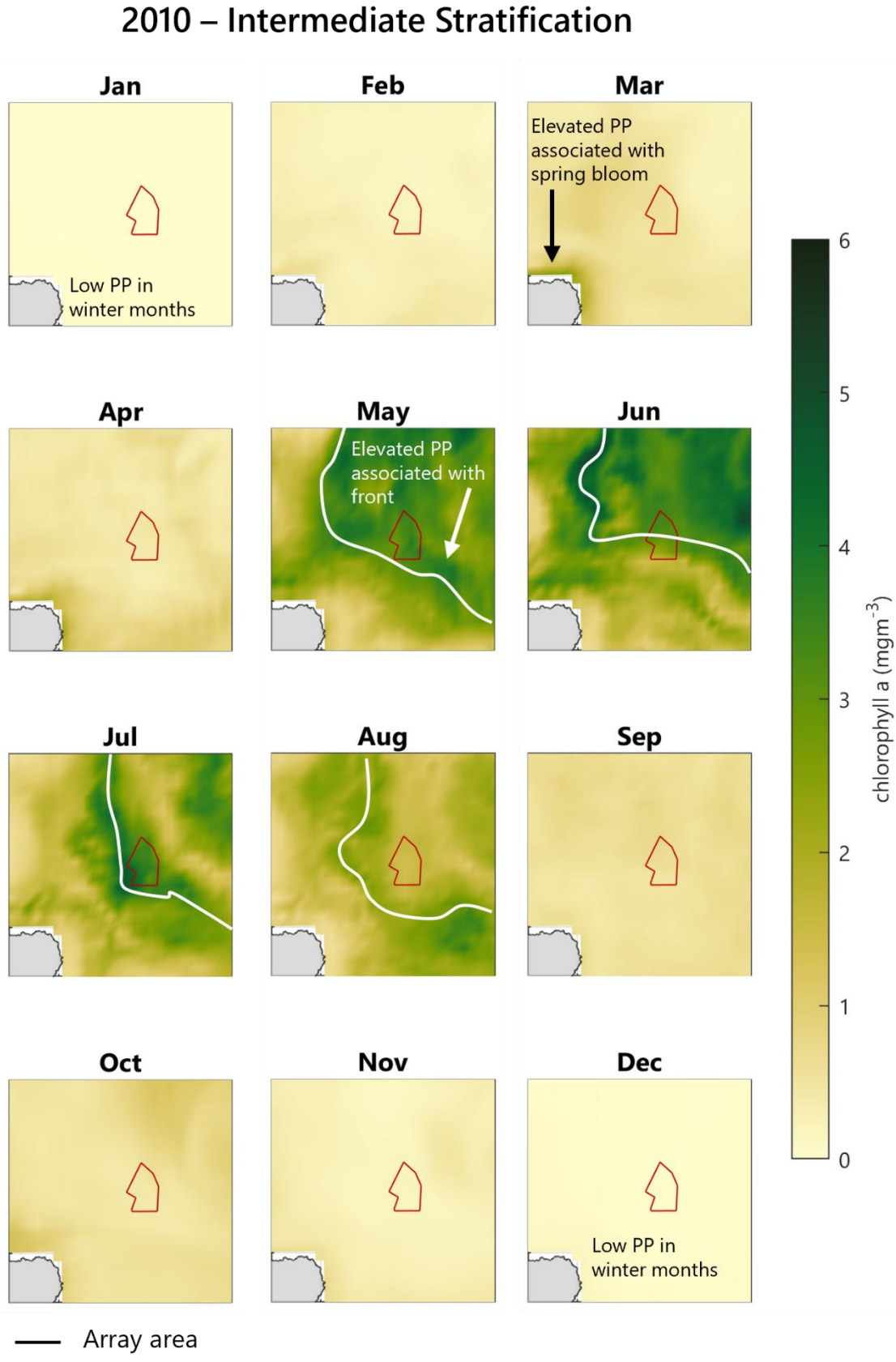

Plate 3.9 Copernicus Reanalysis monthly maximum chlorophyll-a concentration throughout the water column for 2015 a weaker stratification year

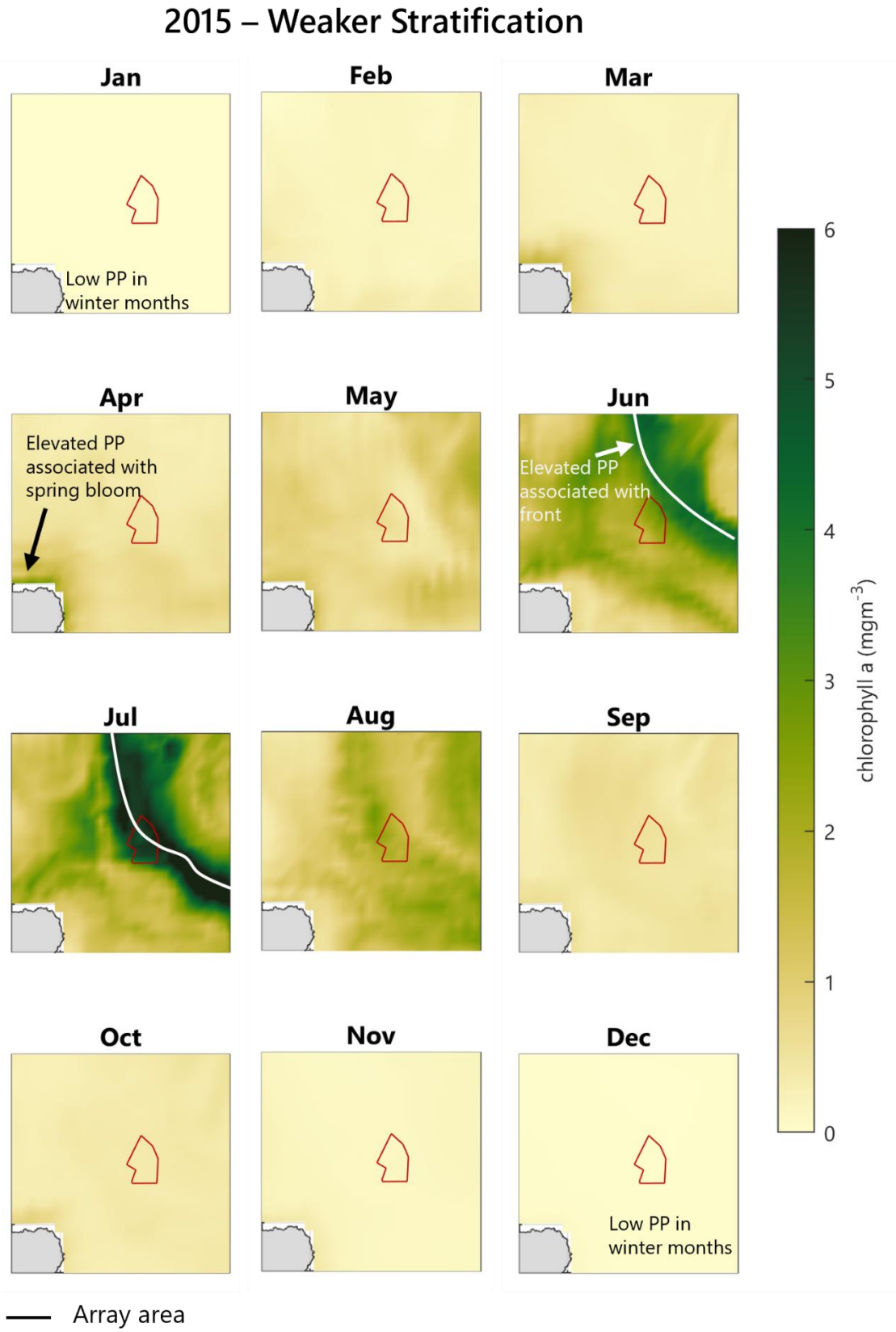

Future change

3.4.1.19 The stratification dynamics in the North Sea are expected to undergo significant changes due to the changing climate. With the Project potentially beginning commercial operation in three phases – 2037, 2040 and 2043, and a project lifetime per phase of ~35 years, it is important to consider how the timing and strength of stratification will evolve during this time.

3.4.1.20 The timing of stratification is influenced by the interplay between solar heating and tidal mixing, with a smaller but notable contribution from wind-driven mixing. Global warming and changes to meteorological conditions is likely to alter the timing of spring stratification, and subsequently the timing of the spring phytoplankton bloom.

3.4.1.21 Model projections suggest that by 2100, the thermal stratification period in UK shelf seas will extend by approximately two weeks (Sharples *et al*., 2025), with stratification occurring about one week earlier and breaking down five days to 10 days later than present (Sharples *et al*., 2022). The dominant driver behind this shift is the increase in air temperature, which accelerates solar heating of the surface waters and thus strengthens thermal gradients. Historically, stratification timing in the north-western North Sea has advanced by about 0.5 days per year since the late 1980s, based on analyses from 1974 to 2003 (Sharples *et al*., 2006; Holt *et al*., 2012). While these observed trends in stratification timing are relatively weak and difficult to separate from inter-annual variability (Jardine *et al*., 2022), they offer some indication of potential future patterns based on a 'business as usual' climate projection (**Plate 3.10**).

Plate 3.10 Comparison between present day (1961 to 1990) and future (2070 to 2098) timing of the onset (a), breakdown (b) and duration (c) of seasonal stratification (from Sharples *et al*., 2025)

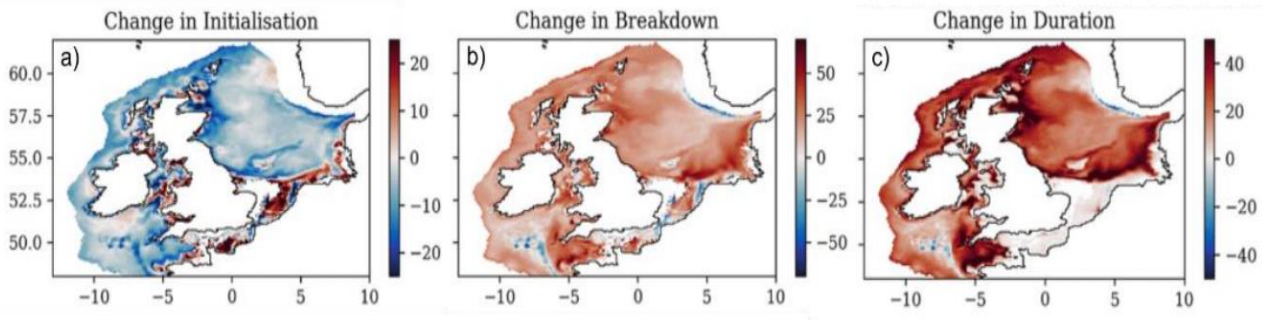

3.4.1.22 Model projections also suggest that seas across the north-west European shelf, including the northern North Sea, will experience greater surface-to-bottom temperature differences as the seasonal heating cycle intensifies (Tinker *et al*., 2016), resulting in stronger stratification (**Plate 3.11**). Alongside the strengthening stratification there will be small shifts in the position of tidal mixing fronts as thermal stratification pushes into shower waters and / or stronger tidal regions.

3.4.1.23 Climate warming is also expected to lead to more frequent Marine Heat Waves (MHWs). MHWs will act to strengthen seasonal stratification through more intense heating of the surface ocean (Sharples *et al*., 2025)

Plate 3.11 Present day (a) and predicted strength of stratification at the end of the century (b) (from Sharples *et al*., 2022)

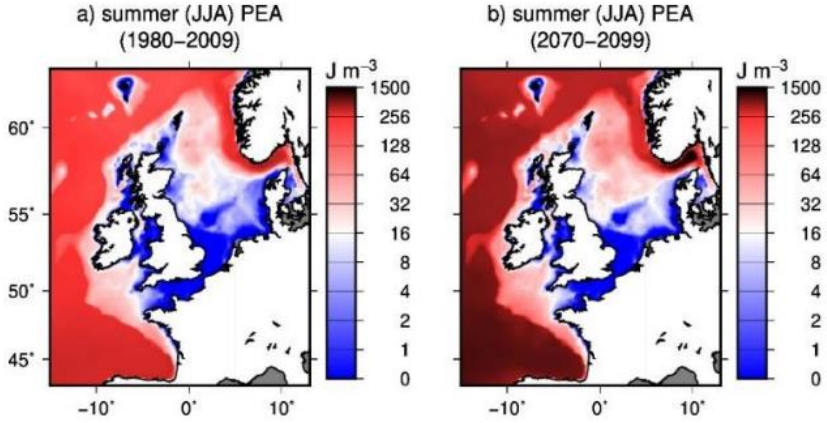

3.4.1.24 Strengthening stratification reduces vertical mixing, limiting the upward transport of nutrients from the deep layers to the surface, where they fuel PP. This could lead to a decline in overall PP, as suggested by Chust *et al*. (2014).

3.4.2 Impact assessment

Maximum design scenario

3.4.2.1 The maximum design scenario for impacts to stratification and frontal systems occurs during the O&M stage of the Project and is associated with the design option providing the largest hydrodynamic blockage within the water column. This is calculated by considering the foundation type, foundation dimensions and foundation number. The maximum design scenario for subsurface blockage contributing to potential impacts on stratification is summarised as follows:

- 225 14MW WTGs on floating units;
- maximum foundation dimension of 120m – conservatively assumed to extend through the whole water column depth (average depth of OAA = 106m); and
- minimum spacing between WTGs of 800m.

3.4.2.2 To the best of the author's knowledge, all of the academic analyses to date which considers the potential impacts from wind farms on mixing processes has focused on flow around monopile (for instance, simple fixed bottom) foundations (for example, Carpenter *et al*. 2016; Cazenave *et al*., 2016; and Dorrell *et al*., 2022). Monopile foundations will not be used in the Project, WTG floating units (semi-submersible / TLP) are likely to be used. The assessment presented in this Section draws upon the research pertaining to fixed bottom monopile foundations, therefore can be seen as a worst-cast estimate of blockage effects, as a monopile structure through the whole water column is likely to impact the vertical structure more than a floating structure near the surface.

Impact on mixing

3.4.2.3 Turbulent mixing acts to breakdown stratification, it is a naturally occurring, omnipresent process driven at the seabed by tidal currents and at the surface by wind and wave action. Flow past individual foundations within the OAA will provide another source of turbulence generation, driving additional water column mixing compared to the baseline scenario.

3.4.2.4 To assess the impact of the foundation structures on the strength of localised water column mixing, the method outlined by Carpenter *et al*. (2016) was employed. This approach uses empirical equations to estimate two key timescales: the mixing timescale, which predicts the time required for complete mixing of stratified layers due to increased TKE generated by the foundation structures, and the advective timescale, which quantifies how long a water parcel remains within the OAA, experiencing enhanced TKE.

3.4.2.5 Power is removed from the flow as it is forced around a foundation. This can be expressed as power consumption per unit area (P_{str}) in watts per square metre (W/m^2) by the following equation:

$$P_{str} = \frac{\rho_0 C_D A \langle |\bar{u}|^3 \rangle}{2L^2}$$

3.4.2.6 Where: ρ_0 is the water density (1026 kilograms per cubic metre (kg/m^3)); C_D is the drag coefficient; A is the cross-sectional area of the foundation in the water column; L is the distance between equally spaced foundations; and, $|\bar{u}|^3$ is the time mean, depth-mean current velocity, cubed (for instance, a measure of the power of the current throughout the year).

3.4.2.7 The drag coefficient of a structure is highly variable, dependent on a range of factors such as roughness, length, scale and turbulence in the approaching flow. A range of values for C_D have been applied in previous studies. The highly conservative value of $C_D = 1$, as used by Carpenter *et al*. (2016) and similar to values suggested by Faltinsen (1990) for floating structures and ships, is applied here.

3.4.2.8 The cross-sectional area (A) providing the maximum total blockage was used – this was for semi-submersible WTG floating unit type which gave a representative individual foundation cross-sectional area of 12,720 square metres (m^2) (calculated assuming maximum foundation dimension of 120m extends through the whole water depth of 106m). The smallest WTG foundation spacing distance provided in **Volume 1, Chapter 4: Project Description**, 800m, was used as L. P_{str} was calculated over a year period from hourly instantaneous tidal velocity magnitudes (extracted for a central point within the OAA from ABPmer's NW European Shelf Hydrodynamic model (ABPmer, 2017), and the mean average power removed from the flow then calculated (**Plate 3.12**).

3.4.2.9 These values and assumptions provide an estimate of power removal per unit area across the OAA of $0.148 W/m^2$, representing a mean value calculated over a year-long period. This approach accounts for the diurnal and spring-neap variability in tidal currents, and thus P_{str}. However, the actual instantaneous P_{str} will fluctuate over time (**Plate 3.12**). For instance, during peak spring tides, higher current velocities (u) will lead to increased P_{str} values - scaling with velocity cubed - effectively shortening the timescale required to break down stratification in the OAA. Conversely, during neap tides, when velocities are lower, P_{str} values will decrease, resulting in a longer stratification breakdown period.

3.4.2.10 Since hydrodynamic conditions constantly shift between these extremes, and stratification response to mixing is not instantaneous, the effects evolve as the hydrodynamics change. Therefore, using a mean value provides a representative measure of the longer-term, persistent impact of power removal - capturing the cumulative effect over time, rather than just transient fluctuations.

Plate 3.12 Year timeseries of tidal current speed (top) and power removed from the tidal flow (P_{str}) by the maximum design scenario for hydrodynamic blockage (bottom)

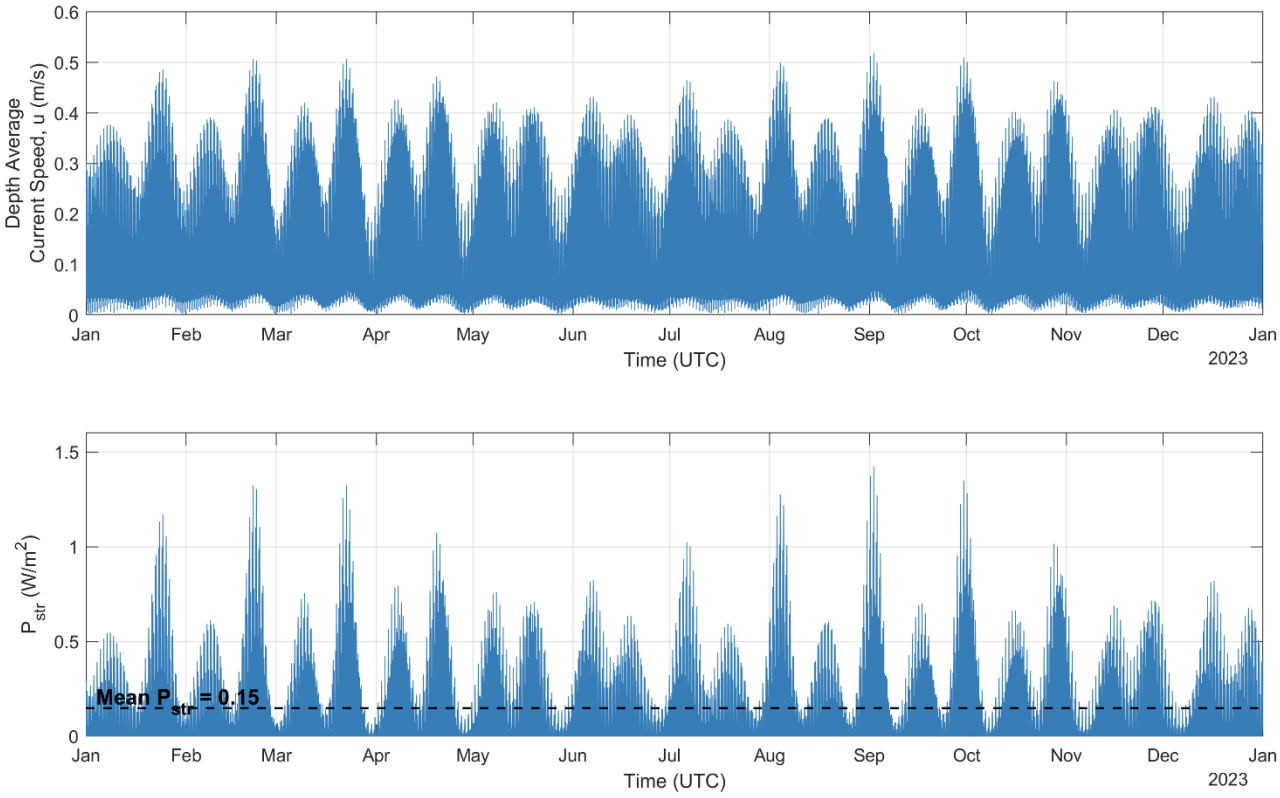

3.4.2.11 The estimate of the power removed by a wind turbine foundation structure is assumed to be equal to the power put into TKE production (Carpenter *et al.*, 2016), which mixes the water column stratification. Therefore, given the strength of the stratification, represented by the PEA, a timescale to mix a water column completely by only the TKE generated by wind turbine structures (T_{mix}) can be estimated by:

$$T_{mix} = \frac{\Phi_{max} h}{R_f P_{str} b}$$

3.4.2.12 Where: R_f is the Richardson number, a value of 0.17 is commonly used in oceanographic studies; h is the representative water depth in the OAA (106 m); ϕ_{max} is the PEA value in joules per square metre (J/m^2) for the maximum stratification case, ϕ_{max} values for a stronger (2014), intermediate (2010) and weaker (2015) stratification year were considered (**Table 3.1**); and, b is the thickness of the pycnocline region during maximum stratification, calculated from density profiles for the most strongly stratified month in the years of interest (**Plate 3.13**), these values are given in **Table 3.1**.

Plate 3.13 OAA density profiles for stronger (2014), intermediate (2010) and weaker (2015) stratification years

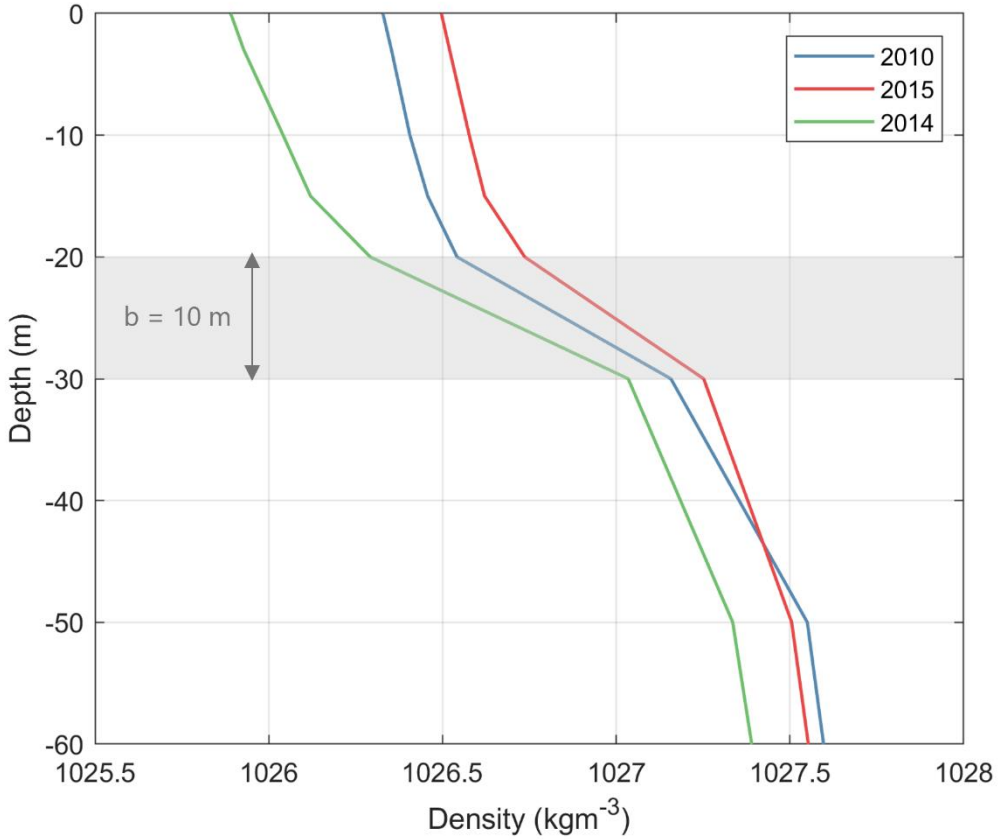

Table 3.1 Mixing timescales for stronger (2014), intermediate (2010) and weaker (2015) stratification years

	Stronger stratification year	Intermediate stratification year	Weaker stratification year
Year	2014	2010	2015
Maximum design scenario blockage (m^2)	12,720	12,720	12,720
h (m)	106	106	106
ϕ_{max} (J/m^3)	170	150	130
ϕ_{max} (J/m^2)	18,020	15,900	13,780
P_{str} (W/m^2)	0.148	0.148	0.148
b (m)	10	10	10
T_{mix} (days)	87.7	77.4	67.1

	Stronger stratification year	Intermediate stratification year	Weaker stratification year
T_{adv} (days)	45.1	45.1	45.1
T_{adv}/T_{mix}	0.51	0.58	0.67

3.4.2.13 The calculated mixing timescales for a range of stratification strengths observed in the OAA are given in **Table 3.1**. To provide context for these values, it is necessary to determine a timescale of advection (T_{adv}), (for instance, how long a parcel of water is likely to experience enhanced turbulent mixing induced by the offshore wind farm structures). This was estimated using ABPmer's NW European Shelf Hydrodynamic model (ABPmer, 2017) to derive the mean residual current speed across the OAA (**Plate 3.14**) and the OAA's length scale, resulting in a T_{adv} value of 45.1 days. This indicates that a parcel of water is not exposed to the elevated TKE from offshore wind farm structures for a sufficiently long time to completely break down the stratification present in the water column, even for more weakly stratified years such as 2015. Stratification will be weakened by the elevated TKE but will not be fully broken down.

Plate 3.14 Residual current speed and direction across the OAA

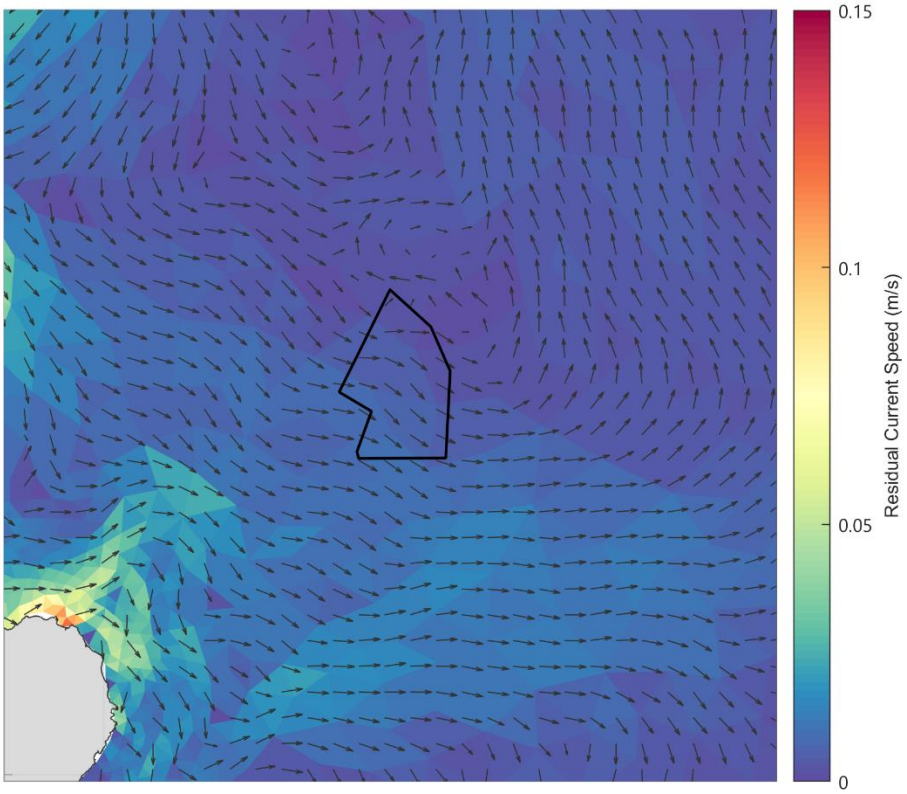

3.4.2.14 To better understand the predicted impact in the context of natural variability, hourly PEA values were calculated for the OAA during a stratified summer month, July 2023, using Copernicus reanalysis data (**Plate 3.15**). The results show that PEA fluctuates significantly over short timescales, with variations of ±20J/m³ within a tidal cycle (12 hours). This

indicates that the stratification weakening caused by elevated turbulent mixing in the wake of foundation structures falls within the natural variability of the system.

Plate 3.15 OAA hourly PEA values for a strong stratification month July 2023

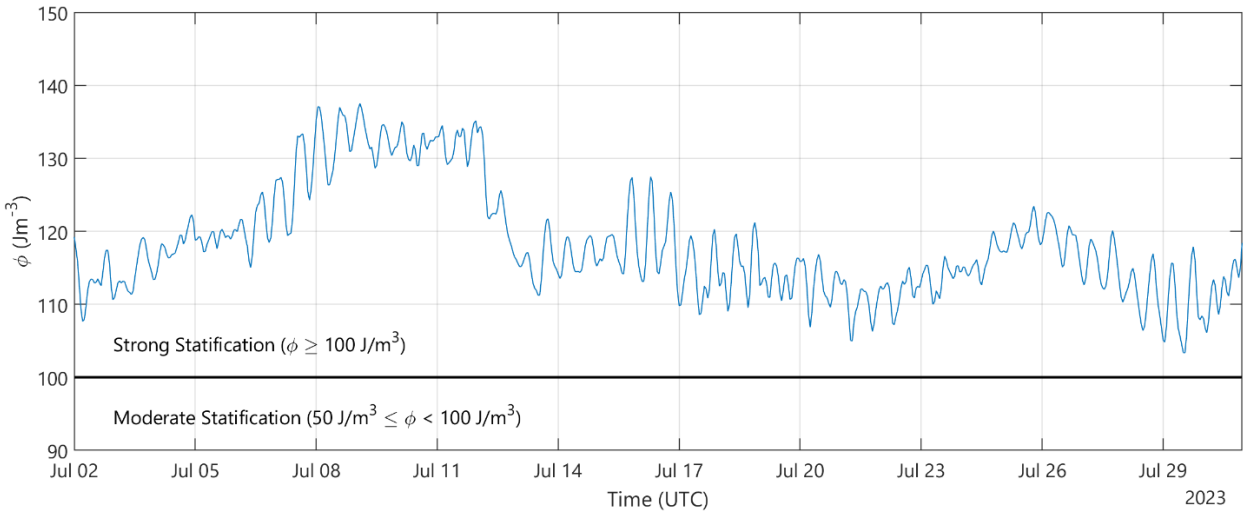

3.4.2.15 The foundation induced mixing described in this Section will primarily occur directly behind individual foundations, extending only a short distance downstream. Research by Miles *et al*. (2017) using scaled flume tank models found that while monopile foundations initially reduced flow velocity and increased turbulence in their wake, these effects largely dissipated within 8.3 pile diameters downstream. This limited spatial influence on flow and turbulence suggests that the impact of foundations on stratification will also be spatially constrained to within a maximum of no more than one spring tidal excursion ellipse from the OAA, and therefore affecting only small portions of the shelf sea and minimising the likelihood of cumulative impacts with other planned offshore wind farms.

Impact on stratification timing and tidal mixing front position

3.4.2.16 The impact of the Project on seasonal stratification is expected to be small. The mixing induced by the foundations is unlikely to be strong enough to fully break down stratification within the timescale that water parcels are exposed to this enhanced mixing. The onset of stratification in spring depends on surface heating overcoming vertical mixing. The foundation-induced mixing could theoretically delay the onset of stratification. Similarly, the breakdown of stratification in autumn may be slightly accelerated by the Project infrastructure's enhanced TKE. However, in years where stratification is naturally weaker, stratification typically develops later and breaks down earlier. Therefore, the Project infrastructure's influence on seasonal timing is expected to be small, falling within the natural variability of the system.

3.4.2.17 Frontal systems form at boundaries between mixed and stratified waters, and their position and intensity can be influenced by vertical mixing. The added turbulence from the offshore infrastructure will act to locally weaken, but not fully break down stratification, within the wakes of foundations. This may create small pockets of elevated primary production within the OAA, where mixing and weakening of the stratification in the foundation wakes acts to vertically mix nutrients into the nutrient depleted, sunlit surface layers of the surrounding more strongly stratified waters.

Impact on primary productivity and the wider ecosystem

3.4.2.18 Potential impacts on PP and the wider marine ecosystem will be reported on separately, within other chapters of this EIA Report, notably **Volume 1, Chapter 11: Marine Mammals, Volume 1, Chapter 12: Offshore and Intertidal Ornithology** and **Volume 1, Chapter 13: Fish Ecology**. However, the potential impact of the Project on PP and the wider ecosystem is expected to be minimal, especially when considering the natural variability and existing patterns of productivity in the region.

3.4.2.19 In terms of the wider ecosystem, the localised mixing effects near the foundation structures are unlikely to affect ecosystem processes beyond the immediate vicinity of the OAA. This limited spatial influence means the likelihood of cumulative impacts with other planned offshore wind farms is minimal.

3.4.2.20 The present day and recent historical PP hotspots and associated biological activities, such as zooplankton blooms and fish aggregations, are concentrated at the tidal front, which is and will continue to be created and controlled by natural processes and will be subject to natural variation in strength and timing.

Impact on near-surface wind speeds and stratification

3.4.2.21 Another potential influence on mixing is the change in near sea surface wind speeds due to the above surface offshore infrastructure. This has been investigated by Christiansen *et al*. (2022). A detailed hydrodynamic model was set up to simulate the seasonal cycle of summer stratification in the southern North Sea, with multiple offshore wind farms in operation. The simulations show the emergence of large-scale attenuation in the wind forcing and associated alterations in the local hydro- and thermodynamics. Induced changes in the vertical and lateral flow were found to be sufficiently strong to influence the residual currents and entail alterations of the temperature and salinity distribution in areas of wind farm operation. Ultimately, these were found to affect the stratification development in the southern North Sea. In the German Bight in particular, the reduction of mixing at offshore wind farms was found to enhance or maintain stratification strength during the autumn breakdown phase of summer stratification.

3.4.2.22 The findings of Christiansen *et al*. (2022) are based on the presence of a very large number of offshore wind farms (>50) in relatively close proximity with a large total number of wind turbines (>2,500) present within the theoretical scenario study area. In contrast, the OAA is further offshore and is not part of such a large group of closely spaced offshore wind farms and is itself much smaller (up to 225 wind turbines). Even when considering cumulative effects of the Project and neighbouring operational / planned offshore wind farms, together the number of wind turbines is lower than those considered by Christiansen *et al*. (2022). Based on this, any associated wind wake effects are therefore only expected to have a very limited aggregated spatial footprint. The potential for widespread changes in the rate of surface mixing and associated water column stratification is therefore considered to be low.

3.4.2.23 Whilst Christiansen *et al*. (2022) provides some evidence on the effects of wind turbines on near surface wind speeds and water column mixing. It is noted that this work focused on a region of the North Sea that does not strongly seasonally stratify, so is not completely analogous to the location of the OAA. Other literature and methodology focusing on this wind wake effect is limited. Therefore, the potential impact is associated with some uncertainty.

3.5 Summary

3.5.1.1 The assessment of potential changes to stratification and frontal systems caused by the Project indicates that the Project will have minimal impacts, with effects generally falling within the range of natural variability.

3.5.1.2 The baseline conditions show that the OAA experiences strong stratification, with significant seasonal and inter-annual variability. Stratification typically peaks during mid-summer when warmer surface waters are separated from colder bottom waters by a thermocline (temperature gradient) and associated pycnocline (density gradient). The area east of the OAA typically experiences stronger stratification, whereas the western region tends to be more weakly stratified - with coastal waters remaining well mixed throughout the year.

3.5.1.3 A region of enhanced PP exists at the boundary between the weak and more strongly stratified waters, associated with the tidal mixing front. This front generally develops to the west of the OAA, but its timing and location vary significantly between years. During weaker stratification, the front forms further offshore. In contrast, years of stronger stratification cause the front to shift closer to the coast.

3.5.1.4 The installation of offshore infrastructure will generate additional turbulence alongside naturally occurring turbulence generated at the seabed by tidal currents and the surface by wind / wave action. The foundation induced TKE will enhance vertical mixing of the water column, acting to break down stratification. However, this mixing effect is expected to be spatially limited.

3.5.1.5 Mixing timescales for a range of stratification strengths observed in the OAA have been calculated. The shortest estimated mixing timescale, associated with a year of weak stratification (2015) is 67.1 days. A parcel of water within the OAA is likely to experience enhanced turbulent mixing induced by the offshore wind farm structures for 45.1 days. Therefore, a parcel of water is not exposed to the elevated TKE from offshore wind farm structures for a sufficiently long time to completely break down the stratification present in the water column, even for more weakly stratified years such as 2015.

3.5.1.6 The calculated mixing timescales presented here are based on a highly conservative description of the WTG floating units, assuming the maximum floating unit dimension extends through the whole water column. In reality, however, the WTG floating unit only occupies the upper portion of the water column. This means the effective blockage cross-sectional area would be significantly reduced - by approximately 50% - and, as a result, the mixing timescale is expected to increase by a similar factor.

3.5.1.7 The Project is not expected to significantly influence the timing of seasonal stratification or the positioning of tidal mixing fronts. While additional mixing may theoretically delay the onset of stratification in spring or accelerate its breakdown in autumn, any changes would be subtle and fall within the bounds of natural variability. Similarly, shifts in frontal systems - regions where mixed and stratified waters meet - are expected to be highly localised.

3.5.1.8 Finally, while changes in near-surface wind speeds due to the Project infrastructure could theoretically influence water column mixing, the scale of these effects is expected to be small. Large-scale wind farms have been shown to reduce surface mixing and enhance stratification in some studies, but the comparatively small size of the Project makes widespread impacts unlikely. However, literature focusing on this wind wake effect is limited. Therefore, this potential impact is associated with some uncertainty.

4. Scour

4.1.1.1 This Section aims to conservatively and quantifiably estimate the area of seabed that will be altered during the operational stage of the Project as a result of sediment scour that may develop adjacent to foundations (in the absence of any scour protection).

4.2 Introduction

4.2.1.1 The term scour refers here to the development of pits, troughs or other depressions in the seabed sediments around the base of foundations. Scour is the result of net sediment removal over time (typically in the order of hours to days from installation in mobile sediments) due to the complex three-dimensional interaction between the foundation and ambient flows (currents and / or waves). Such interactions result in locally accelerated time-mean flow and locally elevated turbulence levels that enhance sediment transport potential in the area of influence. The resulting dimensions of the scour features and their rate of development are, generally, dependent upon the characteristics of the:

- obstacle (dimensions, shape and orientation);
- ambient flow (depth, magnitude, orientation, and variation including tidal currents, waves, or combined conditions); and
- seabed sediment (geotextural and geotechnical properties).

4.2.1.2 Based on the existing literature and evidence base, an equilibrium depth and pattern of scour can be empirically approximated for given combinations of these parameters. Natural variability in the above parameters means that the predicted equilibrium scour condition may also vary over time on, for example, spring-neap, seasonal or annual timescales. The time required for the equilibrium scour condition to initially develop is also dependent on these parameters and may vary from hours to years.

4.2.1.3 Scour assessment for EIA purposes is considered here for several foundation types:

- RCP jacket foundations;
- offshore substation jacket foundations; and
- WTG floating units.

4.2.1.4 Each foundation type may produce different scour patterns therefore, all types with a significant seabed footprint have been considered. Piles have not been considered in the assessment because these will fall within the maximum design scenario envelope of change associated with the other foundation types.

4.2.1.5 The concerns under consideration include the seabed area that may become modified from its natural state (potentially impacting sensitive receptors through habitat alteration) and the volume and rate of additional sediment resuspension, as a result of scour. The seabed area directly affected by scour may be modified from the baseline (pre-development) or ambient state in several ways, including:

- a different (coarser) surface sediment grain size distribution may develop due to winnowing of finer material by the more energetic flow within the scour pit;
- a different surface character will be present if scour protection (for example, rock protection) is used;
- seabed slopes may be locally steeper in the scour pit; and

- flow speed and turbulence may be locally elevated.

4.2.1.6 The magnitude of any change will vary depending upon the foundation type, the local baseline oceanographic and sedimentary environments and the type of scour protection implemented (if needed). In some cases, the modified sediment character within a scour pit may not be so different from the surrounding seabed; however, changes relating to bed slope and elevated flow speed and turbulence close to the foundation are still likely to apply. No direct assessment is offered within this document as to the potential impact on sensitive ecological receptors.

4.2.1.7 The assessment presented here is not intended for use in detailed engineering design. However, methodologies similar to those recommended for the design of offshore wind foundations (for example, Det Norske Veritas, 2016) have been used in some cases where they are applicable.

4.2.2 Evidence base

4.2.2.1 This scour assessment is based on a key publication by Whitehouse (1998) that provides a synthesis of a range of research papers, industry reports, monitoring studies and other evidence available at that time, describing the patterns and dimensions of scour that result from a variety of obstacle shapes, sizes and environmental conditions. Building upon a theoretical understanding of the processes involved, the accepted methods for the prediction of scour mainly rely on stochastic relationships and approaches (for instance, relationships that are based on and describe the available evidence). As such, scour analysis is an evidence-based science where suitable analogues provide the most robust basis for prediction.

4.2.2.2 Since the publication of Whitehouse (1998), evidence continues to be collected, and other predictive relationships have been developed and reported by the research community. In general, more recent observations (for example, summarised in Deltares, 2023) are consistent with the approaches (and associated ranges of uncertainty) presented in Whitehouse (1998). As the evidence base has grown, additional approaches and relationships have been developed to better predict scour for a wider range of more specific obstacle shapes, sizes and environmental conditions.

4.2.2.3 Monitoring evidence regarding scour development around unprotected wind farm monopile installations is provided by HR Wallingford *et al*. (2007) and ABPmer *et al*. (2010) in a series of monitoring data synthesis reports for Department for Trade and Industry and Collaborative Offshore Wind Research into the Environment Ltd. HR Wallingford *et al*. (2007) note that the available data support the view that scour is a progressive process that can occur where the seabed sediment is potentially erodible and there is an adequate thickness of that sediment for scouring to occur. Where the seabed comprises consolidated pre-Holocene sedimentary units, the scour will be slower to develop and limited in depth. For instance, geotechnical surveys at Kentish Flats offshore wind farm (Outer Thames) show that the seabed consists of non-cohesive sands over more resistant London Clay. The post construction monitoring evidence generally indicates that maximum scour rates around the monopiles (of diameter 4.3m) occurred during the first year from installation and then rapidly slowed with near stability occurring by the third anniversary of the works. Scour depths ranged from 1.5m to 1.9m at the monitoring locations and the results indicate that the scour depth is restricted by the cohesive underlying clay formation (Thames Estuary Dredging Association (TEDA), 2012).

4.2.2.4 A research paper by Whitehouse (2004) provides a summary of the field evidence for scour around gravity base foundations in the North Sea used in oil and gas projects. This review emphasised the sensitivity of scour to foundation shape, with foundations in very close proximity sharing similar hydrodynamic / sedimentary environments displaying markedly

different scour characteristics. This review also described field evidence for scour around a rectangular gravity base foundation (75m x 80m x 16m high) located within the North Sea in 42m water depth. Scour was measured as 2.5m to 3.5m deep in 0.15mm (for instance, fine) sand.

4.2.2.5 Scour protection is evidently a mature engineering concept and by design will both prevent primary scour and minimise secondary scour. The evidence base supporting the design of scour protection is therefore strong but is not relevant to this assessment. The evidence base concerning the environmental impacts of scour protection is more limited. Although multi-layered gravel and rock scour protection is being successfully used at the Thornton Bank Offshore Wind Farm in conjunction with six gravity base foundations in a sandy environment with water depths of 28m (ABPmer *et al.*, 2010).

4.3 Methods

4.3.1 Structures considered in scour assessment

4.3.1.1 **Table 4.1** outlines the foundation structures that have been considered within the assessment presented in this Section.

Table 4.1 Maximum design scenario for foundation structures of the Project

Parameter	Maximum design scenario
RCP foundations	2 4-legged jacket foundations – 35m x 25m base. Suction caissons – 0.5m height above seabed and 6.5m diameter.
Offshore substation foundations	4 12-legged jacket foundations – 110m x 90m base. Suction caissons – 0.5m height above seabed and 6.5m diameter.
WTG foundations	225 14MW floating semi-sub foundations. 8 mooring lines – 800m radius. Suction anchors – 0.5m height above seabed and 6.5m diameter.

4.4 Scour calculations

4.4.1.1 In order to quantify the area of seabed that might be affected by scour (either the footprint of scour or scour protection), estimates of the theoretical maximum depth and extent of scour are provided below. Estimates are made of the primary scour, (for instance, the scour pit directly associated with the presence of the main obstacle).

4.4.1.2 The equilibrium primary scour depth for each foundation type has been conservatively calculated assuming the absence of any scour protection, using empirical relationships described in Whitehouse (1998). This analysis considers scour resulting from the characteristic wave and current regime, both alone and in combination.

4.4.1.3 **Volume 1, Chapter 4: Project Description** provides maximum design scenario extents of scour protection for each foundation type. Scour protection might be applied around the base of some or all foundations depending upon the seabed conditions and other

engineering requirements. By design, scour protection will largely prevent the development of primary scour but may itself cause smaller scale secondary scour due to turbulence at the edges of the scour protection area.

4.4.1.4 In the following Sections, the term 'local scour' refers to the local response to individual structure members. 'Global scour' refers to a region of shallower but potentially more extensive scour associated with a multi-member foundation resulting from the change in flow velocity through the gaps between members of the structure and turbulence shed by the entire structure. Global scour does not imply scour at the scale of the wind farm OAA.

4.4.2 Assumptions

4.4.2.1 The following scour assessment for the Project reports the estimated equilibrium scour depth, which assumes that there are no limits to the depth or extent of scour development by time or the nature of the sedimentary or metocean environments. As such, the results of this study are considered to be conservative and provide an (over-) estimation of the maximum potential scour depth, footprint and volume. Several factors may naturally reduce or restrict the equilibrium scour depth locally, with a corresponding reduction in the area and volume of change.

4.4.2.2 This study makes the basic assumption that the seabed comprises an unlimited thickness of uniform non-cohesive and easily eroded sediment. In practice the thickness of more easily erodible surficial sediment is spatially variable across the OAA, typically 0.5m to 2.8m thick (Fugro, 2024).

4.4.2.3 The foundation types, dimensions and numbers used in the assessment are consistent with the project design information.

4.4.2.4 Reported observations of scour under steady current conditions (for example, in rivers) generally show that the upstream slope of the depression is typically equal to the angle of internal friction for the exposed sediment (typically 32° in loose medium sand (Hoffmans and Verheij, 1997)) but the downstream slope is typically less steep.

4.4.2.5 In reversing (tidal) current conditions, both slopes will develop under alternating upstream and downstream forcing and so will tend towards the less steep or an intermediate condition. For the purposes of the present study a representative angle of internal friction (32°) will be used as the characteristic slope angle for scour development.

4.4.3 Equilibrium scour depth

4.4.3.1 The maximum equilibrium scour depth (S_e) is defined as the depth of the scour pit adjacent to the structure, below the mean ambient or original seabed level. The value of S_e is typically proportional to the diameter of the structure and so is commonly expressed in units of structure diameter (D).

4.4.3.2 Scour depth decreases with distance from the edge of the foundation. The scour extent (S_{extent}) is defined as the radial distance from the edge of the structure (and the point of maximum scour depth) to the edge of the scour pit (where the bed level is again equal to the mean ambient or original seabed level). This is calculated on the basis of a linear slope at the angle of internal friction for the sediment:

$$S_{extent} = \frac{S_e}{\tan 32} \approx S_e \times 1.6$$

4.4.3.3 The scour footprint ($S_{footprint}$) is defined as the seabed area affected by scour, excluding the foundation's footprint:

$$S_{footprint} = \pi\left(S_{extent} + \left(\frac{D}{2}\right)\right)^2 - \pi\left(\frac{D}{2}\right)^2$$

4.4.3.4 The scour pit volume is calculated as the volume of an inverted truncated cone described by Equations 1 and 2 above, accounting for the presence of the foundation but excluding its volume.

4.4.4 Jacket foundations

4.4.4.1 Above the seabed jacket foundations comprise a lattice of vertical primary members and diagonal cross-member bracing; it is assumed that either no near-bed horizontal cross-member bracing is required, or that it is sufficiently high above the bed to not induce significant local scour.

4.4.4.2 The RCP 4-legged jacket foundations are assumed to have a nominally square plan view cross-section with base edge dimensions of 35m x 35m. The offshore substation 12-legged jackets have a rectangular base with maximum dimensions 110m x 90m.

4.4.4.3 The RCP and offshore substation jacket foundations will be anchored to the seabed at each primary member by either driven piles (diameter 3m) or suction caissons (diameter 6.5m). The largest near bed structure diameter, for instance, suction caissons, provides the maximum design scenario for scour.

4.4.4.4 A jacket foundation structure may result in the occurrence of both local and group or global scour. The local scour is the local response to individual structure members. Whereas global scour is the formation of a depression around the entire structure.

Under steady currents

4.4.4.5 Under steady currents alone, the equilibrium scour depth around the vertical members of the structure base can be assessed using methods developed for monopiles, unless significant interaction between individual members occurs. The potential for such interaction is discussed below.

4.4.4.6 For monopiles under steady currents Breusers *et al*. (1977) presented a simple expression for scour depth under live-bed scour (for instance, scour occurring in a dynamic sediment environment) which was extended by Sumer *et al*. (1992) who assessed the statistics of the original data to show that:

$$\frac{S_c}{D} = 1.3 \pm \sigma_{Sc/D}$$

4.4.4.7 Where $\sigma_{Sc/D}$ is the standard deviation of observed ratio Sc/D. Based on the experimental data, $\sigma_{Sc/D}$ is approximately 0.7, hence, 95% of observed scour falls within two standard deviations, for instance, in the range 0 < Sc/D < 2.7, with a central value of Sc = 1.3D (as also recommended in Det Norske Veritas, 2016).

4.4.4.8 For a jacket the main scour development will be in proportion to the size of the largest exposed member near to the seabed. For the RCP and offshore substation jacket foundations, the largest exposed member is assumed to be the suction caisson, which will have a diameter of up to 6.5m. Using Equation 3, the scour depth for the largest jacket foundation is therefore estimated as 8.45m.

4.4.4.9 In the case of currents, inter-member interaction has been shown to be a factor when the gap to near bed member diameter ratio (G/D) is less than three. In this case limited experiments by Gormsen and Larson (1984) have shown that the scour depth might increase by between 5% and 15%. However, in the case of the RCP and offshore substation

jackets considered the gap ratio for members at the base of the jacket foundation structure is much greater than 3, and so no significant in combination change is expected.

4.4.4.10 Empirical relationships also presented in Sumer and Fredsøe (2002) indicate that the depth of group scour (measured from the initial sediment surface to the new sediment surface surrounding local scour holes) for an array of members similar to a jacket foundation can be approximated as 0.4D (for instance, for the RCP and offshore substation jackets approximately 2.6m based on 6.5m diameter suction caisson). On the basis of visual descriptions of group scour pits, their extent from the edge of the structure is estimated as half the width of the structure and following a broadly similar plan shape to that of the jacket foundation (for instance, square).

4.4.4.11 On the basis of the proposed jacket design, the diagonal bracing members are not predicted to induce seabed scouring due to the distance of separation from the seabed.

Under waves and combined wave-current forcing

4.4.4.12 The mechanisms of scour associated with wave action are limited when the oscillatory displacement of water at the seabed is less than the length or size of the structure around which it is flowing. This ratio is typically parameterised using the Keulegan-Carpenter (KC) number:

$$KC = \frac{U_{0m}T}{D}$$

4.4.4.13 Where U_{0m} is the peak orbital velocity at the seabed (for example, using methods presented in Soulsby (1997) and T is the corresponding wave period. Sumer and Fredsøe (2001) found that for KC < 6, wave action is insufficient to cause significant scour in both wave alone and combined wave-current scenarios.

4.4.4.14 The value of U_{0m} for given (offshore or deep water) wave conditions depend upon the local water depth, which varies between approximately 87m to 134m within the OAA due to variations in absolute bathymetry and relative water level; the influence of shoaling and wave breaking have been ignored in the present study (a conservative assumption).

4.4.4.15 Values of KC are less than six over the full expected range of tidally affected water depths (approximately 87m to 134m) and extreme wave conditions (**Table 4.2**) expected across the site. Therefore, it is predicted that waves do not have the potential to contribute to scour development around the base of the jacket foundations.

Table 4.2 Extreme omni-directional wave conditions considered

Return period (years)	Significant wave height, Hs (m)	Zero crossing period, Tz (s)
1:1	9.2	8.8
1:10	12.1	10.1
1:50	13.8	10.8

4.4.4.16 The diagonal bracing members will have a smaller diameter and so a larger KC value. However, they are again not predicted to induce seabed scouring due to the likely distance of separation from the seabed. For moderate KC numbers a sufficient distance to avoid scour is approximately one diameter for a horizontal member, increasing to approximately three diameters under increasing KC numbers.

4.4.4.17 As such, little or no significant additional scour is predicted to result from waves, either alone or in combination with currents.

4.4.5 Wind turbine generator floating units

4.4.5.1 The WTG floating unit type comprises a floating surface structure, fixed to the seabed by up eight mooring lines attached to anchors. Anchor options include driven piles (3m diameter, 0.5m height above bed), suction anchor (6.5m diameter, 0.5m height above bed) or drag embedment (fully buried). These individual anchor structures may result in the occurrence of local scour. The largest near bed structure diameter, for instance, suction anchors, provides the maximum design scenario for scour.

Under steady currents

4.4.5.2 The foundation is anchored to the seabed by nine mooring lines attached to piles driven into the seabed. The equation from Sumer and Fredsøe (2002) is used to estimate the scour around a structure with a height above the seabed that is not infinitely large (for instance, a short pile, that is not surface piercing):

$$\frac{S}{S_0} = 1 - e^{-0.55\frac{hp}{Lp}}$$

4.4.5.3 Where hp is the height of the submerged structure measured from the bed, Lp is the structure diameter, and S_o = 2Lp.

4.4.5.4 This gives an estimated scour depth for the suction bucket anchors (6.5m diameter and 0.5m height above seabed) of 0.54m.

4.4.5.5 In the case of currents, inter-member interaction has been shown to be a factor when the G/D is less than three. If this is the case limited experiments by Gormsen and Larson (1984) have shown that the scour depth might increase by between 5% and 15%. The G/D ratio for the eight anchors (assuming equal spacing and a mooring line radius of 800m) is much greater than 3, and so no significant in-combination change is expected.

Under waves and combined wave-current forcing

4.4.5.6 Values of the KC parameter were calculated for a 6.5m diameter structure from the extreme wave conditions found at the site (**Table 4.2**). Values of KC are less than 6 over the full expected range of tidally affected water depths across the site (approximately 87m to 134m) and so it is predicted that waves do not have the potential to contribute to scour development around the base of the suction anchors.

4.4.5.7 As such, little or no significant additional scour is predicted to result from waves, either alone or in combination with currents.

4.5 Results

4.5.1 Baseline conditions

4.5.1.1 Where obstacles are not present on the seabed, normal sediment transport processes can cause spatial and temporal variations in seabed level and sediment character in the baseline environment. Scour is a similar but localised change resulting from particular local patterns of sediment transport. Scour may also occur in the baseline environment in response to natural obstacles such as rocky outcrops or boulders. Key features of the baseline environment pertinent to the assessment of scour due to the presence of wind farm infrastructure are summarised below (Fugro, 2023a; Fugro, 2024):

- The OAA is characterised by the presence of fine to medium-grained unconsolidated sediments predominantly consisting of sandy / silty substrates, interspersed with occasional gravel, cobbles and boulders within seafloor depressions.
- Three types of depositional features were identified in the OAA, sediment ridges, sand ribbons and areas of mottled seafloor, indicating the presence of seafloor currents and mobile sediments.
- Four types of erosional features were identified in the OAA, relict plough marks, seafloor scars, anchor scars and depressions.
- Holocene sediments (very loose, slightly silty fine to medium sand) vary in thickens from <0.5m locally around pockmarks to 2.8m in the south and east of the OAA.
- Underlying the Holocene sediments, the quaternary sequence consist of several layers, with more easily erodible silty and sandy clay deposits (for example, Witch Ground and Swatchway formations) of varying thickness from absent to >20m, overlaying more erosion resistant consolidated clay and glacial till layers (for example, Aberdeen Ground and Ling Bank formations).

4.5.2 Impact assessment

4.5.2.1 **Table 4.3** and **Table 4.4** summarise the key results of the first-order scour assessment undertaken using the methodological approach set out in **Section 4.4**.

4.5.2.2 Results conservatively assume that maximum equilibrium scour depths are symmetrically present around the perimeter of the structure in a uniform and frequently mobile sedimentary environment. Derivative calculations of scour extent, footprint and volume assume an angle of internal friction = 32°. Scour extent is measured from the structure's edge. Scour footprint excludes the footprint of the structure. Scour pit volumes for jacket foundation structures are calculated as the sum of the volume of an inverted truncated cone, minus the structure volume, for each of the corner piles. Scour pit volumes for the WTG floating unit are similarly calculated but as the sum of that predicted for each anchor.

Table 4.3 Summary of predicted maximum scour dimensions for foundation structures

		RCP - four-legged jacket on suction caissons (35m x 35m base, 6.5m diameter)	Offshore substations - 12-legged jacket on suction caissons (80m x 60m base, 6.5m diameter)	WTG - floating on suction anchors (0.5m height, 6.5m diameter)
Equilibrium Scour Depth (m)	Steady current.	8.5	8.5	0.5
	Waves	Insufficient for scour.	Insufficient for scour.	Insufficient for scour.
	Waves and current.	8.5	8.5	0.5
	Global scour.	2.6	2.6	N/A
Extent from foundation* (m)	Local scour.	13.5	13.5	0.9
	Global scour.	35	100	N/A
Footprint* (m^2)	Structure alone.	132.7	398.2	265
	Local scour (excluding structure).	3,403	10,208	159
	Global scour (excluding structure).	3,716	31,018	NA
Volume* (m^3)	Local scour (excluding structure).	11,139	33,418	6
	Global scour (excluding local scour and structure).	9,661	80,646	N/A
	Total scour (excluding structure).	20,800	114,064	6
	Scour protection.	500	500	N/A

*Results assume erodible bed and absence of geological controls**.**
** Based upon the scour depth for steady currents. Footprint and volume values are per foundation.

Table 4.4 Total seabed footprint of all foundation types with and without scour

Maximum number of foundations	**225 WTG + 4 offshore substations + 2 RCPs**
Seabed footprint of all foundations	61,588m^2
Proportion of OAA*	0.009%
Seabed footprint of all local scour	83,513m^2
Proportion of OAA*	0.012%
Seabed footprint of all foundations + local scour	145,101m^2
Proportion of OAA*	0.021%
Seabed footprint of all global scour	131,502m^2
Proportion of OAA*	0.019%
Seabed footprint of all scour protection**	3,000m^2
Proportion of OAA*	<0.001%
Seabed footprint of all foundations + scour protection	64,588m^2
Proportion of OAA*	0.009%

* OAA = 683,770,029m^2
**Assumed scour protection height = 1m.

4.5.2.3 Key findings are summarised below:

- overall, scour development within the OAA (and offshore export cable corridor for RCPs) is expected to be dominated by the action of tidal currents;
- in practice, the thickness of unconsolidated (and more easily erodible) surficial Holocene sediment is relatively thin (typically less than 0.5m, up to 2.8m thick), or absent;
- for the OAA as a whole, the greatest total foundation local scour footprint is associated with an array of 225 14MW WTG floating units with suction anchors, four offshore substations 12-legged jacket foundations on suction caissons and two RCP four-legged jacket foundations on suction caissons (83,513m^2), equivalent to only approximately 0.012% of the total OAA; and
- for the OAA as a whole, the greatest total foundation global scour footprint is associated with an array of 225 14MW WTG floating units with suction anchors, four offshore substations 12-legged jacket foundations on suction caissons and two RCP four-legged jacket foundations on suction caissons (131,502m^2), equivalent to only approximately 0.019% of the total OAA.

Factors effecting equilibrium scour

Engineering controls

4.5.2.4 The greatest preventative influence on local scour depth would arise from the installation of scour protection. If correctly designed and installed, scour protection will essentially prevent the development of local primary scour as described in this Section. The dimensions and nature of scour protection may vary between designs but given its purpose, would likely cover an area of seabed approximately similar to the predicted extent of the scour.

4.5.2.5 Interaction between ambient currents and the scour protection may lead to the development of secondary scour at its edges. The local dimensions of secondary scour are highly dependent upon the specific shape, design and placement of the protection. These parameters are highly variable and so there is no clear quantitative method or evidence base for accurately predicting the dimensions of secondary scour. However, as for foundations, the approximate scale of the scour depth and extent is likely to be proportional to the much smaller size of the individual elements comprising the protection.

Natural controls

4.5.2.6 As summarised in Whitehouse (1998), a number of factors are known to influence equilibrium scour depth, contributing to the range of observed equilibrium scour depths. These factors include the:

- frequency and magnitude of ambient sediment transport;
- ratio of structure diameter to water depth;
- ratio of structure diameter to peak flow speed;
- ratio of structure diameter to sediment grain size;
- sediment grain size, gradation and the geotechnical properties of sedimentary units; and
- the thickness of erodible sediment overlying more erosion resistant sublayers.

4.5.2.7 The influence of these factors where they do apply is to generally reduce the depth, extent and volume of the predicted scour, hence providing a less conservative estimate. For example, a greater frequency and magnitude of sediment transport can actually reduce the equilibrium scour depth, as the scour hole is also simultaneously being (partially) in-filled by ambient sediment transport.

4.5.2.8 The above factors have been considered in the context of the OAA and most (except the thickness of erodible) were not found to significantly or consistently reduce the predicted values for the purposes of EIA. The thickness of unconsolidated (and more easily erodible) surficial Holocene sediment is relatively thin across the OAA, between 0m to 2.8m thick (Fugro, 2023a). In practice, this will fundamentally limit maximum potential scour depth in most of the OAA. The following assessment conservatively assumes that foundations will be located in areas of deeper erodible sediment where the full equilibrium scour depth might eventually occur.

Time for scour to develop

4.5.2.9 Scour depth can vary significantly under combined current and wave conditions through time (Harris *et al*., 2010). Monitoring of scour development around monopile foundations in UK offshore wind farm sites suggest that the timescale to achieve equilibrium conditions can be of the order of 60 days in environments with a potentially mobile seabed (Harris *et*

al., 2011). However, equilibrium scour depths may not be reached for a period of several months or even a few years where erosion resistant sediments / geology are present. These values account for tidal variations as well as the influence of waves. (Near) symmetrical scour will only develop following exposure to both flood and ebb tidal directions.

4.5.2.10 Under waves or combined waves and currents an equilibrium scour depth for the conditions existing at that time may be achieved over a period of minutes, while typically under tidal flows alone equilibrium scour conditions may take several months to develop.

Spatial extent of scour

4.5.2.11 At the Scroby Sands Offshore Wind Farm, narrow, elongated scour features have been observed to extend over tens or hundreds of metres from individual foundations, leading to a more extensive impact than would normally be predicted. The development of elongate scour features at Scroby Sands is considered to have occurred due to the strongly rectilinear nature of the tidal currents (a very well defined tidal current axis with minimal deviation during each half tidal cycle) which allows the narrow turbulent wake behind each foundation to persist over the same areas of seabed for a greater proportion of the time, leading to net erosion in these areas. Due to a relatively higher rate of tidal rotation, the development of such elongate scour features is less likely to occur within the OAA.

4.6 Summary

4.6.1.1 Empirical relationships were used to calculate an equilibrium scour depth and pattern of scour for the range of potential foundation types. Scour development within the OAA is expected to be dominated by the action of tidal currents. For the OAA as a whole, the greatest total foundation local (deeper, limited extent around individual foundation members) scour footprint is 83,513m^2, this is equivalent to 0.012% of the total OAA. For the OAA as a whole, the greatest total foundation global (shallower, larger extent around the foundation as a whole) scour footprint is 131,502m^2, this is equivalent to 0.019% of the total OAA. In practice, the thickness of unconsolidated surficial Holocene sediment (for instance, the thickness of erodible material and so the depth limit for local or global scour) is spatially variable across the OAA and can be locally very thin or absent, which would largely naturally prevent the formation of scour.

5. Suspended Sediment Concentrations and Seabed Levels

5.1.1.1 This Section outlines the assessment of potential changes to suspended sediment concentrations, seabed levels and sediment characteristics due to sediment disturbance caused by construction activities.

5.2 Introduction

5.2.1.1 Local increases in suspended sediment concentration (SSC) may result from the disturbance of sediment by construction related activities, most notably due to:

- drilling for offshore substations foundation installation;
- seabed preparation by dredging for WTG anchors, subsea distribution centres (SDCs), subsea substations and offshore substations foundations;
- sandwave clearance prior to cable burial;
- cable burial; and
- drilling fluid release during horizontal directional drilling (HDD) at the landfall.

5.2.1.2 The mobilised material may be transported away from the disturbance location by the local tidal regime. According to the source-pathway-receptor model:

- disturbance and release of sediment is considered as the source of potential changes to SSC in the water column;
- tidal currents act as the pathway for transporting the suspended sediment; and
- the receptor is a feature potentially sensitive to any increase in suspended sediments and consequential deposition.

5.2.1.3 The magnitude, duration, rate of change and frequency of recurrence of changes to SSC and bed level are variable between operation types and in response to natural variability in the controlling environmental parameters.

5.3 Methods

5.3.1.1 This assessment of changes to SSC and associated deposition of sediment as a result of activities related to the Project is informed by location and project specific numerical (spreadsheet) modelling. The quantitative detail of the modelling results for all individual activities are reported as a descriptive summary and a series of spatial maps.

5.3.1.2 The theoretical basis for, and the results of, the following assessments are consistent with the results of observational (monitoring) evidence (for example, Department for Business Enterprise and Regulatory Reform (BERR), 2008;), previous explicit numerical modelling of sediment plumes for analogous activities and environmental settings (for example, TEDA, 2010; and by ABPmer for East Anglia ONE; Navitus Bay; Hornsea Four; Awel y Môr; Erebus, several confidential floating Scottish offshore wind farms), similar spreadsheet modelling for other wind farms by ABPmer (for example, for Burbo Bank Extension; Walney Extension; Thanet Extension; Hornsea Three; Erebus; several confidential floating Scottish offshore wind farms), and results from other (various) consultants and wind farm EIAs, which normally also use a similar range of methodologies.

5.3.1.3 The maximum design scenario for each activity type is determined using the information contained in the project design description (**Volume 1, Chapter 4: Project Description**). For each activity, the rate and duration of sediment disturbance and the total sediment volume is calculated for individual occurrences and for all occurrences of the activity. Scenarios are identified that are likely to correspond to the realistic 'worst case' in terms of instantaneous and overall effects. The effect of all other options in the design envelope are therefore expected to be equal to or less than the results presented in this Appendix.

5.3.2 Spreadsheet based numerical models

5.3.2.1 In order to inform the assessment of potential changes to SSC and bed levels arising from construction related activities, a number of spreadsheet based numerical models have been developed for use. Similar models were developed and used to inform the EIAs for similar activities at Burbo Bank Extension, Walney Extension, Navitus Bay, Thanet Extension, Hornsea Three, Erebus and several confidential floating Scottish offshore wind farms (DONG Energy, 2013a, b; Navitus Bay Development Ltd, 2014; Vattenfall Wind Power Ltd, 2018; Ørsted, 2018; Blue Gem Wind, 2022 and ABPmer 2025 a, b, respectively).

5.3.2.2 The spreadsheet based numerical models used here are based upon the following information, assumptions and principles:

- Re-suspended coarser sediments (sands and gravels) will settle relatively rapidly to the seabed and their dispersion can therefore be considered on the basis of a 'snapshot' of the ambient conditions which are unlikely to vary greatly between the times of sediment release and settlement to the seabed. Re-suspended finer sediments may persist in the water column for hours or longer and so their dispersion is considered instead according to the longer-term net tidal current drift rate and direction in the area, which vary both temporally and spatially in speed and direction.
- A representative current speed for the OAA and offshore half of the offshore export cable corridor is 0.25 metres per second (m/s), which is representative of higher tidal flow conditions occurring on most flood and ebb cycles for a range of spring and neap conditions (Fugro, 2023b). Assuming a higher value, likely representative of the nearshore half of the offshore export cable corridor (0.5m/s) will increase dispersion and the extent of any effect, but with a proportional decrease in SSC and the thickness of subsequent deposits. In practice, a range of actual local conditions and outcomes are likely.
- Lateral dispersion of SSC in the plume is controlled by the horizontal eddy dispersion coefficient, Ke, estimated as $Ke = \kappa u^* z$ (Soulsby, 1997), where, z is the height above the seabed (a representative value of half the water depth is used), κ is the von Kármán coefficient ($\kappa = 0.4$) and u^* is the friction velocity ($u^* = \sqrt{(\tau/\rho)}$). Where ρ is the density of seawater ($\rho = 1027 kg/m^3$) and τ is the bed shear stress, calculated using the quadratic stress law ($\tau = \rho\ Cd\ U2$, (Soulsby, 1997)) using a representative current speed for the Project (U = 0.25m/s) and a drag coefficient value for a rippled sandy seabed (Cd = 0.006);
- The interpreted geophysical data and sediment grab samples from the OAA (Fugro, 2023a) and offshore export cable corridor (Fugro, 2024) indicate seabed sediments across the study area are highly variable, with coarse (sand and gravels) and fine (muddy) grained sediments present. The distribution broadly reflects spatial variation in current speeds, with coarser material encountered closer to the coast (where current speeds are high) and finer material found further offshore, including within the OAA (where current speeds are much lower).
- To estimate the time-scale in suspension, sediment is assumed to settle downwards at a calculated (theoretical) settling velocity for each grain size fraction (0.0001m/s for

fines, 0.05m/s for (medium) sands and 0.5m/s for gravels and generally coarser sediments, including clastic drill arisings).

5.3.2.3 The numerical model for SSC resulting from the release of sands and gravels is constructed as follows:

- The time required for sediment to settle at the identified settling velocity through a range of total water depths representative of the site is calculated, to yield the duration for settlement.
- The horizontal distance downstream that the plume is advected is found as the product of the representative ambient current speed and the duration for settlement.
- The horizontal footprint area of the plume at different water depths is calculated from the initial dispersion area, increasing at the horizontal dispersion rate over the elapsed time for the plume to reach that depth.
- The estimate of SSC at different elevations is found by dividing the sediment mass in suspension at a given water depth (the product of the sediment release rate and the duration of the impact, divided by the water depth) by the representative plume volume at that depth (horizontal footprint area at that depth x 1m).

5.3.2.4 The numerical model for sediment deposition thickness resulting from the release of sands and gravels is constructed as follows:

- The area over which sediment is deposited depends on the lateral spreading of the sediment plume footprint with depth, but also with tidal variation in current speed and direction, including the possibility of flow reversal. This is an important factor if the release occurs for more than tens of minutes as it affects the distance and direction which the plume is advected from the source.
- The width of the footprint of (instantaneous) deposition onto the seabed is estimated as the square root of the near-bed plume footprint area (calculated using the model for SSC, **paragraph 5.3.2.3**). When drilling anchor piles, the point of sediment release is likely to be static and so the width of deposition is characterised based on the footprint of release and a small amount of lateral dispersion between surface and seabed prior to deposition.
- The length of the footprint of deposition onto the seabed over multiple tidal cycles is estimated as twice the advected distance of the plume at the representative current speed, representing the maximum length over consecutive flood and ebb tides. If the operation lasts less than 12.4 hours (one full tidal cycle), the length is reduced proportionally.
- The average seabed deposition thickness is calculated as the total volume of sediment released, divided by the footprint area (width times length) of deposition.
- This model provides a conservative estimate of deposition thickness as it assumes that the whole sediment volume is deposited locally in a relatively narrow corridor. In practice, the deposition footprint on the seabed will probably be normally wider and frequently longer than is assumed, and the proportion of all sediment deposited locally will vary with the distribution in grain size (leading to a greater area but a correspondingly smaller average thickness).

5.3.2.5 The numerical model for SSC resulting from dispersion of fine sediment is constructed on the basis of the initial dispersion into the receiving waters, and then further dispersion of the plume as a whole, as per the following example for overspill for a trailing suction hopper dredger:

- The vessel is likely to be stationary during precision dredging operations so the water movement relative to the vessel is dominantly tidal (at the representative current speed 0.25m/s).
- Sediment is discharged at a representative rate (for example, 30 kilogram per second (kg/s) for dredging over-spill) into a minimum volume of water 100 cubic metres (m^3) = 10m x 10m x 1m deep.
- This volume of water will be refreshed every 40s (10m / 0.25m/s).
- The total sediment input is 40s x 30kg/s = 120 kilogram (kg).
- The resulting initial concentration in the receiving water is 1200kg / 100m^3 = 12kg/m^3 = 12,000mg/l.
- The initial concentration plume would then be subject to turbulent dispersion both laterally and vertically. Given the starting mass of sediment and water volume above, levels of SSC will vary rapidly in proportion to the dilution of the same sediment mass as the plume dimensions and volume increase.
- Assuming a faster current speed, faster vessel motion or larger footprint of release would reduce the mass of sediment introduced to the fixed volume of the receiving waters (and so SSC) at the point of initial dispersion, and vice versa.

5.4 Description of activities causing sediment disturbance

5.4.1 Drilling for offshore substations foundation installation

Overview

5.4.1.1 Driven piles for fixed offshore substation foundations will be installed into the seabed using standard piling techniques. In some locations, the particular geology may present some obstacle to piling, in which case, some or all of the seabed material might be drilled from within the pile footprint to assist in the piling process.

5.4.1.2 The impact of drilling operations mainly relates to the release of drilling spoil at or above the water surface which will put sediment into suspension and the subsequent re-deposition of that material to the seabed. The nature of this disturbance will be mostly determined by the rate and total volume of material to be drilled, the seabed and subsoil material type, and the drilling method (affecting the texture and grain size distribution of the drill spoil). The environmental conditions (total water depth, current speed and direction) over the period of active drilling will also affect the dimensions and concentration pattern of the plume and any subsequent deposition, to some extent; however, such conditions are likely to be continuously varying over time.

Evidence base

5.4.1.3 The evidence-base does not presently include many measurements of SSC resulting from drilling operations for driven pile installation. This is due to the relatively small number of occasions that such works have been necessary and the likely limited nature (extent, duration and SSC magnitude) of actual measurable impacts in practice.

5.4.1.4 Limited evidence from the field is provided by the during- and post-construction monitoring of monopile installation using drill-drive methods into chalk at the Lynn and Inner Dowsing Offshore Wind Farms (Centrica Renewable Energy Ltd, 2008). For the Project, it is recognised that the geological properties of the consolidated material, the drilling

dimensions and drilling apparatus will differ to some degree. In the Project OAA, it is also not yet known how the drilled sub-soils will disaggregate as a result of the final chosen tools and method for drilling if and where needed. All of the above factors limit the extent to which the Lynn and Inner Dowsing monitoring evidence can be considered to be indicative of the proposed construction activities for the Project.

5.4.1.5 The installation of steel monopiles (4.7m diameter and up to 20m penetration depth) was assisted in some cases by a drill-drive methodology. The drill arisings were mainly in the form of rock (chalk) chippings that were released onto the seabed a short distance away in a controlled manner using a pumped riser. The particular concern in that case was the possibility of sub-surface chalk arisings leading to high levels of SSC of an atypical sediment type. The result of sediment trap monitoring (located as close as 100m from the operation) was that the chalk was not observed to collect in significant quantities. However, direct measurements of SSC were not possible at the time of the operation.

5.4.1.6 The dimensions of the chalk drill arisings deposit created was measured by geophysical survey and characterised as a conical mound, approximately 3m thick at the peak, extending laterally (from the peak to ambient bed level) up to 10m in what is assumed the downstream direction and 5m in the other. The volume of the deposit (measured as approximately 290m^3) was similar to the total volume of the drilled hole (347m^3) indicating that the majority of the total drill arisings volume had been deposited locally. The difference in volumes might be partially explained by different patterns of settling or transport leading to some material settling away from the main deposit location. It is also possible that the combination of drill and drive did not necessarily release a volume of material equivalent to 100% of the internal volume of the pile, or that the full burial depth may not have been achieved in this example. Seabed photographs indicate that the material in the deposit is clearly horizontally graded, with the largest clasts closer to the centroid of the deposit.

5.4.2 Seabed preparation by dredging

Overview

5.4.2.1 To provide a stable footing for WTG anchors, offshore substations fixed foundations, SDCs and subsea substations, standard dredging techniques may be used to remove or lower the level of the mobile seabed sediment veneer within a footprint slightly larger than the anchor / foundation / structure base. Dredging may also be used to reduce the level of sandwaves where they are present in the footprint of foundations and in a narrow corridor where they intersect array, interconnector and offshore export cable routes in the OAA. There are areas of sandwaves present in the offshore export cable corridor as evidenced in the **Appendix 6.3: Marine Geology, Oceanography and Physical Processes Baseline Report**.

5.4.2.2 Dredging has the potential to cause elevated SSC by, sediment over-spill at the water surface during dredging and by the subsequent release of the dredged material from the dredger during spoil disposal at a nearby location. The subsequent settlement of the sediment disturbed by dredging will lead to sediment accumulation of varying thickness and extent on the seabed. These changes are quantitatively characterised in this Section using spreadsheet based numerical models.

Evidence base

5.4.2.3 The evidence-base with regards to dredging and elevated levels of SSC is broad and well established through a variety of monitoring and numerical modelling studies. The following text from the UK Marine Special Area of Conservation Project is representative of the wider evidence base.

"Dredging activities often generate no more increased suspended sediments than commercial shipping operations, bottom fishing or generated during severe storms (Parr et al., 1998). Furthermore, natural events such as storms, floods and large tides can increase suspended sediments over much larger areas, for longer periods than dredging operations (Environment Canada, 1994). It is therefore often very difficult to distinguish the environmental effects of dredging from those resulting from natural processes or normal navigation activities (Pennekamp et al., 1996).

…In general, the effects of suspended sediments and turbidity are generally short term (<1 week after activity) and near-field (<1 km from activity). There generally only needs to be concern if sensitive species are located in the vicinity of the maintained channel."

5.4.3 Cable burial

Overview

5.4.3.1 The impact of cable burial operations mainly relates to a localised and temporary re-suspension and subsequent settling of sediments (BERR, 2008). The exact nature of this disturbance will be determined by the soil conditions within the OAA and offshore export cable corridor, the length of installed cable, the burial depth and burial method. These changes are quantitatively characterised in this Section for export, array and substation interconnector cables.

5.4.3.2 The impact of dredging sandwaves as part of cable burial is assessed in **Section 5.4.2**. There are areas of sandwaves present in the offshore export cable corridor as evidenced in **Appendix 6.3**.

Evidence base

5.4.3.3 The evidence base with respect to cable burial activities is broad and includes a range of theoretical, numerical modelling and monitoring studies considering a range of installation methodologies, sediment types, water depths and other environmental conditions. The evidence base is widely applicable as the dimensions of the cables, the installation techniques used and the target depths of burial do not vary significantly with the scale of the development (small or large wind farm arrays) or the type of cable being installed (wind farm export, array or inter-connector cables, or non-wind farm electrical and communications cables).

5.4.3.4 SSC monitoring during cable laying operations has been undertaken at Nysted Wind Farm (BERR, 2008). During the works, both jetting and trenching were used, where the latter method involves pre-trenching and back-filling using back-hoe dredgers. Superficial sediments within the site were predominantly medium sands, approximately 0.5m to 3m in thickness, underlain by clay. SSC was recorded at a distance of 200m from jetting and trenching activities and the following values were observed:

- trenching – mean (14 milligrams per litre (mg/l)) and max (75mg/l); and
- jetting – mean (2mg/l) and max (18mg/l).

5.4.3.5 The higher sediment concentrations from the trenching activities were considered to be a result of the larger volume of seabed strata disturbed during operations and the fact that the material disturbed during trenching was lifted to the surface for inspection. This meant that the sediment was transported through the full water column before being placed alongside the trench (BERR, 2008).

5.4.3.6 Cable laying monitoring also took place at Kentish Flats where ploughing methods were used to install three offshore export cables (EMU Limited, 2005). Cefas agreed pre-defined threshold limits against which SSC monitoring would be compared. The monitoring 500m down-tide (where the concentrations would be greatest) of the cable laying activities showed:

- marginal, short-term increases in background levels (approximately nine times increase to the background concentrations); and
- peak concentrations occasionally reaching 140mg/l (equivalent to peaks in the naturally occurring background concentrations).

5.4.3.7 The observations at Nysted and Kentish Flats provide confidence that cable laying activities do not create a long-term, significant disruption to the background sediment concentrations. Furthermore, it also illustrates that there is little sediment dispersal, indicating that there is unlikely to be much deposition on the seabed other than immediately adjacent to the cable route.

5.4.3.8 Reach (2007) describes plume dispersion studies for a cable laying jetting operation in Hong Kong with an assumption that 20% of a trench cross-section of 1.75m² would be disturbed by the jetting process and the speed of the jetting machine would be 300m/hour (0.083m/s). Applied Science Associates (2006) describes similar studies for a cable laying operation near Cape Cod in the USA and assumed that 30% of a trench cross-section of 3m² would be disturbed by the jetting process and the speed of the jetting machine would be 91m/hour (0.025m/s). This latter study also assumed that any sand particles would quickly return to the bed and only the fine sediment particles (particles with a diameter less than 63 micrometres (µm)) would form a plume in the water column.

5.4.3.9 SeaScape Energy (2008) describes cable installation plume dispersion monitoring studies carried out at the Burbo Offshore Wind Farm in Liverpool Bay, UK.

- Three offshore export cables were installed to a target depth of approximately 3m by vertical injector ploughing while array cables were installed to a similar depth by jetting assisted ploughing.
- The monitoring demonstrated clearly that both cable installation techniques had only small scale impacts on localised SSC. Changes were measurable to a few hundreds of metres only and suspended sediment levels were not elevated more than five times background. Suspended sediment levels never approached the threshold level (3,000mg/l) agreed with regulatory authorities beforehand, even in very close proximity to the works (less than 50m).
- Local changes in SSC over a relatively fine sediment seabed area (most likely to lead to plume impacts) was in the region of 250mg/l to 300mg/l within 200m of the operation, falling to the measured baseline level (100mg/l) by 700m downstream. It is assumed, therefore, that coarser sediments were associated with even lower levels.

5.4.3.10 The post-burial impacts of cable burial on sandy seabed morphology were also considered by BERR (2008) with reference to a wide range of desktop and monitoring studies. The report concludes that impacts will also be limited in terms of both the thickness of re-deposited sediments and the potential for affecting the surficial sediment type:

"The low levels of sediment that are mobilised during cable laying mean that there will be only low levels of deposition around the cable route. The finer material will generally remain in suspension for longer but will settle and remobilise on each tide with no measurable material left in place. Coarser sediments are expected to settle within a few metres of the cable route and following disturbance is likely to recover rapidly, given similar communities in the vicinity." (BERR, 2008).

5.4.4 Drilling fluid release during horizontal directional drilling at the landfall

5.4.4.1 HDD is the preferred option to transition the Project offshore export cable to the onshore grid at the landfall. The drill punch-out location will be in the subtidal area. Up to eight HDD conduits might be required.

5.4.4.2 The release of drilling fluid (a suspension of natural bentonite clay in water) into the coastal waters at the punch-out location may cause a sediment plume in the nearshore area.

5.4.4.3 Drilling fluid is a composite made of bentonite and water with the following functions:

- to remove cuttings from in front of the drill bit;
- power the mud motor;
- to transport cuttings from the drill face through the annular space towards the surface;
- lubricate the drill string during drilling phases and high-density polyethylene strings during pull back;
- cooling the reamers (cutting tools);
- hole stabilisation; and
- creation of a filter cake against the wall of the hole to minimize the risk of loss of drilling fluid or influx of groundwater penetration into the borehole.

5.4.4.4 The drilling fluid typically consists of a low concentration bentonite - water mixture. Depending on the formation to be drilled through, the concentration is typically between 13 litres (l) (30kg) and 35l (80kg) of dry bentonite clay per 1m³ of water (30,000mg/l to 80,000mg/l).

5.4.4.5 The use of bentonite has limited potential to cause environmental impacts:

- it is a natural material, so has no chemical constituents;
- it is recyclable;
- it is on the OSPAR List of Substances Used and Discharged Offshore which Are Considered to Pose Little or No Risk to the Environment (OSPAR, 2013); and
- owing to the large diameter pipe and long length, the total volume of fluid used may be relatively large, but, owing to the low concentration, the total amount of bentonite used is limited.

5.4.4.6 At the point of ‘punch out’ some of the total volume of drilling fluid may be released into the surrounding seawater by residual pressure in the system, and further movement of the equipment. The size of the plume will be initially very small in extent and localised to the end of the drill bit and borehole (order of a few metres diameter); the SSC of the undiluted drilling fluid at this point will be very high (30,000mg/l to 80,000mg/l). The free end of the plume will be advected (transported passively) at the speed and direction of the ambient tidal current at the time of the release and the narrow plume will gradually grow in length for the (limited) period of time that drilling fluid continues to be released.

5.4.4.7 The plume will be subject to turbulent dispersion over time and distance as it is advected. The width and the height of the plume will gradually increase, but the SCC within the plume will rapidly decrease in proportion to the increase in volume.

5.4.4.8 Bentonite clay grains are very small and so are likely to stay in suspension for long periods of time (days to weeks or longer) in the relatively turbulent marine environment. As a result,

the Bentonite clay in the drilling fluid is expected to become progressively dispersed to very low concentrations (not measurably different from ambient natural turbidity levels) over periods of hours to days and will therefore not settle or accumulate onto the seabed in measurable thickness in any location more than a few tens of metres from the main point of release.

5.5 Results

5.5.1 Baseline conditions

5.5.1.1 A more detailed description of naturally varying SSC in the study area can be found in the **Appendix: 6.3**.The following summary information is repeated here.

5.5.1.2 Monthly-averaged satellite imagery of Suspended Particulate Matter (SPM) concentration in surface waters suggests that, within the OAA, average surface SPM is generally very low, between approximately 0.5mg/l to 2.0mg/l (Cefas, 2016). During the summer months, values within the OAA are generally <1mg/l, increasing slightly in the winter months to ~ 2mg/l to 3mg/l. Still small, but relatively higher values, are anticipated during larger spring tides and storm conditions. Higher suspended sediment concentrations are also likely to be observed at any given time closer to the seabed due to local resuspension by currents and wave action.

5.5.1.3 SPM values along the offshore export cable corridor are also generally very low but increase slightly from the OAA towards the landfall. In the winter months, SPM values range from 1mg/l to 5mg/l, decreasing to an average of <1mg/l in summer months.

5.5.2 Impact assessment

5.5.2.1 This Section provides a description of the realistically possible combinations of magnitude and extent of impact for local increases in SSC and seabed deposition, due to sediment disturbance potentially caused by:

- drilling for offshore substations foundation installation;
- seabed preparation by dredging for WTG anchors, SDCs, subsea substations and offshore substations foundations;
- sandwave clearance prior to cable burial;
- cable burial; and
- drilling fluid release during HDD at the landfall.

5.5.2.2 The actual magnitude and extent of such impacts will depend in practice on a range of factors, such as the actual total volumes and rates of sediment disturbance, the local water depth and current speed at the time of the activity, the local sediment type and grain size distribution, the local seabed topography and slopes, etc. There will be a wide range of possible combinations of these factors and so it is not possible to predict specific dimensions with complete certainty. To provide a robust assessment, a range of realistic combinations have been considered, based on conservatively representative location (environmental) and project (maximum design scenario) specific information, including a range of water depths, heights of sediment ejection / initial resuspension, and sediment types.

5.5.2.3 This wider range of results can be summarised broadly in terms of four main zones of effect, based on the distance from the activity causing sediment disturbance.

- 0m to 25m - zone of highest SSC increase and greatest likely thickness of deposition. All gravel sized sediment likely deposited in this zone, also a large proportion of sands that are not resuspended high into the water column, and also most or all dredge spoil in the active phase. Plume dimensions and SSC, and deposit extent and thickness, are primarily controlled by the volume of sediment released and the manner in which the deposit settles:
  - At the time of active disturbance - very high SSC increase (tens to hundreds of thousands of mg/l) lasting for the duration of active disturbance plus up to 30 minutes following end of disturbance; sands and gravels may deposit in local thicknesses of tens of centimetres to several metres; fine sediment is unlikely to deposit in measurable thickness.
  - More than one hour after the end of active disturbance - no change to SSC; no measurable ongoing deposition.
- 25m to 250m - zone of measurable SSC increase and measurable but lesser thickness of deposition. Mainly sands that are released or resuspended higher in the water column and resettling to the seabed whilst being advected by ambient tidal currents. Plume dimensions and SSC, and deposit extent and thickness, are primarily controlled by the volume of sediment released, the height of resuspension or release above the seabed, and the ambient current speed and direction at the time:
  - At the time of active disturbance - high SSC increase (hundreds to low thousands of mg/l) lasting for the duration of active disturbance plus up to 30 minutes following end of disturbance; sands and gravels may deposit in local thicknesses of up to tens of centimetres; fine sediment is unlikely to deposit in measurable thickness.
  - More than one hour after end of active disturbance - no change to SSC; no measurable ongoing deposition.
- 250m to the tidal excursion buffer distance - zone of lesser but measurable SSC increase and no measurable thickness of deposition. Mainly fines that are maintained in suspension for more than one tidal cycle and are advected by ambient tidal currents. Plume dimensions and SSC are primarily controlled by the volume of sediment released, the patterns of current speed and direction at the place and time of release and where the plume moves to over the following 24 hours:
  - At the time of active disturbance - low to intermediate SSC increase (tens to low hundreds of mg/l) as a result of any remaining fines in suspension, only within a narrow plume (tens to a few hundreds of metres wide, SSC decreasing rapidly by dispersion to ambient values within one day after the end of active disturbance; fine sediment is unlikely to deposit in measurable thickness.
  - One to six hours after end of active disturbance - decreasing to low SSC increase (tens of mg/l); fine sediment is unlikely to deposit in measurable thickness.
  - Six to 24 hours after end of active disturbance - decreasing gradually through dispersion to background SSC (no measurable local increase); fine sediment is unlikely to deposit in measurable thickness. No measurable change from baseline SSC after 24 hours to 48 hours following cessation of activities.
- Beyond the tidal excursion buffer distance or anywhere not tidally aligned to the active sediment disturbance activity - there is no expected impact or change to SSC nor a measurable sediment deposition.

5.5.2.4 **Figure 2** illustrates the maximum spatial extent of these zones in relation to the whole of the Project OAA and offshore export cable corridor, and in relation to selected receptors in the surrounding area. **Figure 3** provides an example schematic illustration of the footprint

of effect for a single occurrence of an activity causing local sediment disturbance. In practice the MDS impact will be a limited number of discrete areas of effect (similar to that shown in the example), separated by areas of lesser impact.

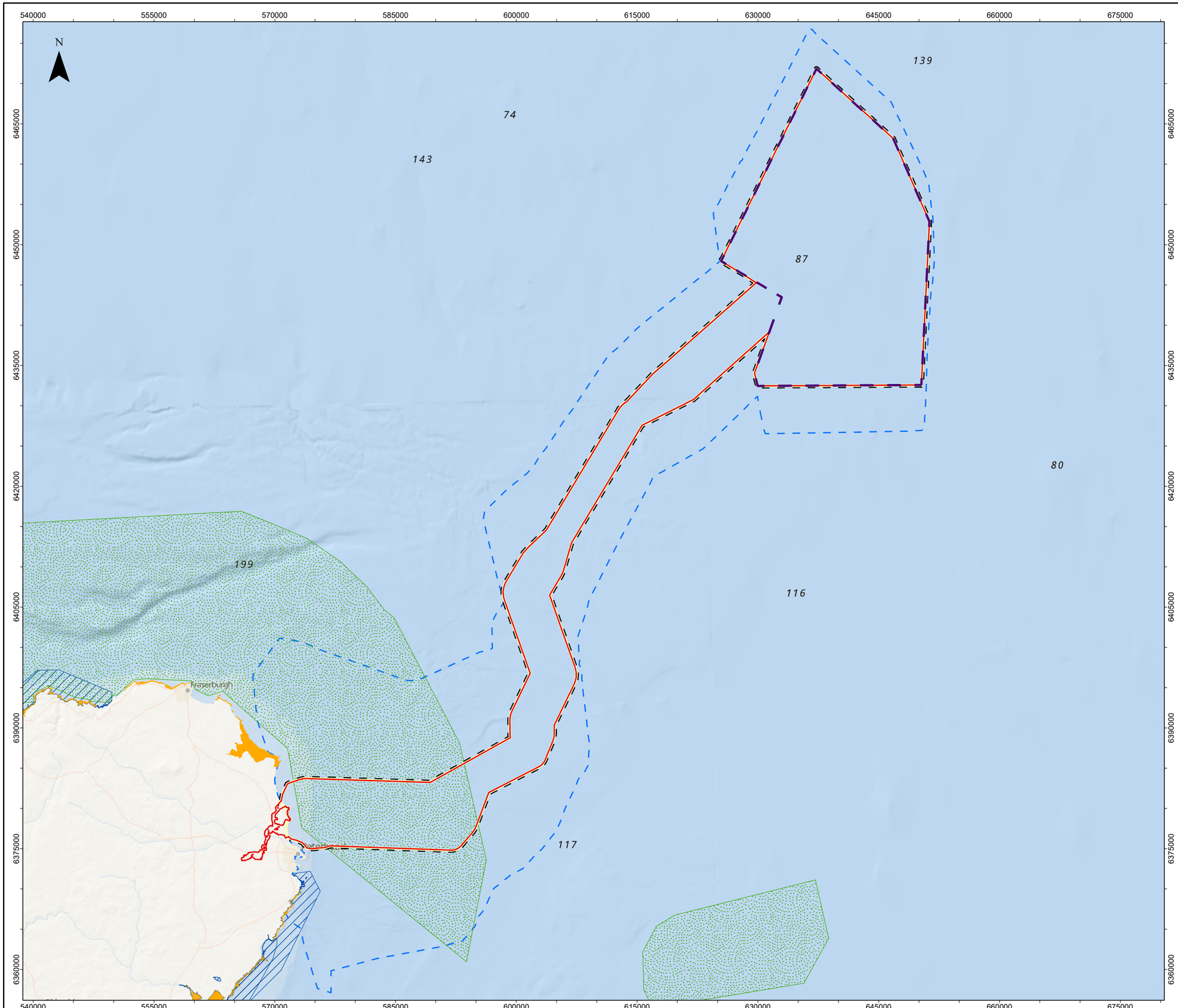

Red Line Boundary

Option Agreement Area

25m buffer around the Red Line Boundary

250m buffer around the Red Line Boundary

Spring tidal excursion ellipse buffer

Site of Special Scientific Interest

Marine Protected Area

Special Protection Area

0 10 20 Kilometres

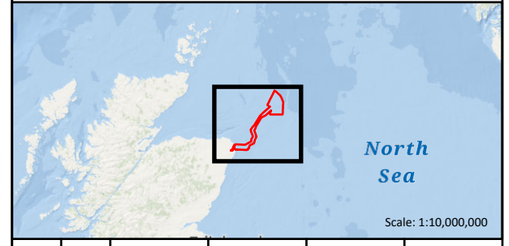

	dd/mm/yyyy	--	--	--	--
	dd/mm/yyyy	--	--	--	--
2	18/09/2025	AW		DL	DL
REV	REV DATE	GIS CREATOR	GIS REVIEWER	TECHNICAL CHECKER	TECHNICAL APPROVER

WSP DRAWING NUMBER	808368-WEIS-IA-E5-FG-M7-10099
MarramWind DRAWING NUMBER	MAR-GEN-ENV-MAP-WSP-000360

DATUM	ETRS 89	PROJECTION	UTM Zone 30N
SCALE	1:450,000	PAGE SIZE	A3

PROJECT TITLE

MarramWind Offshore Wind Farm

DRAWING TITLE

Figure 2 Spring tidal excursion buffer, 25m and 250m buffers outside of the OAA and offshore export cable corridor

Environmental Impact Assessment Report

Appendix 6.1

NOT TO BE USED FOR NAVIGATION

wsp

MarramWind

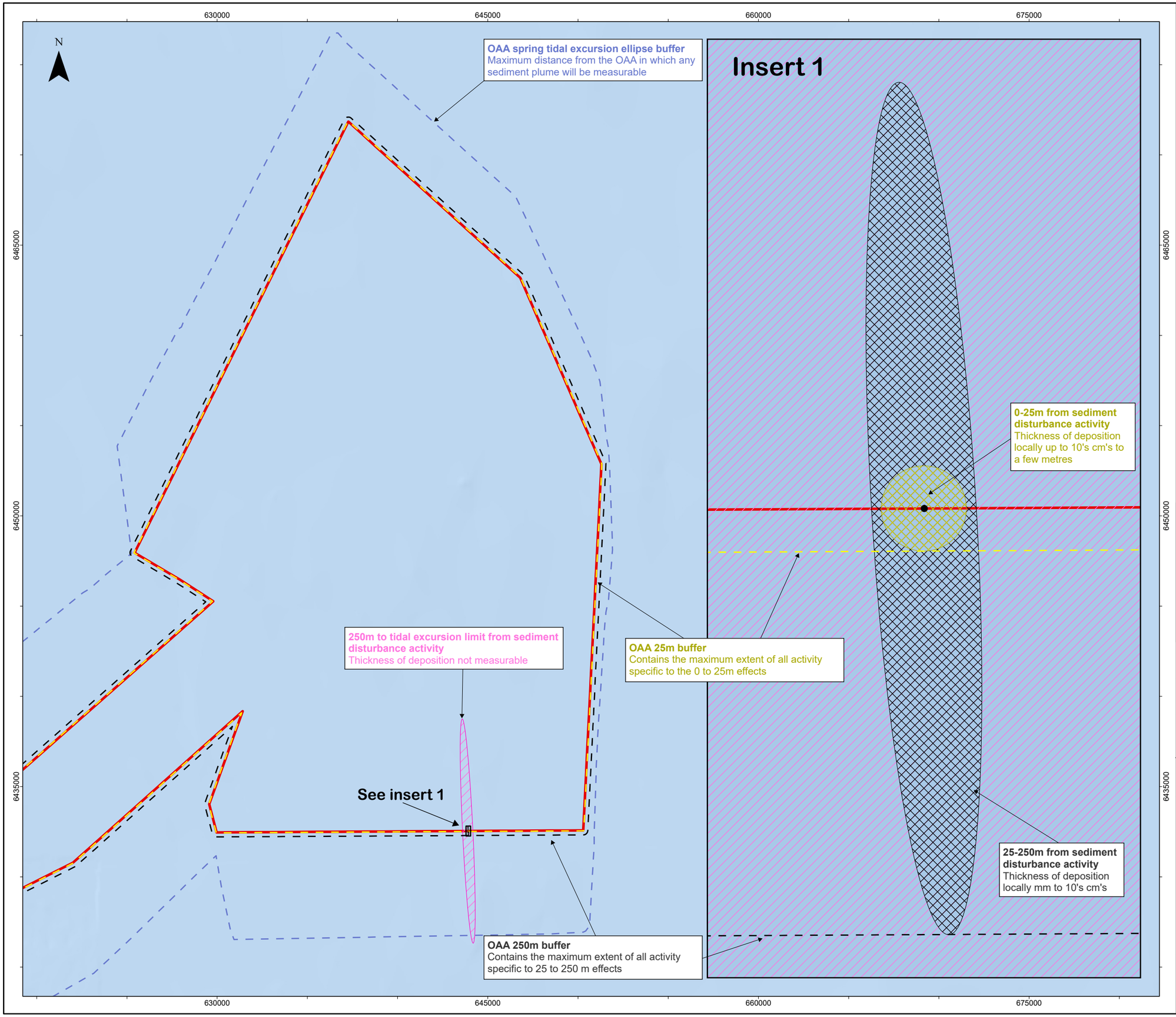

- Red line boundary
- OAA 25m buffer
- OAA 250m buffer
- OAA Spring tidal excursion ellipse buffer
- Activity sediment release location
- Activity 25m buffer
- Activity 250m buffer
- Activity tidal excursion ellipse maximum zone of influence

0 10 Kilometres

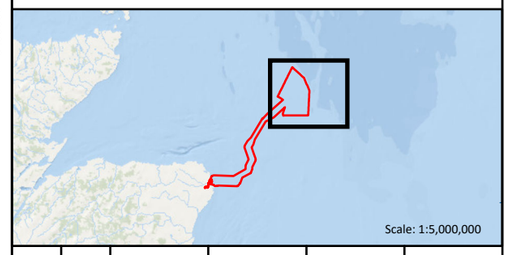

	dd/mm/yyyy	--	--	--	--
	dd/mm/yyyy	--	--	--	--
2	18/09/2025	AW		DL	DL
REV	REV DATE	GIS CREATOR	GIS REVIEWER	TECHNICAL CHECKER	TECHNICAL APPROVER

WSP DRAWING NUMBER	808368-WEIS-IA-E5-FG-M7-30044
MarramWind DRAWING NUMBER	MAR-GEN-ENV-MAP-WSP-000361

DATUM	ETRS 89	PROJECTION	UTM Zone 30N
SCALE	1:200,000	PAGE SIZE	A3

PROJECT TITLE

MarramWind Offshore Wind Farm

DRAWING TITLE

Figure 3 Sediment deposition footprints associated with a single disturbance activity at an example location in the OAA

Environmental Impact Assessment Report

Appendix 6.1

NOT TO BE USED FOR NAVIGATION

wsp MarramWind

5.5.3 Cumulative impacts

Overview

5.5.3.1 A Cumulative Effects Assessment (CEA) has been undertaken to consider the impact associated with the Project together with other projects and plans (see **Volume 1, Chapter 33: Cumulative Effects Assessment**). Each project on the CEA long list has been considered on a case-by-case basis for scoping in or out of the **Volume 1, Chapter 6: Marine Geology Oceanography and Physical Processes**, based upon data confidence, effect-receptor pathways and the spatial / temporal scales involved.

5.5.3.2 In terms of the potential for cumulative changes to SSC, bed levels and sediment type, the screening approach described above was informed using modelled spring tidal excursion ellipses. This is because meaningful sediment plume interaction generally only has the potential to occur if the activities generating the sediment plumes are located within one spring tidal excursion ellipse from one another and occur at the same time.

5.5.3.3 Detailed consideration of cumulative changes to SSC, bed levels and sediment type is provided in **Volume 1, Chapter 6: Marine Geology, Oceanography and Physical Processes**.

5.6 Summary

5.6.1.1 Location and project specific numerical (spreadsheet) modelling were used to assess changes to suspended sediment concentration and associated deposition of sediment as a result of construction activities related to the Project (drilling, seabed preparation, cable burial and HDD punchout).

5.6.1.2 The actual magnitude and extent of SSC and bed deposition will depend in practice on a wide range of factors, such as the actual total volumes and rates of sediment disturbance, the local water depth and current speed at the time of the activity, the local sediment type and grain size distribution, the local seabed topography and slopes, etc. Applying realistic and conservative combinations of these factors has allowed a robust assessment over a range of conditions.

5.6.1.3 A representative current speed for the OAA and offshore half of the offshore export cable corridor is 0.25m/s, which is representative of higher tidal flow conditions occurring on most flood and ebb cycles for a range of spring and neap conditions (Fugro, 2023b). Assuming a higher value, likely representative of the nearshore half of the offshore export cable corridor (0.5m/s) will increase dispersion and the extent of any effect, but with a proportional decrease in SSC and the thickness of subsequent deposits. In practice, a range of actual local conditions and outcomes are likely.

5.6.1.4 This wider range of results can be summarised broadly in terms of four main zones of effect, based on the distance from the activity causing sediment disturbance. Assuming a representative current speed of 0.25m/s these zones are:

- 0m to 25m - zone of highest SSC increase and greatest likely thickness of deposition.
- 25m to 250m - zone of measurable SSC increase and measurable but lesser thickness of deposition.
- 250m to the tidal excursion buffer distance - zone of lesser but measurable SSC increase and no measurable thickness of deposition.

- Beyond the tidal excursion buffer distance or anywhere not tidally aligned to the active sediment disturbance activity - there is no expected impact or change to SSC nor a measurable sediment deposition.

6. References

ABPmer, HR Wallingford, and Cefas, (2010). *Further review of sediment monitoring data*. (Collaborative Offshore Wind Research into the Environment Ltd ScourSed-09).

ABPmer., (2013). *SEASTATES Wave Hindcast Model, Calibration and Validation Report,* August 2013. [online] Available at: https://www.seastates.net/downloads/ [Accessed: 06 May 2025].

ABPmer, (2017). *SEASTATES North West European Continental Shelf Tide and Surge Hindcast Database, Model validation report*, March 2017. [online] Available at: https://www.seastates.net/downloads/ [Accessed: 06 May 2025].

ABPmer, (2021). *Awel y Môr Offshore Windfarm Environmental Impact Assessment*, *Volume 4, Annex 2.3: Marine Geology, Oceanography and Physical Processes Technical Assessment*. ABPmer Report No. R3628. A report produced by ABPmer for GoBe Consultants Ltd, March 2022.

ABPmer, (2024). *Five Estuaries Offshore Windfarm Environmental Impact Assessment, Volume 6, Part 5, Annex 2.3: Physical Processes Technical Assessment*. ABPmer Report No. R.3628. A report produced by ABPmer for GoBe Consultants Ltd.

ABPmer, (2025a). *Confidential Scottish Floating Offshore Windfarm Environmental Impact Assessment*.

ABPmer, (2025b). *Confidential Scottish Floating Offshore Windfarm Environmental Impact Assessment*.

Applied Science Associates, (2006). *Simulation of Sediment Transport and Deposition from Cable Buria Operation for the Alternative Site of the Vape Wind Energy Project*. Prepared for Cape Wind Associates, LLC.

Blue Gem Wind, (2022). *Environmental Statement for Erebus Floating Offshore Wind Farm: Coastal Processes Chapter and Associated Appendices*.

Breusers, H.N.C., Nicollet, G., and Shen, H.W., (1977). *Local scour around cylindrical piers*. J. of Hydraulic Res., IAHR, Vol. 15, No. 3, pp. 211 252.

Carpenter, J.R., Merckelbach, L., Callies, U., Clark, S., Gaslikova, L., and Baschek, B., (2016). *Potential Impacts of Offshore Wind Farms on North Sea Stratification*. PLoS ONE 11(8).

Cazenave, P. W., Torres, J., and Icarus Allen, J., (2016). *Unstructured grid modelling of offshore wind farm impacts on seasonally stratified shelf seas*. Progress in Oceanography, 145, pp. 25-41.

Centre for Environment, Fisheries and Aquaculture Science (Cefas), (2016). Suspended Sediment Climatologies around the UK. Report for the UK. Department for Business, Energy & Industrial Strategy offshore energy Strategic Environmental Assessment programme

Centrica Renewable Energy Ltd, (2008). *Environmental Report for Monitoring of the Disposal of Drill arisings, Lynn & Inner Dowsing*.

Christiansen, N., Daewl, U., Djath, B., and Schrum, C., (2022). *Emergence of Large-Scale Hydrodynamic Structures Due to Atmospheric Offshore Wind Farm Wakes*. Frontier Marine Science, Vol. 9.

Chust, G., Allen, J.I., Bopp, L., Schrum, C., Holt, J., Tsiaras, K., Zavatarelli, M., Chifflet, M., Cannaby, H., Dadou, I., Daewel, U., Wakelin, S. L., Machu, E., Pushpadas, D., Butenschon, M., Artioli, Y., Petihakis, G., Smith, C., Garçon, V., Goubanova, K., Le Vu, B., Fach, B.A., Salihoglu, B., Clementi, E., and Irigoien, X., (2014). *Biomass changes and trophic amplification of plankton in a warmer climate*. Global Change Biology, 20(7), 2124-2139, doi: 10.1111/gcb.12562.

Ciavatta, S., Brewin, R.J.W., Skákala, J., Polimene, L., de Mora, L., Artioli, Y., and Allen, J.I., (2018). *Assimilation of ocean-color plankton functional types to improve marine ecosystem simulations*. Journal of Geophysical Research: Oceans, 123, 834–854.

Copernicus Marine Service, (2024a). *Atlantic- European Northwest Shelf- Ocean Physics Reanalysis*. [online] Available at: https://data.marine.copernicus.eu/product/NWSHELF_MULTIYEAR_PHY_004_009/description [Accessed on: 06 May 2025].

Copernicus Marine Service, (2024b). *Atlantic- European Northwest Shelf- Ocean Biogeochemistry Reanalysis*. [online] Available at: https://data.marine.copernicus.eu/product/NWSHELF_MULTIYEAR_BGC_004_011/description?view=-&option=-&product_id=- [Accessed on: 06 May 2025].

Deltares, (2023). *Handbook of scour and cable protection methods*. [online] Available at: https://www.deltares.nl/en/expertise/publications/handbook-of-scour-and-cable-protection-methods [Accessed on: 06 May 2025]

Department for Business Enterprise and Regulatory Reform (BERR), (2008). *Review of Cabling Techniques and Environmental Effects applicable to the Offshore Wind farm Industry Technical Report*. Department for Business Enterprise and Regulatory Reform in association with Defra.

Det Norske Veritas, (2016). *Support structures for Wind Turbines*. Offshore Standard DNVGL-ST-0126, 182pp.

DHI, (2025). *MIKE 21 Spectral Wave Module Scientific Documentation*.

DONG Energy, (2013a). *Environmental Statement for Burbo Bank Extension Offshore Wind Farm: Chapter 10 – Metocean and Physical Processes*.

DONG Energy, (2013b). *Environmental Statement for Walney Extension Offshore Wind Farm*.

Dorrell, R.M., Lloyd, C.J., Lincoln, B.J., Rippeth, T. P., Taylor, J. R., Caulfield, C.P., Sharples, J., Polton, J.A., Scannell, B.D., Greaves, D.M., Hall, R.A., and Simpson, J.H., (2022). *Anthropogenic Mixing in Seasonally Stratified Shelf Seas by Offshore Wind Farm Infrastructure*. Front. Mar. Sci. 9:830927.

EMODnet, (2025). *Bathymetry Data Portal*. [online] Available at: https://www.emodnet-bathymetry.eu/ [Accessed on: 06 May 2025].

EMU Limited, (2005). *Kentish Flats Offshore Wind Farm Post-construction Debris Survey*. Report to Kentish Flats Ltd, Report Ref 05/J/1/02/0869/0563.

Faltinsen, O. M., (1990). *Sea Loads on Ships and Offshore Structures*. Cambridge University Press, Cambridge, CB2 1RP, UK.

Fugro, (2023a). *Geophysical and Environmental Offshore Windfarm Survey, MarramWind Floating Offshore Windfarm, NE7, Volume 1 of 11: Geophysical Results Report*. Fugro Report No. 220154-OWF-01. A report produced by Fugro GB for MarramWind Limited.

Fugro, (2023b). *MarramWind Floating Offshore Windfarm: Metocean Survey Data*.

Fugro, (2024). *Geophysical, Environmental and Geotechnical Export Cable Corridor Survey, MarrramWind Floating Offshore Windfarm ECC, NE7, Volume 1 of 8: Geophysical Interpretive Report.* Fugro Report No. 230308-ECC-01. A report produced by Fugro GB for MarramWind Limited.

Garcia-Nieto, P.J., Garcia-Gonzalo, E., Fernandez, J.R.A, Muiz, C.D., (2024), *Forecast of chlorophyll-a concentration as an indicator of phytoplankton biomass in El Val reservoir by utilizing various machine learning techniques: A case study in Ebro River basin, Spain*. Journal of Hydrology, 639.

Gormsen, C. and Larsen, T., (1984). *Time development of scour around offshore structures*. ISVA, Technical University of Denmark, 139pp. (In Danish).

Gowen, R., Stewart, B., Mills, D., and Elliott, P., (1995). *Regional differences in stratification and its effect on phytoplankton production and biomass in the northwestern Irish Sea*. J. Plankton Res. 17, 753–769.

Harris, J.M., Whitehouse, R.J.S. and Benson, T., (2010). *The time evolution of scour around offshore structures*. Proceedings of the Institution of Civil Engineers, Maritime Engineering, 163, March, Issue MA1, pp. 3 – 17.

Harris, J.M., Whitehouse, R.J.S. and Sutherland, J., (2011). *Marine scour and offshore wind - lessons learnt and future challenges*. Proceedings of the ASME 2011 30th International Conference on Ocean, Offshore and Arctic Engineering, OMAE2011, June 19-24, 2011, Rotterdam, The Netherlands, OMAE2011-50117.

Hill, V. and Cota, G., (2005). *Spatial patterns of primary production on the shelf, slope and basin of the Western Arctic in 2002.* Deep Sea Res. II 52, 3344–3354.

Hill, A.E., Brown, J. Fernand, L. Holt, J., Horsburgh, K. J., Proctor, R., Raine R. and Turrell, W.R., (2008). *Thermohaline circulation of shallow tidal seas*. Geophysical Research Letters. 35(11).

Hoffmans, G.J.C.M. and Verheij, H.J., (1997). *Scour Manual*. Balkema.

Holt, J., Hughes, S., Hopkins, J., Wakelin, S.L., Holliday, N.P., Dye, S., González-Pola, C., Hjøllo, S.S., Mork, K.A., Nolan, G., Proctor, R., Read, J., Shammon, T., Sherwin, T., Smyth, T., Tattersall, G., Ward, B., and Wiltshire, K.H., (2012) *Multi-decadal variability and trends in the temperature of the northwest European continental shelf: A model-data synthesis*. Progress in Oceanography, 106, 96-117, doi:10.1016/j.pocean.2012.08.001.

HR Wallingford, ABPmer and Cefas, (2007). *Dynamics of scour pits and scour protection - Synthesis report and recommendations.* (Sed02)

Jardine, J.E., Palmer, M.R., Mahaffey, C., Holt, J., Wakelin, S. and Artioli, Y., (2022). *Climatic controls on the spring phytoplankton growing season in a temperate shelf sea*. Journal of Geophysical Research: Oceans, e2021JC017209.

MarramWind Limited, (2023). *MarramWind Offshore Wind Farm Environmental Impact Assessment – Scoping Report.* [online] Available at: https://marramwind.co.uk/scoping-report [Accessed: 07 August 2025].

Miles, J., Martin, T., Goddard, L., (2017). *Current and wave effects around windfarm monopile foundations*. Coastal Engineering 121, 167-178.

Miller, P.I., Xu, W., Lonsdale, P., (2014). *Seasonal shelf-sea front mapping using satellite ocean colour to support development of the Scottish MPA network*. Scottish Natural Heritage Commissioned Report No. 538.

Navitus Bay Development Ltd, (2014). *Navitus Bay Wind Park Environmental Statement. Volume B – Offshore: Chapter 5 – Physical Processes.* Document 6.1.2.5.

Ørsted, (2018). *Hornsea Project Three Offshore Wind Farm Environmental Statement*.

OSPAR Commission, (2013). *OSPAR List of Substances Used and Discharged Offshore which Are Considered to Pose Little or No Risk to the Environment (PLONOR) – Update 2024*. [online] Available at: https://www.ospar.org/documents?v=32939 [Accessed: 08 August 2025].

Ramsay D.L., and Brampton A.H., (2000a). *Coastal Cells in Scotland: Cell 2 – Fife Ness to Cairnbulg Point*. Scottish Natural Heritage Research, Survey and Monitoring Report No 144.

Ramsay D.L., and Brampton A.H., (2000b). *Coastal Cells in Scotland: Cell 3 – Cairnbulg Point to Duncansby Head*. Scottish Natural Heritage Research, Survey and Monitoring Report No 145.

Reach, (2007). *Asia-America Gateway (AAG) Cable Network, South Lantau, Project Profile 2007*. Report prepared by Atkins and EGS for Reach Networks Hong Kong Ltd. 2007.

SeaScape Energy, (2008). *Burbo Offshore Wind Farm: Construction Phase Environmental Monitoring Report*. CMACS for SeaScape Energy. April 2008.

Sharples, J., Ross, O.N., Scott B.E., Greenstreet, S.P.R., and Fraser, H., (2006). *Inter-annual variability in the timing of stratification and the spring bloom in the North-western North Sea*. Continental Shelf Research, 26(6), 733–751, doi:10.1016/j.csr.2006.01.011.

Sharples, J., Holt, J., Wakelin, S., Palmer, M.R., (2022). *Climate change impacts on stratification relevant to the UK and Ireland*. Marine Climate Change Impacts Partnership Science Review, 11pp.

Sharples, J., Holt, J., Wakelin, S., Palmer, M.R., Graham, J.A., (2025). *Climate change impacts on stratification relevant to the UK and Ireland*. Marine Climate Change Impacts Partnership Science Review, 13pp.

Simpson, J.H., and Bowers, D., (1981). *Models of stratification and frontal movement in shelf seas*. Deep Sea Research Part A. Oceanographic Research Papers. 28, 7, pp. 727-738.

Simpson, J.H. and Sharples, J., (2012). *Physical and Biological Oceanography of shelf Seas*. Cambridge University Press, CBO9781139034098

Soulsby, R., (1997). *Dynamics of Marine Sands*. Thomas Telford, London. pp249

Sumer, B.M. and Fredsøe, J., (2001). *Wave scour around a large vertical circular cylinder*. J. Waterway, Port, Coastal, and Ocean Engineering. May/June 2001.

Sumer, B.M. and Fredsøe, J., (2002). *The mechanics of scour in the marine environment*. Advanced series in Ocean Engineering - Volume 17.

Sumer, B.M., Fredsøe, J. and Christiansen, N., (1992). *Scour around a vertical pile in waves*. J. Waterway, Port, Coastal, and Ocean Engineering. ASCE, Vol. 118, No. 1, pp. 15 - 31.

Thames Estuary Dredging Association (TEDA), (2010). *Thames Estuary Marine Aggregates Regional Environmental Assessment (MAREA)*. Reports produced on behalf of the Thames Estuary Dredging Association. October 2010

Thames Estuary Dredging Association (TEDA), (2012). *Thames Estuary Marine Aggregates Regional Environmental Assessment (MAREA)*. Reports produced on behalf of the Thames Estuary Dredging Association. October 2012.

Tinker, J., Lowe, J., Pardaens, A., Holt, J., and Barciela. R., (2016). *Uncertainty in climate projections for the 21st century northwest European shelf seas*. Progress in Oceanography, 148 (Supplement C), 56-73. doi: https://doi.org/10.1016/j.pocean.2016.09.003.

Tonani, M., Ascione, I. and Saulter, A., (2022). *Product User Manual v.1.3 – Ocean Physical and Biogeochemical reanalysis*. Copernicus Marine Service.

Vattenfall Wind Power Ltd., (2018). *Thanet Extension Offshore Wind Farm Environmental Statement.*

University College London and United Kingdom Hydrographic Office, (2005). *Vertical Offshore Reference Frames (VORF)*. [online] Available at: https://www.ucl.ac.uk/civil-environmental-geomatic-engineering/research/groups-and-centres/vertical-offshore-reference-frames-vorf [Accessed: 06 May 2025].

van Leeuwen, S., Tett, P., Mills, D., and van der Molen, J., (2015). *Stratified and non-stratified areas in the North Sea: Long-term variability and biological and policy implications*. Journal of Geophysical Research-Oceans, 120(7), 4670-4686.

Whitehouse, R.J.S., (1998). *Scour at marine structures: A manual for practical applications*. Thomas Telford, London, 198 pp.

Whitehouse, R.J.S., (2004). *Marine scour at large foundations*. In: Proc. 2nd Int. Conf. On Scour and Erosion, (eds). Chiew, Y-M., Lim, S-Y. and Cheng, N-S., Singapore, 14 - 17 Nov, Vol. 2, pp. 451 to463.

Yamaguchi, R., Toshio, S., Richards, K.J. and Qiu, B., (2019). *Diagnosing the development of seasonal stratification using the potential energy anomaly in the North Pacific*. Climate Dynamics.

7. Glossary of Terms and Abbreviations

7.1 Abbreviations

Acronym	Definition
CEA	Cumulative Effects Assessment
DirM	Mean Wave Direction
DirStd	Directional Standard Deviation
E	East
EIA	Environmental Impact Assessment
ENE	East Northeast
EVA	Extreme Value Analysis
G/D	Gap to Near Bed Member Diameter Ratio
GOTM	General Ocean Turbulence Model
HDD	Horizontal Directional Drilling
Hs	Significant Wave Height
KC	Keulegan-Carpenter
LAT	Lowest Astronomical Tide
MHW	Marine Heat Wave
MSL	Mean Sea Level
MW	Megawatt
N	North
NCMPA	Nature Conservation Marine Protected Area
NE	Northeast
NNE	North Northeast
O&M	Operation and Maintenance
OAA	Option Agreement Area
PEA	Potential Energy Anomaly
PP	Primary Productivity
RCP	Reactive Compensation Platform

Acronym	Definition
RP	Return Period
SDC	Subsea Distribution Centre
SPM	Suspended Particulate Matter
SSC	Suspended Sediment Concentration
SSSI	Site Of Special Scientific Interest
SW	Spectral Wave
TEDA	Thames Estuary Dredging Association
TKE	Turbulent Kinetic Energy
Tp	Peak Wave Period
WTG	Wind Turbine Generator

7.2 Glossary

Term	Definition
50% non-exceedance	A statistical threshold indicating that a given value is expected to be exceeded only 50% of the time. It represents the median condition in a dataset and is used to describe average conditions.
Global scour	Scour within and closely around the footprint of a multi-legged structure, such as a jacket structure
Holocene	The current geological epoch, which began approximately 11,700 years ago after the end of the last Ice Age.
Intertidal area	The area between MHWS and Mean Low Water Springs (MLWS).
Local scour	Scour around an individual structure, for example around a single monopile or around one leg of a jacket structure.
Morphology	Term used to describe channel form and its process of change in shape and direction over time
Primary production	The process by which phytoplankton convert inorganic into organic material using sunlight through photosynthesis.
Pycnocline	A depth layer in a body of water where the water density changes rapidly with depth due to variations in temperature and/or salinity.
Return period	The average time interval between occurrences of a specific event.

Term	Definition
Seastate	The ocean surface conditions at a given time and location, typically defined by wave height, wave period, and wind conditions.
Scour protection	Protective materials to avoid sediment being eroded away from the base of the foundations due to the flow of water.
Significant wave height	The average height of the highest one-third of waves observed over a given period.
Subtidal	Areas of the coastal marine environment that lie below the level of MLWS and are continuously submerged by seawater.
Tidal excursion ellipse	The approximate displacement path of water during a representative tidal cycle.

MarramWind